JAERI 1327

JAERI 1327

Development of BERMUDA: A Radiation Transport Code System Part I. Neutron Transport Codes

May 1992

日本原子力研究所

Japan Atomic Energy Research Institute

JAERI レポートは，日本原子力研究所が研究成果編集委員会の審査を経て不定期に公刊している研究報告書です。

入手の問合わせは，日本原子力研究所技術情報部情報資料課（〒319－11 茨城県那珂郡東海村）あて，お申しこしください。なお，このほかに財団法人原子力弘済会資料センター（〒319－11 茨城県那珂郡東海村日本原子力研究所内）で複写による実費頒布をおこなっております。

JAERI reports are reviewed by the Board of Editors and issued irregularly.

Inquiries about availability of the reports should be addressed to Information Division Department of Technical Information, Japan Atomic Energy Research Institute, Tokai-mura, Naka-gun, Ibaraki-ken 319－11, Japan.

編集兼発行　日本原子力研究所
印　　刷　いばらき印刷㈱

Development of BERMUDA: A Radiation Transport Code System Part I. Neutron Transport Codes

Tomoo SUZUKI, Akira HASEGAWA, Shun-ichi TANAKA
and Hiroshi NAKASHIMA

Department of Reactor Engineering
Tokai Research Establishment,
Japan Atomic Energy Research Institute
Tokai-mura, Naka-gun, Ibaraki-ken

(Received 13 February, 1992)

Abstract

A radiation transport code system BERMUDA has been developed for one-, two- and three-dimensional geometries. Purpose of the development is to establish a basis of an accurate shielding calculation method for general use. The time-independent transport equation is numerically solved using a direct integration method in a multigroup model, to obtain spatial, angular and energy distributions of neutron, gamma rays or adjoint neutron flux. In order to mitigate the ray effect, the spherical harmonics expansion is not used in representing anisotropy of both angular flux and scattering cross sections. Group-angle transfer matrices are calculated by numerically integrating double-differential cross section data, taking energy-angle correlation into account. In addition, a first collision source method is used for a case of point source. Angular flux distribution is obtained by integrating the transport equation over the line segment along each angular discrete ordinate at each spatial mesh point. A fine energy grid (subgroup having equal lethargy width) method is used, with a rebalancing scheme concerning the number of gain and loss of particles over each coarse mesh region and also in each energy grid. As to group constants, a library with any structure of energy groups is capable to be produced from a data base JSSTDL, or by a processing code PROF-GROUCH-G/B, selecting objective nuclear data through a retrieval system EDFSRS. Validity of the present code system has been tested by analyzing the shielding benchmark experiments performed at the FNS facility in the JAERI. The test has shown that accurate results are obtainable with this system especially in deep penetration calculation. In this report as Part I, described are the devised calculation method and the results of validity tests. Input data specification, job control languages and output data are also described as a user's manual for the following four neutron transport codes:

BERMUDA-1DN	: sphere, slab	(S_{20})
BERMUDA-2DN	: cylinder	(S_8)
BERMUDA-2DN-S16	: cylinder	(S_{16})
BERMUDA-3DN	: rectangular parallelpiped	(S_8)

Development of gamma rays and adjoint neutron transport codes will be reported after validity test of them as Part II and Part III, respectively.

Keywords: BERMUDA, Radiation Transport, Shielding, Code System, Direct Integration Method, Energy Group, Neutron Angular Flux, Double-Differential Cross Section, Anisotropy, Angular Discrete Ordinates, JSSTDL, PROF-GROUCH-G/B, EDFSRS, Gamma Rays, Adjoint Neutron Flux, Benchmark Experiment, FNS, Validity Test

放射線輸送コードシステムBERMUDAの開発 第Ⅰ部 中性子輸送コード

日本原子力研究所東海研究所原子炉工学部

鈴木 友雄・長谷川 明・田中 俊一・中島 宏

(1992年2月13日受理)

要 旨

高精度の遮蔽計算を行うコードシステムの完成を目標に，その計算手法の基礎を確立するため，1～3次元の各形状に対する放射線輸送コードシステムBERMUDAを開発した。本コードシステムでは直接積分法と，エネルギーに関する多群モデルを組合わせて定常状態での輸送方程式を数値的に解き，中性子，ガンマ線あるいは随伴中性子の各線束の空間，角度，エネルギー分布を求めている。レイイフェクトを緩和するため，線束や散乱断面積の非等方性の表現に球面調和関数展開を用いていない。散乱による群・角度遷移マトリックスの算出には，エネルギーと散乱角の相関を考慮して，二重微分散乱断面積の数値積分を行う。さらに，点線源の場合は一回散乱源を求めてから輸送方程式を解く方法を用いている。線束の空間・角度分布は各格子点で各角度分点の方向へ輸送方程式を積分し，エネルギー群をレサジーで等分割した微細群毎に，領域毎の粒子バランスが成立つように規格化を行いつつ求める。群定数は任意の群構造のものが，データベースJSSTDLから，あるいは処理コードPROF-GROUCH-G/Bで核データ収納検索システムEDFSRSをもとにライブラリーとして作成される。コードの適用性はFNSを用いて行ったベンチマーク実験の解析により行い，特に，深層透過計算の精度が良いことが確認された。本報告書は第Ⅰ部として，次の4個の中性子輸送コード

BERMUDA-1 DN (1次元球，平板体系，S_{20})
BERMUDA-2 DN (2次元円柱体系，S_8)
BERMUDA-2 DN-S 16 (2次元円柱体系，S_{16})
BERMUDA-3 DN (3次元直方体体系，S_8)

の計算法と適用性検討結果について述べている。また使用マニュアルとしてジョブ制御文と入力データの準備，更に出力データの概要について述べた。ガンマ線及び随伴中性子輸送コードについてはテストの終了後，それぞれ第Ⅱ部，第Ⅲ部で報告する。

Contents

目　　次

List of Tables

List of Figures

This is a blank page.

1. Introduction

Since 1979, development of a radiation transport code system BERMUDA has been carried out in the Japan Atomic Energy Research Institute. Purpose of the development is to establish a basis of an accurate shielding analysis system for general use including fission and fusion reactors.

BERMUDA has been designed as a deterministic-type transport equation code for one-, two- and three-dimensional geometries. It is not a modification of the formerly existing codes. We have tried to attain high accuracy of the results with a precise simulation. Efficiency in computation is not considered because an exact calculation method must be first achieved.

There have been good many discrete ordinates transport codes based on the Sn method[1),2)] using the Legendre expansion approximation in dealing with anisotropy in both neutron angular flux and scattering cross sections. However, it is difficult to apply this spherical harmonics expansion in low order to represent the extremely anisotropic angular distribution of fast neutron flux in a spatial region where a source is localized in a small part. Similar difficulty is in dealing with the strong anisotropy of scattering in the high energy region. The Sn codes are very excellent now for practical use even though the Sn codes sometimes produce negative values or inaccurate distributions even for scalar flux in the high energy region above 10MeV.

To overcome these difficulties, Takeuchi et al.[3)] have developed the PALLAS code series without using the Legendre expansion. They use the direct integration method to obtain the angular flux for each direction of discrete ordinates at each spatial mesh point. In addition, they apply the exact energy-angle correlation method in dealing with anisotropy of elastic scattering by integrating numerically the double -differential cross section. Thus PALLAS has an advantage in calculating neutron flux having a strong anisotropy. However, the energy group model is not used in PALLAS. With respect to energy variable, PALLAS solves the transport equation in a continuous energy model, arraying discrete energy points E_i with equal lethargy intervals. This method is good for computer efficiency, though it is difficult to maintain neutron balance in an energy interval between E_{i-1} and E_i unless the energy meshes are made extremely fine.

Several codes[17),20)] have been developed applying double-differential cross sections to the Sn codes. They are now useful in fusion neutronics analyses. We aim at developing a new-type transport code incorporating various accurate simulation methods. For solving transport equation in space and angle, we selected the direct integration method like PALLAS. This method is very natural, direct and simple in simulating neutron transport phenomenon. Moreover, this method never calculates negative results and does not need a so-called Diamond-Difference Approximation technique used in the Sn codes.

For energy variable, we have, on the contrary, selected the energy group model as in the Sn codes. It is because the model is convenient to maintain neutron balance in each group. In addition, it is easy to derive adjoint equation in the group model with the same scattering kernel.

These are the reasons why BERMUDA is designed using the direct integration method in the usual energy group model. Moreover, it considers neutron balance in each region called a coarse mesh. Scattering kernel is obtained numerically so as to conserve the number of neutrons after scattering.

Neutron transport calculation architecture in the present code system has become a combination of the following models:

(a) Direct integration method for obtaining space-angle distribution of flux,
(b) Numerical integration of double-differential cross section of elastic and inelastic (discrete levels) scatterings for obtaining group-angle transfer matrices,

(c) Group dividing method into fine energy groups (grids) with a few iterations for each grid for the groups except thermal energy group (For the thermal group, the usual energy group model is adopted with iteration procedure for scattering source from the self group.) ,
(d) Neutron balance adjustment in each grid or group by renormalizing the obtained flux after space–angle calculation sweep in each spatial region called a coarse mesh,
(e) First collision source method in case of a point source, in which the flux is obtained as the sum of the solution and the uncollided flux and
(f) Scalar flux calculation after all angular fluxes are obtained by numerically integrating them over the angular space for each spatial mesh point and for each energy grid or group.

Shortcoming of the present code system is to spend very much computer resources. The radiation transport problems often involve a steep distribution function behaving like a delta function, and so, an approximation with separation of variables like $F(x, y) = f(x)\, g(y)$ is usually difficult to be applied. Each variable of space, angle and energy needs to be discretized into very fine segments for numerical calculation. Then the shielding calculation becomes very expensive especially in three–dimensional case. In this case a precise solution is not obtained without consuming too much computer resources. One practical solution is to devise some simplified approximation method. But it is necessary to validate the approximated solutions by comparing with an exact solution or at least by an experimental value. To resolve the shortcoming of the present three–dimensional code, more improvements will be necessary to attain efficiency. A progress in computer hardware capability is also expected to solve this problem.

We have achieved an accurate calculation method especially for a penetration calculation up to two–dimension. This has been confirmed through validity tests by comparison with benchmark experiments performed at the Fusion Neutronics Source (FNS) facility[21] in JAERI. Required computation time is also in practical range except a three–dimensional case.

In Chapter 2, the nuclear data base system[4], the processing code[5] and several libraries of group constants set for BERMUDA are briefly described. The numerical methods to solve the neutron transport equation in the present version of the code system are introduced in detail in Chapter 3. In Chapter 4, some examples of validity tests are given in comparison with the benchmark experiments. Chapter 5 is a guide for users to prepare input data as well as the job control languages for the FACOM/VP2600 computer. In addition, a brief description is given about the output data on printer or disk. Chapter 6 is for concluding remarks.

The above–mentioned output data file on disk contains the space, angle and energy distributions of flux. This data are processed to produce distributions and integrated values of various kinds of physical quantities and to plot them in figures by some separate codes' aid. These post–processing codes will be released in the future.

The gamma rays and adjoint neutron transport versions in the BERMUDA code system will also be reported after their validity tests as Part II and Part III, respectively.

2. Group Constants Library

It is necessary to prepare group constants as the coefficients of each term in the Boltzmann transport equation. The coefficients are the macroscopic cross sections; the sum of products of atomic number density and microscopic cross section. The neutron cross sections of nuclei are usually given to a transport code as averaged values for each energy group. For reactions having resonances in a group, resonance self-shielding factors are also prepared to give effective values of cross sections in a material or mixture.

A group constants library thus consists of microscopic cross sections and resonance self-shielding factors; the parameters invariable through various problems having different composition and configuration. Compiling them in a magnetic disk as a library file in binary form, the number of input parameters for a transport code becomes quite few. Microscopic cross sections and other parameters commonly used in the present code are supplied almost automatically from the library file.

In this chapter, we only mention the data source of the neutron cross section, processing code used, data structure and brief descriptions of the stored data in the library.

2.1 Nuclear Data and Group Constants Processing System

The basic cross section data with respect to fine discrete energy points are first prepared from measured raw data or theoretical calculations known as 'evaluated nuclear data file.' For example, there are ENDF/B, ENDL, JEF, JENDL, KEDAK and UKNDL. Hasegawa has completed a data base management system, namely 'Evaluated Data Files Storage and Retrieval System, EDFSRS,'[4] and stored almost all obtainable nuclear data files in the world into the system.

To test the present code system, we made some libraries using JENDL files as well as ENDF/B-IV. Those from JENDL files correspond to the latest version of JENDL files available at the development stage of BERMUDA.

Group constants are made from those evaluated nuclear data files by processing them for each energy 'group' defined by dividing the energy space into some number of intervals. The structure of energy group is defined fine enough for the problem to be analyzed. In general, weighting spectrum to produce group constants are assumed for each energy region as fission or DT neutron source, $1/E$, $1/\Sigma_t$, Maxwellian spectrum or detailed thermal neutron spectrum based on a thermal neutron scattering kernel. In the present work, adopted fundamental weighting spectrum is Maxwellian and $1/E$ (joined at 0.32eV) to enhance the generality of applications not only for fusion neutronics but also for fission reactors.

For the processing, a code 'PROF-GROUCH-G/B' was used. As to the details of the processing for the group constants generation, they will be described in a report[5] 'PROF-GROUCH-G/B, a Code System to Produce Group Constants for BERMUDA or Other Transport Codes.'

2.2 Neutron Group Constants

A common 295-group (neutron group) constants data base JSSTDL-295 (the JAERI Shielding Standard Library of 295 groups) has been produced. The energy space below 16.5MeV is divided into 295 energy intervals (groups) in such a manner that the group structures of various kinds of existing libraries can be reproduced by collapsing the 295 groups into less number of groups.

There are three neutron group constants libraries prepared for BERMUDA test calculations;

(a) J2585. BERMUDA1. DATA (ENDF/B-IV,[14] 120 groups, 30 nuclides),

(b) J2585. BERMUDAJ. DATA (JENDL-2[15] and JENDL-3PR1,[16]
120 groups, 30 nuclides) and
(c) J3931. BERM125X. DATA (JENDL-2, JENDL-3PR1 and JENDL-3PR2,[16]
125 groups, 24 nuclides).

In Table 2.1, the boundary energies, middle energies and lethargy widths are given for the library with 125 energy groups (J3931.BERM125X.DATA). Table 2.2 shows nuclides contained, together with their code numbers (identification numbers for use in BERMUDA) and their atomic weights. This library consists of 3876 binary records as follows:

(1) The first header record is

(EUP (I) , I=1, 126) , (EMID (I) , I=1, 125) , (DELU (I) , I=1, 125) ,
(CHI (I) , I=1, 125) , (NCODEL (N) , N=1, 30) , (AW (N) , N=1, 30) ,
(LEVEL (N) , N=1, 30) , ((Q (L-1, N) , L=2, 41) , N=1, 30) , NS0, NTP,
(CSIG0 (IS0) , IS0=1, NS0) , (TP (ITP) , ITP=1, NTP) , (INDXFT (N) , N=1, 30) ,

where
- EUP : upper energy boundary (eV) ,
- EMID : group mid-point in lethargy (eV) ,
- DELU : group lethargy width,
- CHI : dummy,
- NCODEL : nuclide code number,
- AW : atomic weight (in unit of neutron mass) ,
- LEVEL : number of levels for elastic (=1) and inelastic (discrete levels) scattering,
- Q : Q value (positively defined) for each level L,
- NS0 : number of σ_0 points for f (σ_0,T) table (=9) ,
- NTP : number of temperature points for f (σ_0,T) table (=4) ,
- CSIG0 : value of σ_0 for f (σ_0,T) table (barn),
- TP : value of T for f(σ_0,T) table (Kelvin),
- INDXFT : index for f(σ_0,T) table existence and
- σ_0 : admixture cross section defined as a ratio of 'sum of macroscopic total cross sections of other nuclides in a mixture' to 'atomic number density of the nuclide of interest.'

The remaining $3875=31\times125$ records are corresponding to the number of products obtained by repeating 31 times of a group cross section record for 125 groups. The 31 records for each group consists of 30 anisotropic data records (repeated for each nuclide) , and one record containing isotropic data of all (30) nuclides.

(2) Anisotropic data record for each of 30 nuclides are given as,

LEV, (LGEN (L) , SSS (L) , (FC (LG, L) , LG=1, LGEN (L)) , L=1, LEV) ,

where
- LEV : number of levels including elastic level (Q=0 and L=1) ,
- LGEN : number of Legendre coefficients for level L (anisotropic scattering data as group constants are given in a form of Legendre coefficients. LGEN (L) value does not contain the Legendre first (isotropic) term.) ,
- SSS : scattering cross section for level L and

Table 2.1 Energy group structure

GROUP NO.	UPPER ENERGY	LOWER ENERGY	MIDDLE ENERGY	LETHARGY WIDTH
1	1.64870E+07	1.62310E+07	1.63585E+07	0.0156
2	1.62310E+07	1.59800E+07	1.61050E+07	0.0156
3	1.59800E+07	1.57320E+07	1.58555E+07	0.0156
4	1.57320E+07	1.54880E+07	1.56095E+07	0.0156
5	1.54880E+07	1.52480E+07	1.53675E+07	0.0156
6	1.52480E+07	1.50120E+07	1.51295E+07	0.0156
7	1.50120E+07	1.47790E+07	1.48950E+07	0.0156
8	1.47790E+07	1.45500E+07	1.46641E+07	0.0156
9	1.45500E+07	1.43240E+07	1.44366E+07	0.0157
10	1.43240E+07	1.41020E+07	1.42126E+07	0.0156
11	1.41020E+07	1.38830E+07	1.39921E+07	0.0157
12	1.38830E+07	1.36680E+07	1.37751E+07	0.0156
13	1.36680E+07	1.34560E+07	1.35616E+07	0.0156
14	1.34560E+07	1.32480E+07	1.33516E+07	0.0156
15	1.32480E+07	1.30420E+07	1.31446E+07	0.0157
16	1.30420E+07	1.28400E+07	1.29406E+07	0.0156
17	1.28400E+07	1.26410E+07	1.27401E+07	0.0156
18	1.26410E+07	1.24450E+07	1.25426E+07	0.0156
19	1.24450E+07	1.22520E+07	1.23481E+07	0.0156
20	1.22520E+07	1.20620E+07	1.21566E+07	0.0156
21	1.20620E+07	1.18750E+07	1.19681E+07	0.0156
22	1.18750E+07	1.16910E+07	1.17826E+07	0.0156
23	1.16910E+07	1.15100E+07	1.16001E+07	0.0156
24	1.15100E+07	1.13310E+07	1.14201E+07	0.0157
25	1.13310E+07	1.11560E+07	1.12432E+07	0.0156
26	1.11560E+07	1.09830E+07	1.10692E+07	0.0156
27	1.09830E+07	1.08120E+07	1.08972E+07	0.0157
28	1.08120E+07	1.06450E+07	1.07282E+07	0.0156
29	1.06450E+07	1.04800E+07	1.05622E+07	0.0156
30	1.04800E+07	1.03170E+07	1.03982E+07	0.0157
31	1.03170E+07	1.01570E+07	1.02367E+07	0.0156
32	1.01570E+07	9.99990E+06	1.00781E+07	0.0156
33	9.99990E+06	9.39400E+06	9.69222E+06	0.0625
34	9.39400E+06	8.82490E+06	9.10500E+06	0.0625
35	8.82490E+06	8.29020E+06	8.55337E+06	0.0625
36	8.29020E+06	7.78790E+06	8.03513E+06	0.0625
37	7.78790E+06	7.31610E+06	7.54832E+06	0.0625
38	7.31610E+06	6.87280E+06	7.09099E+06	0.0625
39	6.87280E+06	6.45640E+06	6.66135E+06	0.0625
40	6.45640E+06	6.06520E+06	6.25774E+06	0.0625
41	6.06520E+06	5.69780E+06	5.87863E+06	0.0625
42	5.69780E+06	5.35250E+06	5.52245E+06	0.0625
43	5.35250E+06	5.02820E+06	5.18782E+06	0.0625
44	5.02820E+06	4.72360E+06	4.87352E+06	0.0625
45	4.72360E+06	4.43740E+06	4.57826E+06	0.0625
46	4.43740E+06	4.16860E+06	4.30090E+06	0.0625
47	4.16860E+06	3.91600E+06	4.04033E+06	0.0625
48	3.91600E+06	3.67870E+06	3.79550E+06	0.0625
49	3.67870E+06	3.45590E+06	3.56556E+06	0.0625
50	3.45590E+06	3.24650E+06	3.34956E+06	0.0625

Table 2.1 Energy group structure (continued)

GROUP NO.	UPPER ENERGY	LOWER ENERGY	MIDDLE ENERGY	LETHARGY WIDTH
51	3.24650E+06	3.04980E+06	3.14661E+06	0.0625
52	3.04980E+06	2.86500E+06	2.95596E+06	0.0625
53	2.86500E+06	2.69140E+06	2.77684E+06	0.0625
54	2.69140E+06	2.52840E+06	2.60863E+06	0.0625
55	2.52840E+06	2.37520E+06	2.45060E+06	0.0625
56	2.37520E+06	2.23130E+06	2.30213E+06	0.0625
57	2.23130E+06	2.09610E+06	2.16264E+06	0.0625
58	2.09610E+06	1.96910E+06	2.03161E+06	0.0625
59	1.96910E+06	1.84980E+06	1.90852E+06	0.0625
60	1.84980E+06	1.73770E+06	1.79287E+06	0.0625
61	1.73770E+06	1.53350E+06	1.63241E+06	0.1250
62	1.53350E+06	1.35330E+06	1.44059E+06	0.1250
63	1.35330E+06	1.19430E+06	1.27132E+06	0.1250
64	1.19430E+06	1.05400E+06	1.12196E+06	0.1250
65	1.05400E+06	9.30130E+05	9.90130E+05	0.1250
66	9.30130E+05	8.20840E+05	8.73778E+05	0.1250
67	8.20840E+05	7.24380E+05	7.71103E+05	0.1250
68	7.24380E+05	6.39270E+05	6.80496E+05	0.1250
69	6.39270E+05	5.64150E+05	6.00537E+05	0.1250
70	5.64150E+05	4.97860E+05	5.29970E+05	0.1250
71	4.97860E+05	4.39360E+05	4.67696E+05	0.1250
72	4.39360E+05	3.87740E+05	4.12744E+05	0.1250
73	3.87740E+05	3.42170E+05	3.64243E+05	0.1250
74	3.42170E+05	3.01970E+05	3.21442E+05	0.1250
75	3.01970E+05	2.66490E+05	2.83676E+05	0.1250
76	2.66490E+05	2.35170E+05	2.50341E+05	0.1250
77	2.35170E+05	2.07540E+05	2.20923E+05	0.1250
78	2.07540E+05	1.83150E+05	1.94964E+05	0.1250
79	1.83150E+05	1.61630E+05	1.72054E+05	0.1250
80	1.61630E+05	1.42640E+05	1.51838E+05	0.1250
81	1.42640E+05	1.25880E+05	1.33998E+05	0.1250
82	1.25880E+05	1.11090E+05	1.18254E+05	0.1250
83	1.11090E+05	9.80350E+04	1.04359E+05	0.1250
84	9.80350E+04	8.65150E+04	9.20951E+04	0.1250
85	8.65150E+04	7.63490E+04	8.12732E+04	0.1250
86	7.63490E+04	6.73780E+04	7.17234E+04	0.1250
87	6.73780E+04	5.94610E+04	6.32958E+04	0.1250
88	5.94610E+04	5.24740E+04	5.58584E+04	0.1250
89	5.24740E+04	4.63080E+04	4.92947E+04	0.1250
90	4.63080E+04	4.08670E+04	4.35025E+04	0.1250
91	4.08670E+04	3.60650E+04	3.83910E+04	0.1250
92	3.60650E+04	3.18270E+04	3.38798E+04	0.1250
93	3.18270E+04	2.80870E+04	2.98986E+04	0.1250
94	2.80870E+04	2.47870E+04	2.63855E+04	0.1250
95	2.47870E+04	2.18740E+04	2.32850E+04	0.1250
96	2.18740E+04	1.93040E+04	2.05489E+04	0.1250
97	1.93040E+04	1.50340E+04	1.70357E+04	0.2500
98	1.50340E+04	1.17090E+04	1.32677E+04	0.2500
99	1.17090E+04	9.11860E+03	1.03329E+04	0.2500
100	9.11860E+03	7.10160E+03	8.04715E+03	0.2500

Table 2.1 Energy group structure (continued)

GROUP NO.	UPPER ENERGY	LOWER ENERGY	MIDDLE ENERGY	LETHARGY WIDTH
101	7.10160E+03	5.53070E+03	6.26712E+03	0.2500
102	5.53070E+03	4.30730E+03	4.88082E+03	0.2500
103	4.30730E+03	3.35460E+03	3.80122E+03	0.2500
104	3.35460E+03	2.61250E+03	2.96039E+03	0.2500
105	2.61250E+03	2.03460E+03	2.30551E+03	0.2500
106	2.03460E+03	1.58460E+03	1.79556E+03	0.2500
107	1.58460E+03	1.23410E+03	1.39841E+03	0.2500
108	1.23410E+03	9.61100E+02	1.08908E+03	0.2500
109	9.61100E+02	5.82930E+02	7.48501E+02	0.5000
110	5.82930E+02	3.53570E+02	4.53990E+02	0.5000
111	3.53570E+02	2.14450E+02	2.75360E+02	0.5000
112	2.14450E+02	1.30070E+02	1.67014E+02	0.5000
113	1.30070E+02	7.88910E+01	1.01298E+02	0.5000
114	7.88910E+01	4.78500E+01	6.14405E+01	0.5000
115	4.78500E+01	2.90230E+01	3.72659E+01	0.5000
116	2.90230E+01	1.76030E+01	2.26029E+01	0.5000
117	1.76030E+01	1.06770E+01	1.37094E+01	0.5000
118	1.06770E+01	6.47580E+00	8.31517E+00	0.5000
119	6.47580E+00	3.92780E+00	5.04338E+00	0.5000
120	3.92780E+00	2.38230E+00	3.05895E+00	0.5000
121	2.38230E+00	1.44490E+00	1.85531E+00	0.5000
122	1.44490E+00	8.76400E-01	1.12530E+00	0.5000
123	8.76400E-01	5.31560E-01	6.82539E-01	0.5000
124	5.31560E-01	3.22410E-01	4.13981E-01	0.5000
125	3.22410E-01	1.00100E-05	1.79648E-03	10.3800

FC : Legendre coefficients for level L.

(3) Isotropic data record for each group are given as,

(SST (N) , N=1, 30), (SSFNU (N) , N=1, 30) , (SSF (N) , N=1, 30) ,
(SSC (N) , N=1, 30) , ((SS0 (J, N) , J=1, 125) , N=1, 30) ,
(((FFF (IS0, ITP, N) , IS0=1, NS0) , ITP=1, NTP) , N=1, 30) ,
(((FFC (IS0, ITP, N) , IS0=1, NS0) , ITP=1, NTP) , N=1, 30) ,
(((FFE (IS0, ITP, N) , IS0=1, NS0) , ITP=1, NTP) , N=1, 30) ,
(((FFT (IS0, ITP, N) , IS0=1, NS0) , ITP=1, NTP) , N=1, 30) ,

where SST : total cross section σ_t,
SSFNU : fission yield cross section $\nu\,\sigma_f$,
SSF : fission cross section σ_f,
SSC : capture cross section σ_c,
SS0 : isotropic scattering matrix $\sigma_s^{i\to i+j-1}$ as the sum of inelastic continuum level and (n, 2n) , (n, 3n) etc.,

FFF : resonance self-shielding factor for fission cross section,
FFC : resonance self-shielding factor for capture cross section,
FFE : resonance self-shielding factor for elastic scattering cross section and
FFT : resonance self-shielding factor for total cross section.

The total 31 records of (2) and (3) are repeated for each of 125 energy groups.

Other cross sections for detector responses for seven reactions are also prepared in the first header record (after INDXFT). These data are no more referred by BERMUDA directly, because editing of reaction rates is now performed by other post-processing codes[6] after the angular, scalar and uncollided fluxes are calculated and stored on the ouput disk of BERMUDA.

Table 2.2 Nuclides in the library J3931. BERM125X. DATA

ORDER IN LIBRARY	NUCLIDE NAME	CODE NUMBER	ATOMIC MASS (IN NEUTRON MASS UNIT)
1	H	11	0.9992
2	VACANCY	0	0.0
3	VACANCY	0	0.0
4	LI-6	36	5.9635
5	LI-7	37	6.9557
6	BE	40	8.9348
7	B-10	50	9.9269
8	VACANCY	0	0.0
9	C	60	11.8970
10	N	70	13.8830
11	O	80	15.8580
12	NA	110	22.7920
13	AL	130	26.7680
14	CR	240	51.5490
15	MN	250	54.4660
16	FE	260	55.3670
17	NI	280	58.2010
18	CU	290	63.5000
19	VACANCY	0	0.0
20	MO	420	95.0660
21	PB	820	205.4000
22	F	90	18.8350
23	CA	200	39.7360
24	V-51	230	50.5060
25	CO-59	270	58.4270
26	NB	410	92.1080
27	TA	730	179.3900
28	VACANCY	0	0.0
29	VACANCY	0	0.0
30	SI	140	27.8480

3. Numerical Method to Solve Neutron Transport Equation

In this chapter, we describe the numerical method developed for the BERMUDA code system to solve accurately the time-independent neutron transport equation. The method is almost numerical in the meaning that neither expansion nor transformation with orthogonal functions is used. However, analytical, geometrical (i. e. spherical trigonometry used in Sec. 3.4) and physical equations describing neutron transport and scattering are utilized as far as possible. Once the basic algorismic procedure is made up and confirmed through validity tests, it will be applicable also to gamma rays and adjoint neutron transport calculations with some modifications.

3.1 Transport Equation in Multigroup Model

The time-independent transport equation,[7]

$$\vec{\Omega} \cdot grad\ \phi\ (\vec{r}, E, \vec{\Omega}) + \Sigma_t (\vec{r}, E)\ \phi\ (\vec{r}, E, \vec{\Omega})$$

$$= \int dE' \int d\vec{\Omega}'\, \phi\ (\vec{r}, E', \vec{\Omega}')\ \Sigma_s (E' \to E, \vec{\Omega}' \to \vec{\Omega}) + S (\vec{r}, E, \vec{\Omega}),$$

is rewritten in a usual energy group model, where the flux ϕ and the independent source S are integrated over a group width ΔE_i, and the macroscopic cross sections are averaged in the group as described in Chap.2, as

$$\vec{\Omega} \cdot grad\ \phi^{\,i} (\vec{r}, \vec{\Omega}) + \Sigma_t^{\,i} (\vec{r})\ \phi^{\,i} (\vec{r}, \vec{\Omega}) = q^{\,i} (\vec{r}, \vec{\Omega}). \tag{3.1}$$

Symbols in Eq. (3.1) are as follows:

$\vec{\Omega}$: unit direction vector drawn from the spatial point $\vec{r}$,

$\cdot$: sign for inner product of vectors, i. e. $\vec{\Omega} \cdot$ means direction cosine between directions of $\vec{\Omega}$ and gradient operator,

$$q^{\,i} (\vec{r}, \vec{\Omega}) = q_{aniso}^{\,i} (\vec{r}, \vec{\Omega}) + (1/4\pi) \sum_{j=1}^{i} \Sigma_{iso}^{j \to i} (\vec{r})\ \Phi^{\,j} (\vec{r}) + S^{\,i} (\vec{r}, \vec{\Omega}) \tag{3.2}$$

(In Eq. (3.2), anisotropic and isotropic scattering sources are separately written. The former is treated with double-differential cross section for elastic and inelastic (discrete levels only) scatterings as described below. The latter involves inelastic (continuum level) scattering and (n, 2n) and (n, 3n) reactions),

$$q_{aniso}^{\,i} (\vec{r}, \vec{\Omega}) = \sum_{j=1}^{i} \int d\vec{\Omega}'\, \phi^{\,j} (\vec{r}, \vec{\Omega}') / \Delta E_j \int_{\Delta E_j} dE' \int_{\Delta E_i} dE$$

$$\times \sum_m N^m (\vec{r}) \sum_L F_L^{mj} \sigma_L^{\,m} (E' \to E, \vec{\Omega}' \to \vec{\Omega}), \tag{3.3}$$

i, j : group indeces numbered from the highest energy group as 1, 2, ···, IMAX,

$\Sigma_{iso}^{j \to i} (\vec{r}) = \sum_m N^m (\vec{r})\ \sigma_s^{m,\, j \to i}$: isotropic scattering cross section corresponding to SS0 in Sec. 2.2 (This is an averaged value for group j but is an integrated value for group i),

$\Phi^j(\vec{r}) = \int \phi^j(\vec{r}, \vec{\Omega})\, d\vec{\Omega}$: scalar flux for group j,

m : nuclide,

N^m : atomic number density of nuclide m in a mixture,

L : level (L=0 for elastic and L≠0 for inelastic (discrete levels) scatterings),

$$F_L^{mj} = \begin{cases} \bar{f}_e^{mj}\ (L=0): & \text{resonance self-shielding factor (elastic) interpolated from the table FFE (see Sec. 2.2) to the actual } (\sigma_0, T) \text{ point,} \\ 1 \quad (L \neq 0) \end{cases}$$

and

$\sigma_L^m(E' \to E, \vec{\Omega}' \to \vec{\Omega})$: double-differential cross section.

The other symbols are used as usual.

Equation (3.1) is solved first for group 1, then the soludion ϕ^1 is used in Eq. (3.2) to obtain the slowing down source from the group 1. In this manner, Eq. (3.1) is solved consecutively up to the final (lowest energy) group IMAX.

3.2 Direct Integration Method

Taking the gradient along the linear path of direction $\vec{\Omega}$ at the spatial point $\vec{r}$, direction cosine becomes unity. Then, Equation (3.1) is written by using x which is a coefficient used as $\vec{r}' = \vec{r} + x\vec{\Omega}$,

$$(d/dx)\,\phi(x) + \Sigma_t(x)\,\phi(x) = q(x), \tag{3.4}$$

where the group index i is suppressed.

We consider a line segment $[x_{p-1}, x_p]$ where x_p coincides the mesh point $\vec{r}_p$, that is, $\vec{r}' = \vec{r}_p - (x_p - x)\,\vec{\Omega}$. If the values of $\phi(x_{p-1})$, $q(x_{p-1})$ and $q(x_p)$ are known, and the medium is homogeneous over the line segment, the solution of Eq. (3.4) gives

$$\phi(x_p) = \phi(x_{p-1})\, exp\,[-(x_p - x_{p-1})\,\Sigma_t] + \int_{x_{p-1}}^{x_p} exp\,[-(x_p - x)\Sigma_t]\, q(x)\, dx. \tag{3.5}$$

Usually the point $\vec{r}_{p-1} = \vec{r}_p - (x_p - x_{p-1})\,\vec{\Omega}$ does not coincide with an adjacent mesh point of space and angle, except in the case of one-dimensional slab. So, the values of $\phi(x_{p-1})$ and $q(x_{p-1})$ are obtained from the values at the mesh points nearest to $\vec{r}_{p-1}$ by interpolation with respect to space and angle coordinates. The q (x) over $[x_{p-1}, x_p]$ is also interpolated usually by an exponential function using the values of $q(x_{p-1})$ and $q(x_p)$. As to angular ordinates, $\vec{\Omega}$ space is on the surface of a unit sphere, whose center is $\vec{r}_p$. The surface is divided into a number of regions $\Delta\vec{\Omega}_n$, in which a representative direction $\vec{\Omega}_n$ is defined. The definition of these $\vec{\Omega}_n$ and $\Delta\vec{\Omega}_n$ is given in Sec. 3.4. At the beginning, the exact value of $q(x_p)$ is not known because Eq. (3.2) contains $\phi(x_p)$ for the self group. By this reason, an iteration procedure is necessary, which is introduced in Sec.3.6.

3.3 Group-Angle Transfer Matrices

This Section introduces the method of calculation for the anisotropic scattering source given in Eq. (3.3).

Omitting $\sum_j$, m, $\sum_m$, N_m, L, $\sum_L$ and F_L^{mj} for simplicity, Eq. (3.3) becomes,

$$q_{aniso}^{j\to i}(\vec{r},\vec{\Omega})=\int d\vec{\Omega}'\phi^{j}(\vec{r},\vec{\Omega}')/\Delta E_j\int_{\Delta E_j}dE'\int_{\Delta E_i}dE\ \sigma\ (E'\to E,\ \vec{\Omega}'\to\vec{\Omega}).$$

When the angular space $\vec{\Omega}$ is discretized into a finite number of regions $\Delta\vec{\Omega}_n$ (see Sec. 3.4),

$$\begin{aligned}q_{aniso}^{j\to i,\ n'\to n}(\vec{r})&=\phi^{j}(\vec{r},\vec{\Omega}_{n'})/\Delta E_j\int_{\Delta E_j}dE'\int_{\Delta E_i}dE\int_{\Delta\vec{\Omega}_{n'}}d\vec{\Omega}'\\&\quad\times\sigma\ (E'\to E,\vec{\Omega}'\to\vec{\Omega}_n)\\&=\phi^{j}(\vec{r},\vec{\Omega}_{n'})\ K_{aniso}^{j\to i,\ n'\to n}.\end{aligned}$$

Thus, the group–angle transfer matrices are defined as,

$$K_{aniso}^{j\to i,\ n'\to n}=\int_{\Delta E_j}dE'/\Delta E_j\int_{\Delta E_i}dE\int_{\Delta\vec{\Omega}_{n'}}d\vec{\Omega}'\ \sigma\ (E'\to E,\vec{\Omega}'\to\vec{\Omega}_n).\qquad(3.6)$$

For the $\vec{\Omega}$ space, we consider a sphere of radius 1 (a unit sphere drawn by unit direction vectors) whose center is $\vec{r}$ (Fig. 3.1). Symbols given in Fig.3.1 are defined as follows:

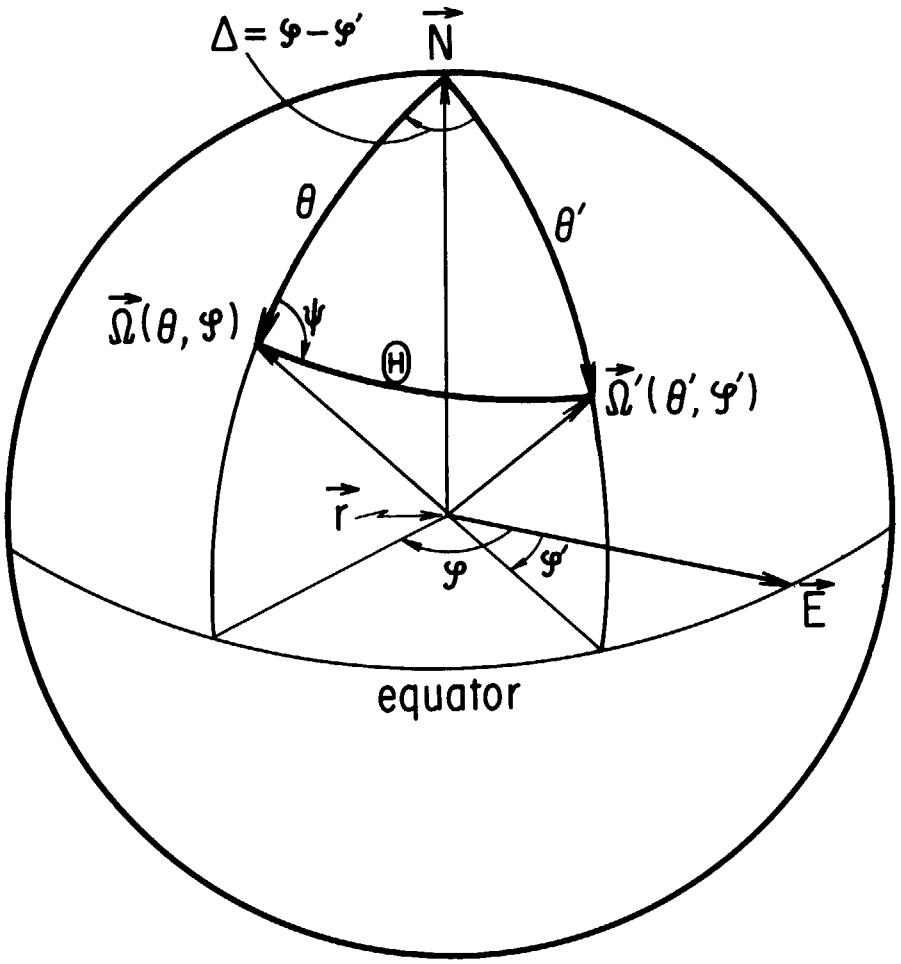

Fig. 3.1 Spherical triangle $\vec{N}\vec{\Omega}'\vec{\Omega}$ on the unit sphere (BERMUDA triangle)

θ, θ' : polar angle (zero on the north pole),
φ, φ' : azimuthal angle (zero on eastside longitude),
$\vec{\Omega}'$ (θ', φ') : neutron direction before collision,
$\vec{\Omega}$ (θ, φ) : neutron direction after collision,
Θ : scattering angle in the laboratory system,
Θ_c : scattering angle in the center-of-mass system,
ϕ : angle at $\vec{\Omega}$ between $\vec{N}$ and $\vec{\Omega}'$,
$\Delta = \varphi - \varphi'$,
$\omega' = \cos\theta'$,
$\omega = \cos\theta$,
$\xi = \cos\Theta$ and
$\mu = \cos\Theta_c$.

Furthermore,

E' = neutron kinetic energy before collision and $E' \geqq [(A+1)/A]\ Q$ (threshold energy),
E = neutron kinetic energy after collision,
$\beta^2 = 1 - [(A+1)/A]\ Q/E'$,
A : atomic mass of target nucleus (in the unit of incident neutron mass $m_o/\sqrt{1-(v/c)^2}$),
m_o : neutron rest mass,
Q : Q-value (defined positive, and Q=0 for elastic scattering) and
$\alpha = [(A-1)/(A+1)]^2$

From the law of conservation of energy and momentum concerning the system of a neutron and a nucleus suffering a collision, we obtain,

$$E/E' = [(A\beta+1)^2 - 2A\beta(1-\mu)]/(A+1)^2$$
$$= [\pm\sqrt{A^2\beta^2 - 1 + \xi^2} + \xi]^2/(A+1)^2, \tag{3.7}$$

$$\mu = 1 - [(A\beta+1)^2 - (A+1)^2 E/E']/2A\beta$$
$$= [\pm\sqrt{A^2\beta^2 - 1 + \xi^2} \cdot \xi - 1 + \xi^2]/A\beta \text{ and} \tag{3.8}$$

$$\xi = [(A+1)/2]\sqrt{E/E'} - [(A^2\beta^2 - 1)/2(A+1)]\sqrt{E'/E}$$
$$= (1 + A\beta\mu)/\sqrt{1 + 2A\beta\mu + A^2\beta^2}. \tag{3.9}$$

The negative sign in the duplicate signs in Eqs. (3.7) and (3.8) are meaningful only when $E' \leqq [A/(A-1)]\ Q$. Otherwise only the plus sign is used.

In case of $[(A+1)/A]\ Q < E' \leqq [(A/(A-1)]\ Q$, the neutron energy after collision, E, has two values, because the curve of E has two branches in the graph drawn on the [E', E] plane. However, the calculated value of scattering kernel from E' in this interval is considered to be very small, so that we adopt only one branch corresponding to the plus sign, and make the value of the calculated kernel half when E' is in this interval.

From Eq. (10.7a) in Ref. 7,

$$\sigma(E' \to E, \vec{\Omega}' \to \vec{\Omega}) = \sigma(E', \mu)\ (d\mu/d\xi)\ \delta\{E - E(E')\},$$

where $E(E') = E' - [2AE'/(A+1)^2](1-\beta\mu) - [A^2E'/(A+1)^2](1-\beta^2)$,

and by using the relation,

$$\delta\{E-E(E')\}\,dE=\delta\{\xi-\xi(\mu)\}\,d\xi,$$

where $\xi(\mu)=(1+A\beta\mu)/\sqrt{1+2A\beta\mu+A^2\beta^2}$,

we obtain

$$\sigma(E'\to E,\ \vec{\Omega}'\to\vec{\Omega})=\sigma(E',\mu)\ (d\mu/dE)\ \delta\{\xi-\xi(\mu)\}$$

$$=\sigma(E')\,f(E',\mu)\ (d\mu/dE)\ \delta\{\xi-\xi(\mu)\},\qquad(3.10)$$

where the angular distribution function is normalized as

$$\int_{-1}^{1} f(E',\mu)\ d\mu=1/2\pi.$$

From Fig. 3.1, it is clear that

$$\vec{\Omega}=(\sin\theta\cos\varphi,\ \sin\theta\sin\varphi,\ \cos\theta)\ \text{and}$$
$$\vec{\Omega}'=(\sin\theta'\cos\varphi',\ \sin\theta'\sin\varphi',\ \cos\theta').$$

Using the above equations, we obtain,

$$\cos\Theta=(\vec{\Omega}\cdot\vec{\Omega}')=\cos\theta\cos\theta'+\sin\theta\sin\theta'\cos\Delta.\qquad(3.11)$$

On the triangle $(\vec{N}\,\vec{\Omega}'\,\vec{\Omega})$, we can consider "$\theta'$ and Θ" and "Δ and ϕ" interchanged simultaneously, then we obtain

$$\cos\theta'=\cos\theta\cos\Theta+\sin\theta\sin\Theta\cos\phi.\qquad(3.12)$$

Equations (3.11) and (3.12) are the formulae of spherical trigonometry and can be rewritten with our pre-defined symbols,

$$\xi=\omega\omega'+\sqrt{1-\omega^2}\sqrt{1-\omega'^2}\cos(\varphi-\varphi'),\qquad(3.13)$$

$$\omega'=\omega\xi+\sqrt{1-\omega^2}\sqrt{1-\xi^2}\cos\phi.\qquad(3.14)$$

As the Jacobian $\begin{vmatrix}\partial\omega'/\partial\xi & \partial\omega'/\partial\phi\\ \partial\varphi'/\partial\xi & \partial\varphi'/\partial\phi\end{vmatrix}$ is easily proved to be unity, we can write

$$\int d\vec{\Omega}'=\int_{-1}^{1}d\omega'\int_{0}^{2\pi}d\varphi'=\int_{-1}^{1}d\xi\int_{0}^{2\pi}d\phi.\qquad(3.15)$$

When Eqs. (3.10) and (3.15) are substituted into Eq. (3.6),

$$K_{aniso}^{j\to i,\ n'\to n}=\int_{\Delta E_j}dE'/\Delta E_j\int_{\Delta E_i}dE\int_{-1}^{1}d\xi\int_{\Delta\vec{\Omega}_{n'}}d\phi_{n'}\sigma^j f^j(\mu)$$

$$\times(d\mu/dE)\ \delta\{\xi-\xi(\mu)\}$$

$$=\sigma^j\int_{\Delta E_j}dE'/\Delta E_j\int_{\Delta E_i}dE\ (d\mu/dE)\ f^j(\mu)$$

$$\times\int_{-1}^{1}d\xi\,\delta\{\xi-\xi(\mu)\}\int_{\Delta\vec{\Omega}_{n'}}d\phi_{n'}\qquad(3.16)$$

The σ^j and $f^j(\mu)$ are supplied as group constants and

$$\Delta\phi_{n',nm'}=\int_{-1}^{1}d\xi\delta\ (\xi-\xi_{m'})\int_{\Delta\vec{\Omega}_{n'}}d\phi_n \tag{3.17}$$

is prepared as a table for discrete values of $\xi_{m'}=\cos\ [(2m'-1)\pi/160]$. A description of the table is given in Sec. 3.4.

Then Eq. (3.16) is reduced to

$$K_{aniso}^{j\to i,\ n'\to n}=\sigma^{j}\int_{\Delta E_j}dE'/\Delta E_j\int_{\mu\epsilon\Delta E_i}f^{j}\ (\mu)\ d\mu$$
$$\times\Delta\phi_{n',nm'}\delta\{\xi\ (\mu),\ \xi_{m'}\}. \tag{3.18}$$

Numerical integration with E' and μ (E) are performed by separating the ranges ΔE_j and $\Delta\mu$ (ΔE_i) into fine intervals. For each combination of the fine E' and E values, the ratio E/E' determines μ from Eq. (3.8) and ξ from Eq. (3.9), δ means m' in the table of $\Delta\phi_{n',nm'}$ is picked out and used, if ξ (E/E') happens to fall in the fine interval of $\xi_{m'}$. The data of $f^j\ (\mu)$ is prepared for 81 values of μ as $\mu_{k'}=(41-k')/40$ ($k'=1,\cdots,81$).

The range of E' is limited by the kinematics relation of Eq. (3.7) if E is given as,

$$E'_{max}=E\ [(A\beta'+1)/(A-1)]^{2},$$
$$E'_{min}=E\ [(A\beta'-1)/(A-1)]^{2}\ and\ E'_{min}\geqq\ [(A+1)/A]Q,$$

where $\beta'^{2}=1+\ [(A-1)/A]\ Q/E$, and conversely,

$$E_{max}=E'\ [(A\beta+1)/(A+1)]^{2}\ and$$
$$E_{min}=E'\ [(A\beta-1)/(A+1)]^{2},$$

where $\beta^{2}=1-\ [(A+1)/A]\ Q/E'$.

Then actual intervals for numerical integration are given between group j and i ($j<i$ or $E^j>E^i$) as,

$$[E']=\Delta E_j\cap[E'_{min}\ (E_{lower}^{i}),\ E'_{max}\ (E_{upper}^{i})]\ and$$
$$[E]=\Delta E_i\cap[E_{min}\ (E'),\ E_{max}(E')].$$

For self-group scattering ($j=i$), we at first use as the range [E']

$$[E']=\Delta E_i\cap[E'_{min}\ (E_{lower}^{i}),\ E'_{max}\ (E_{lower}^{i})]$$

for elastic scattering.

Then the kernel for self-group scattering $K_{aniso}^{i\to i,\ n'\to n}$ must be added by a component integrated over the full range of μ when $E_{upper}^{i}>E_{lower}^{i}/\alpha$ as,

$$[(E_{upper}^{i}-E_{lower}^{i}/\alpha)\Delta E_i]\int_{-1}^{1}d\mu\sigma^{i}f^{i}(\mu)\ \Delta\phi_{n'nm'}\delta\{\xi\ (\mu),\ \xi_{m'}\}.$$

3.4 Angular Discrete Ordinates and Azimuthal Weights of Scattering Angle

As shown in Fig. 3.1, the angular space $\vec{\Omega}$ is considered as a unit sphere. In order to solve the transport equation numerically, the surface of the unit sphere must be divided into an appropriate number of regions $\Delta\vec{\Omega}_n$. In each region, a representative direction $\vec{\Omega}_n$ is defined. The angular flux $\phi^i\ (\vec{r},\vec{\Omega}_n)$ must be calculated as an average value in $\Delta\vec{\Omega}_n$ in order to obtain the scalar flux $\Phi^i\ (\vec{r})$ by simple numerical integration over $\vec{\Omega}$.

3.4.1 One-Dimensional Case

In the one-dimensional case for sphere or infinite slab, the angular flux distribution is calculated only along r or z coordinate, respectively. We fix this r or z direction to the north pole $\vec{N}$ of the unit sphere. As no variation is considered about azimuthal rotation, angular discrete ordinates are distributed with respect to only polar angle $\theta(0 \leqq \theta \leqq \pi)$ on a longitude, in other words, on the axis between the north and the south poles, i.e. the space of $\omega = \cos\theta$. For this case, the Gaussian quadrature set consisting of abscissae ω_n and weights W_n is appropriate for numerical integration. We have selected the set of 20 points (Table 3.1). Surface of the unit sphere is divided by latitudes into 20 zones having areas $2\pi W_n$.

Next, we consider the scattering angle between $\vec{\Omega}_{n'}$ (before collision) and $\vec{\Omega}_n$ (after collision) on the unit sphere. The scattering angle between them is given as Θ in Eq. (3.11). Taking Θ as a polar angle from $\vec{\Omega}_n$, the azimuthal angle extension of $\Delta\vec{\Omega}_{n'}$ to $\vec{\Omega}_n$ is defined as $\Delta\phi$ illustrated in Fig.3.2, which depends on the magnitude of Θ, the radius of the small circle drawn on the unit sphere around $\vec{\Omega}_n$. This $\Delta\phi$ is the measure (weight) of integration with ϕ. In order to tabulate $\Delta\phi_{n',nm'}$ of Eq. (3.17), 80 points of $\Theta_{m'}$ are selected over the range $[0, \pi]$ as

$$\Theta_{m'} = (\pi/80)\ (m' - 1/2),\ m' = 1, \cdots, 80 \ \textit{and}$$
$$\xi_{m'} = \cos\Theta_{m'}.$$

Then using Eq. (3.14), we have W^* as the weight (symbol $W^*_{n',nm'}$ is used for $\Delta\phi_{n',nm'}$ not yet normalized) as follows:

$$\begin{aligned} W^*_{n',nm'} &= 2\int_{\omega_{BS,n'-1}}^{\omega_{BS,n'}} d\phi = 2\Delta\phi \\ &= 2\left[\cos^{-1}\{(\omega_{BS,n'} - \omega_n\xi_{m'})/D\}\right. \\ &\quad \left. - \cos^{-1}\{(\omega_{BS,n'-1} - \omega_n\xi_{m'})/D\}\right], \end{aligned} \tag{3.19}$$

Table 3.1 Gaussian quadrature set for n = 20

N	ABSCISSA	WEIGHT	SOUTH BOUNDARY
1	0.9931286	0.0176140	0.9823860
2	0.9639719	0.0406014	0.9417846
3	0.9122344	0.0626721	0.8791125
4	0.8391170	0.0832768	0.7958357
5	0.7463319	0.1019301	0.6939056
6	0.6360537	0.1181945	0.5757111
7	0.5108670	0.1316886	0.4440225
8	0.3737061	0.1420961	0.3019264
9	0.2277859	0.1491730	0.1527534
10	0.0765265	0.1527534	0.0
11	-0.0765265	0.1527534	-0.1527534
12	-0.2277859	0.1491730	-0.3019264
13	-0.3737061	0.1420961	-0.4440225
14	-0.5108670	0.1316886	-0.5757111
15	-0.6360537	0.1181945	-0.6939056
16	-0.7463319	0.1019301	-0.7958357
17	-0.8391170	0.0832768	-0.8791125
18	-0.9122344	0.0626721	-0.9417846
19	-0.9639719	0.0406014	-0.9823860
20	-0.9931286	0.0176140	-1.0000000

where (1) BS means the south boundary (Table 3.1), (2) D is equal to $\sqrt{1-\omega_n{}^2}\times\sqrt{1-\xi_{m'}{}^2}$ and (3) the factor 2 means the contribution from the left hand side of the longitude passing $\vec{\Omega}_n$. It is clear from Fig. 3.2 that the relation

$$\sum_{n'} W^*{}_{n',nm'}=2\pi \tag{3.20}$$

holds.

For a small value of Θ, the circle of radius Θ is completely contained in the domain $\Delta\vec{\Omega}_n$ ($\theta_{BS,\,n-1}\leqq\theta\leqq\theta_{BS,\,n}$), so that the relation

$$W^*{}_{n',nm'}=2\pi\delta_{n',n}$$

holds. This is inadequate for accounting the slight neutron migration from the adjacent areas. To account it, 5 points are taken uniformly over the $W_n\equiv\Delta\omega_n$ range $[\omega_{BS,\,n},\omega_{BS,\,n-1}]$. The values of W^* obtained by Eq. (3.19) with the 5 different values of ω_n are averaged. Even so, Eq. (3.20) holds. This procedure is applied not only for small Θ, but for all 80 values of Θ, i.e. the kernel K in Sec. 3.3 is obtained as an average in the region $\Delta\vec{\Omega}_n$.

Here let us consider the conservation of the number of neutrons after collision. As $f(E',\mu)$ in Eq. (3.10) is normalized to $1/2\pi$ when integrated over μ, $\Delta\phi_{n',nm'}$ in Eq. (3.17) is necessary to satisfy

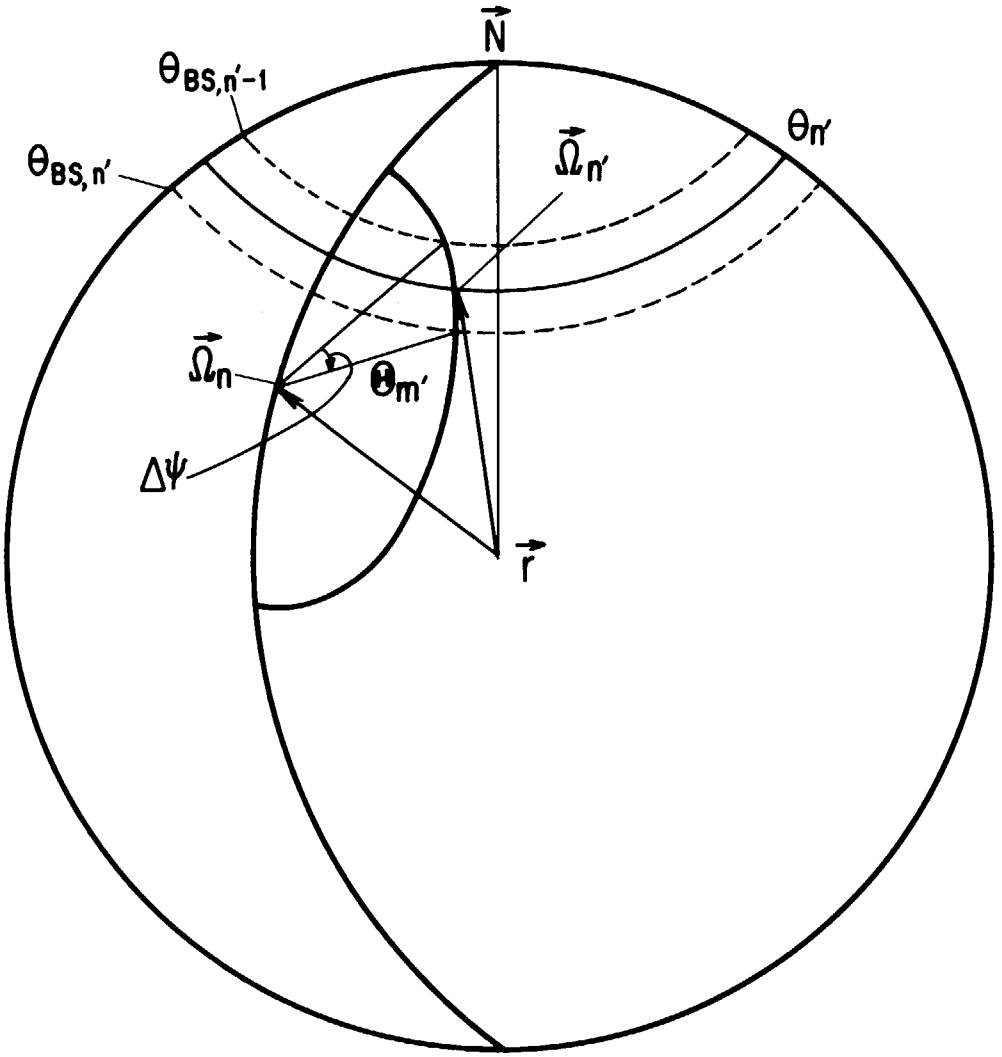

Fig. 3.2 Azimuthal angle extension ($\Delta\phi$) of scattering on the unit sphere

$$\sum_n \Delta\vec{\Omega}_n \Delta\psi_{n',nm'} / \Delta\vec{\Omega}_{n'} = 2\pi. \tag{3.21}$$

So, we obtain $\Delta\psi_{n',nm'}$ as

$$\Delta\psi_{n',nm'} = [2\pi\Delta\vec{\Omega}_{n'} / \sum_L \Delta\vec{\Omega}_L W^*_{n',Lm'}] W^*_{n',nm'} \tag{3.22}$$

We note that if W^* were strictly calculated as the average of not 5 but infinite number of ω_n points, the reciprocity relation,

$$\Delta\vec{\Omega}_n W^*_{n',nm'} = \Delta\vec{\Omega}_{n'} W^*_{nn',m'},$$

would hold, because $W^*_{n',nm'}$ is the quantity integrated over $\Delta\vec{\Omega}_{n'}$ but not over $\Delta\vec{\Omega}_n$.

3.4.2 Two-Dimensional Case

In the two-dimensional (r, z) cylindrical geometry, we fix r and z directions to the east and north poles of the unit sphere, respectively. Angular distribution of flux is symmetric with respect to the (r, z) plane, so that angular discrete ordinates $\vec{\Omega}_n$ are necessary to be distributed over the hemisphere (Figs. 3.3 and 3.4). The ordinates and their territorial boundaries are fixed as shown in Table 3.2 for S_8 case and in

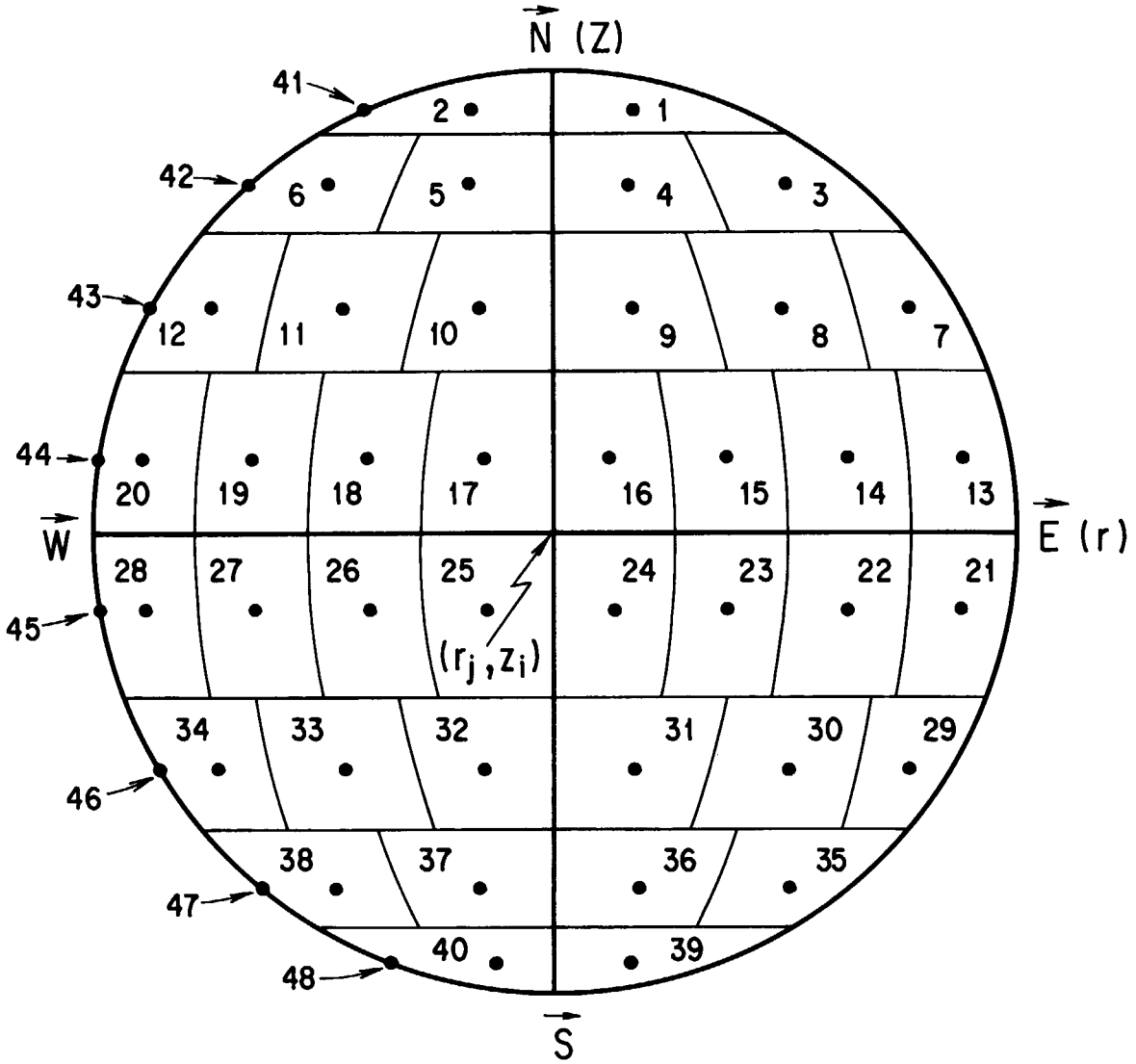

Fig. 3.3 S_8 angular ordinates (•) and their territories on the unit hemisphere in case of two-dimensional (r, z) geometry

Table 3.3 for S_{16} case.[8] There, the $W^*_{n',nm'}$ must be defined with both latitudes and longitudes for the boundary lines of $\Delta\vec{\Omega}_{n'}$ (Fig. 3.5).

For an example case of Fig. 3.5, $\Delta\vec{\Omega}_{n'}$ locates north-west of $\vec{\Omega}_n$, and the circle of radius $\Theta_{m'}$ cuts only the south-east part of $\Delta\vec{\Omega}_{n'}$. Then, $W^*_{n',nm'}$ is given as

$$W^*_{n',nm'} = \cos^{-1}[(b_2-\omega_n\xi_{m'})/D] - \cos^{-1}[(b_1-\omega_n\xi_{m'})/D],$$

where
$$b_1 = (\omega_n\xi_{m'} + c_1\sqrt{c_2-\xi_{m'}^2})/c_2,$$
$$c_1 = \sqrt{1-\omega_n^2}\cos(\varphi_n-\varphi_{BE,n'}),$$
$$c_2 = \omega_n^2 + c_1^2,$$
$$b_2 = \omega_{BS,n'} \text{ and}$$
$$D = \sqrt{1-\omega_n^2}\sqrt{1-\xi_{m'}^2}.$$

When the circle $\Theta_{m'}$ passes the back side of the unit sphere and crosses the $\Delta\vec{\Omega}_{\bar{n}}$ (just the symmetric domain to the $\Delta\vec{\Omega}_{n'}$ with respect to the (r, z) plane), the value $W^*_{\bar{n}',nm'}$ is added to $W^*_{n',nm'}$.

The $W^*_{n',nm'}$ is calculated as the average value of $W^*_{n',nm'}$ by 25 different $\vec{\Omega}_n$ points uniformly distributed in the domain of $\Delta\vec{\Omega}_n$ ($\Delta\omega_n$, $\Delta\varphi_n$). The $\Delta\phi_{n',nm'}$ is obtained as Eq. (3.22),

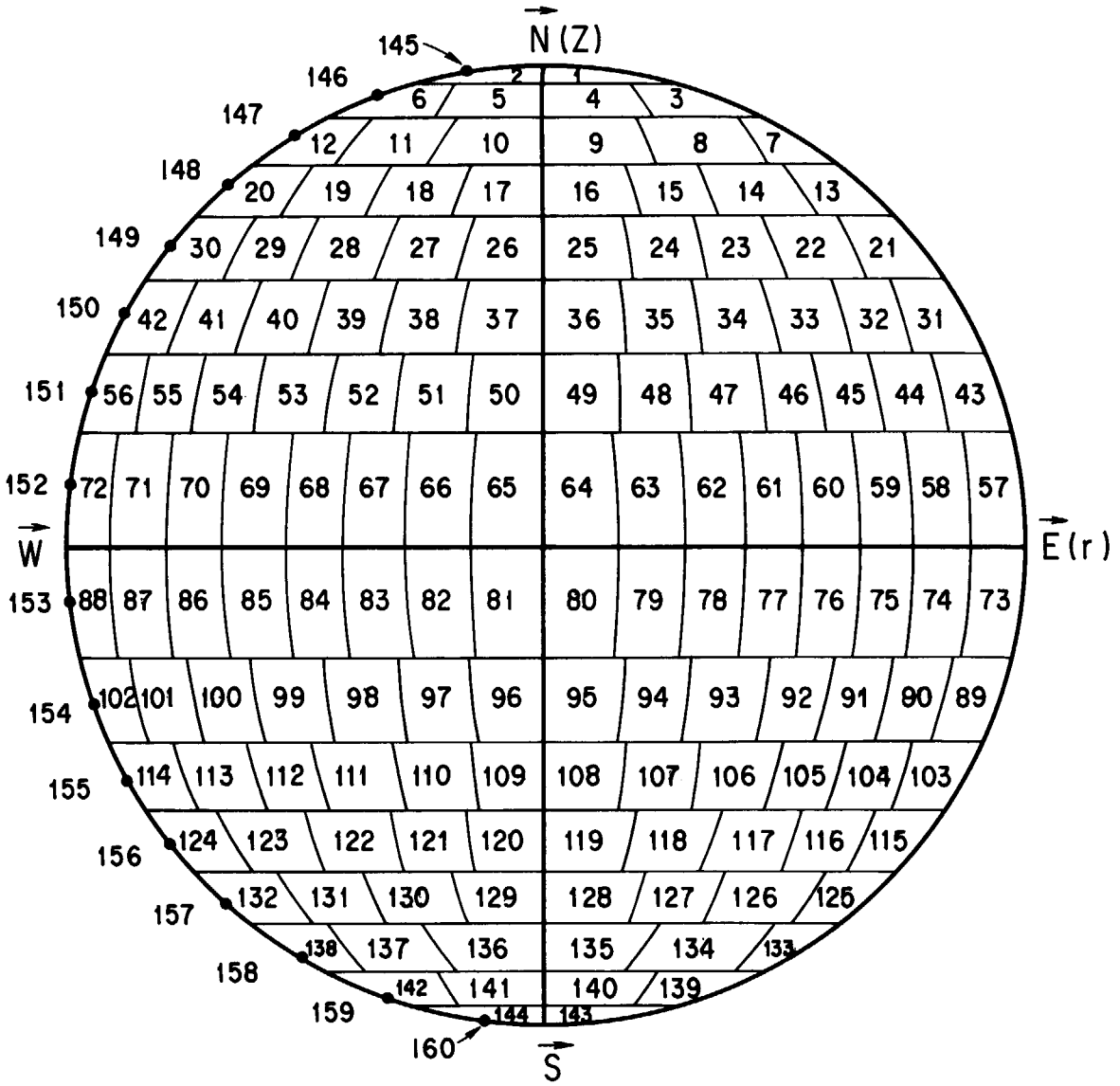

Fig. 3.4 S_{16} angular ordinates and their territories on the unit hemisphere in case of two-dimensional (r, z) geometry

Table 3.2 S_8 angular discrete ordinates and their boundaries in case of two-dimensional (r, z) geometry

N	POLAR ANG (COS)	(DEG)	AZIMU ANG	(DEG)	NORTH BND (COS)	(DEG)	SOUTH BND (COS)	(DEG)	EAST BOUND	(DEG)	WEST BOUND	(DEG)	WEIGHT
1	0.9511897	(17.98)	0.7853982	(45.00)	1.0000000	(0.0)	0.8790123	(28.48)	0.0	(0.0)	1.5707963	(90.00)	0.3800939
2	0.9511897	(17.98)	2.3561945	(135.00)	1.0000000	(0.0)	0.8790123	(28.48)	1.5707963	(90.00)	3.1415927	(180.00)	0.3800939
3	0.7867958	(38.11)	0.3613671	(20.70)	0.8790123	(28.48)	0.6975309	(45.77)	0.0	(0.0)	0.7853982	(45.00)	0.2850704
4	0.7867958	(38.11)	1.2094292	(69.30)	0.8790123	(28.48)	0.6975309	(45.77)	0.7853982	(45.00)	1.5707963	(90.00)	0.2850704
5	0.7867958	(38.11)	1.9321635	(110.70)	0.8790123	(28.48)	0.6975309	(45.77)	1.5707963	(90.00)	2.3561945	(135.00)	0.2850704
6	0.7867958	(38.11)	2.7802255	(159.30)	0.8790123	(28.48)	0.6975309	(45.77)	2.3561945	(135.00)	3.1415927	(180.00)	0.2850704
7	0.5773503	(54.74)	0.2705498	(15.50)	0.6975309	(45.77)	0.4234568	(64.95)	0.0	(0.0)	0.5200610	(29.80)	0.2850704
8	0.5773503	(54.74)	0.7853982	(45.00)	0.6975309	(45.77)	0.4234568	(64.95)	0.5200610	(29.80)	1.0507353	(60.20)	0.2908882
9	0.5773503	(54.74)	1.3002466	(74.50)	0.6975309	(45.77)	0.4234568	(64.95)	1.0507353	(60.20)	1.5707963	(90.00)	0.2850704
10	0.5773503	(54.74)	1.8413461	(105.50)	0.6975309	(45.77)	0.4234568	(64.95)	1.5707963	(90.00)	2.0908573	(119.80)	0.2850704
11	0.5773503	(54.74)	2.3561945	(135.00)	0.6975309	(45.77)	0.4234568	(64.95)	2.0908573	(119.80)	2.6215317	(150.20)	0.2908882
12	0.5773503	(54.74)	2.8710429	(164.50)	0.6975309	(45.77)	0.4234568	(64.95)	2.6215317	(150.20)	3.1415927	(180.00)	0.2850704
13	0.2182179	(77.40)	0.2255134	(12.92)	0.4234568	(64.95)	0.0	(90.00)	0.0	(0.0)	0.4487990	(25.71)	0.3800939
14	0.2182179	(77.40)	0.6330518	(36.27)	0.4234568	(64.95)	0.0	(90.00)	0.4487990	(25.71)	0.7853982	(45.00)	0.2850704
15	0.2182179	(77.40)	0.9377445	(53.73)	0.4234568	(64.95)	0.0	(90.00)	0.7853982	(45.00)	1.1219974	(64.29)	0.2850704
16	0.2182179	(77.40)	1.3452829	(77.08)	0.4234568	(64.95)	0.0	(90.00)	1.1219974	(64.29)	1.5707963	(90.00)	0.3800939
17	0.2182179	(77.40)	1.7963097	(102.92)	0.4234568	(64.95)	0.0	(90.00)	1.5707963	(90.00)	2.0195953	(115.71)	0.3800939
18	0.2182179	(77.40)	2.2038482	(126.27)	0.4234568	(64.95)	0.0	(90.00)	2.0195953	(115.71)	2.3561945	(135.00)	0.2850704
19	0.2182179	(77.40)	2.5085408	(143.73)	0.4234568	(64.95)	0.0	(90.00)	2.3561945	(135.00)	2.6927937	(154.29)	0.2850704
20	0.2182179	(77.40)	2.9160792	(167.08)	0.4234568	(64.95)	0.0	(90.00)	2.6927937	(154.29)	3.1415927	(180.00)	0.3800939
21	-0.2182179	(102.60)	0.2255134	(12.92)	0.0	(90.00)	-0.4234568	(115.05)	0.0	(0.0)	0.4487990	(25.71)	0.3800939
22	-0.2182179	(102.60)	0.6330518	(36.27)	0.0	(90.00)	-0.4234568	(115.05)	0.4487990	(25.71)	0.7853982	(45.00)	0.2850704
23	-0.2182179	(102.60)	0.9377445	(53.73)	0.0	(90.00)	-0.4234568	(115.05)	0.7853982	(45.00)	1.1219974	(64.29)	0.2850704
24	-0.2182179	(102.60)	1.3452829	(77.08)	0.0	(90.00)	-0.4234568	(115.05)	1.1219974	(64.29)	1.5707963	(90.00)	0.3800939
25	-0.2182179	(102.60)	1.7963097	(102.92)	0.0	(90.00)	-0.4234568	(115.05)	1.5707963	(90.00)	2.0195953	(115.71)	0.3800939
26	-0.2182179	(102.60)	2.2038482	(126.27)	0.0	(90.00)	-0.4234568	(115.05)	2.0195953	(115.71)	2.3561945	(135.00)	0.2850704
27	-0.2182179	(102.60)	2.5085408	(143.73)	0.0	(90.00)	-0.4234568	(115.05)	2.3561945	(135.00)	2.6927937	(154.29)	0.2850704
28	-0.2182179	(102.60)	2.9160792	(167.08)	0.0	(90.00)	-0.4234568	(115.05)	2.6927937	(154.29)	3.1415927	(180.00)	0.3800939
29	-0.5773503	(125.26)	0.2705498	(15.50)	-0.4234568	(115.05)	-0.6975309	(134.23)	0.0	(0.0)	0.5200610	(29.80)	0.2850704
30	-0.5773503	(125.26)	0.7853982	(45.00)	-0.4234568	(115.05)	-0.6975309	(134.23)	0.5200610	(29.80)	1.0507353	(60.20)	0.2908882
31	-0.5773503	(125.26)	1.3002466	(74.50)	-0.4234568	(115.05)	-0.6975309	(134.23)	1.0507353	(60.20)	1.5707963	(90.00)	0.2850704
32	-0.5773503	(125.26)	1.8413461	(105.50)	-0.4234568	(115.05)	-0.6975309	(134.23)	1.5707963	(90.00)	2.0908573	(119.80)	0.2850704
33	-0.5773503	(125.26)	2.3561945	(135.00)	-0.4234568	(115.05)	-0.6975309	(134.23)	2.0908573	(119.80)	2.6215317	(150.20)	0.2908882
34	-0.5773503	(125.26)	2.8710429	(164.50)	-0.4234568	(115.05)	-0.6975309	(134.23)	2.6215317	(150.20)	3.1415927	(180.00)	0.2850704
35	-0.7867958	(141.89)	0.3613671	(20.70)	-0.6975309	(134.23)	-0.8790123	(151.52)	0.0	(0.0)	0.7853982	(45.00)	0.2850704
36	-0.7867958	(141.89)	1.2094292	(69.30)	-0.6975309	(134.23)	-0.8790123	(151.52)	0.7853982	(45.00)	1.5707963	(90.00)	0.2850704
37	-0.7867958	(141.89)	1.9321635	(110.70)	-0.6975309	(134.23)	-0.8790123	(151.52)	1.5707963	(90.00)	2.3561945	(135.00)	0.2850704
38	-0.7867958	(141.89)	2.7802255	(159.30)	-0.6975309	(134.23)	-0.8790123	(151.52)	2.3561945	(135.00)	3.1415927	(180.00)	0.2850704
39	-0.9511897	(162.02)	0.7853982	(45.00)	-0.8790123	(151.52)	-1.0000000	(180.00)	0.0	(0.0)	1.5707963	(90.00)	0.3800939
40	-0.9511897	(162.02)	2.3561945	(135.00)	-0.8790123	(151.52)	-1.0000000	(180.00)	1.5707963	(90.00)	3.1415927	(180.00)	0.3800939
41	0.9511897	(17.98)	3.1415927	(180.00)									0.0
42	0.7867958	(38.11)	3.1415927	(180.00)									0.0
43	0.5773503	(54.74)	3.1415927	(180.00)									0.0
44	0.2182179	(77.40)	3.1415927	(180.00)									0.0
45	-0.2182179	(102.60)	3.1415927	(180.00)									0.0
46	-0.5773503	(125.26)	3.1415927	(180.00)									0.0
47	-0.7867958	(141.89)	3.1415927	(180.00)									0.0
48	-0.9511897	(162.02)	3.1415927	(180.00)									0.0

Table 3.3 S_{16} angular discrete ordinates and their boundaries in case of two-dimensional (r, z) geometry (1/4 quadrant only)

N	POLAR ANG (COS)	(DEG)	AZIMU ANG	(DEG)	NORTH BND (COS)	(DEG)	SOUTH BND (COS)	(DEG)	EAST BOUND	(DEG)	WEST BOUND	(DEG)	WEIGHT
1	0.9775252	(12.17)	0.7853982	(45.00)	1.0000000	(0.0)	0.9456541	(18.98)	0.0	(0.0)	1.5707963	(90.00)	0.1707326
3	0.9067647	(24.94)	0.3613671	(20.70)	0.9456541	(18.98)	0.8675089	(29.83)	0.0	(0.0)	0.7853982	(45.00)	0.1227502
4	0.9067647	(24.94)	1.2094292	(69.30)	0.9456541	(18.98)	0.8675089	(29.83)	0.7853982	(45.00)	1.5707963	(90.00)	0.1227502
7	0.8299933	(33.90)	0.2705498	(15.50)	0.8675089	(29.83)	0.7955626	(37.29)	0.0	(0.0)	0.5653644	(32.39)	0.0813517
8	0.8299933	(33.90)	0.7853982	(45.00)	0.8675089	(29.83)	0.7955626	(37.29)	0.5653644	(32.39)	1.0054319	(57.61)	0.0633224
9	0.8299933	(33.90)	1.3002466	(74.50)	0.8675089	(29.83)	0.7955626	(37.29)	1.0054319	(57.61)	1.5707963	(90.00)	0.0813517
13	0.7453560	(41.81)	0.2255134	(12.92)	0.7955626	(37.29)	0.6869559	(46.61)	0.0	(0.0)	0.3739277	(21.42)	0.0812221
14	0.7453560	(41.81)	0.6330518	(36.27)	0.7955626	(37.29)	0.6869559	(46.61)	0.3739277	(21.42)	0.7853982	(45.00)	0.0893769
15	0.7453560	(41.81)	0.9377445	(53.73)	0.7955626	(37.29)	0.6869559	(46.61)	0.7853982	(45.00)	1.1968686	(68.58)	0.0893769
16	0.7453560	(41.81)	1.3452829	(77.08)	0.7955626	(37.29)	0.6869559	(46.61)	1.1968686	(68.58)	1.5707963	(90.00)	0.0812221
21	0.6497863	(49.47)	0.1973956	(11.31)	0.6869559	(46.61)	0.6092065	(52.47)	0.0	(0.0)	0.5223326	(29.93)	0.0812221
22	0.6497863	(49.47)	0.5455338	(31.26)	0.6869559	(46.61)	0.6092065	(52.47)	0.5223326	(29.93)	0.6385535	(36.59)	0.0180722
23	0.6497863	(49.47)	0.7853982	(45.00)	0.6869559	(46.61)	0.6092065	(52.47)	0.6385535	(36.59)	0.9322428	(53.41)	0.0456683
24	0.6497863	(49.47)	1.0252625	(58.74)	0.6869559	(46.61)	0.6092065	(52.47)	0.9322428	(53.41)	1.0484637	(60.07)	0.0180722
25	0.6497863	(49.47)	1.3734008	(78.69)	0.6869559	(46.61)	0.6092065	(52.47)	1.0484637	(60.07)	1.5707963	(90.00)	0.0812221
31	0.5374838	(57.49)	0.1777106	(10.18)	0.6092065	(52.47)	0.4714439	(61.87)	0.0	(0.0)	0.2952606	(16.92)	0.0813517
32	0.5374838	(57.49)	0.4866950	(27.89)	0.6092065	(52.47)	0.4714439	(61.87)	0.2952606	(16.92)	0.6196480	(35.50)	0.0893769
33	0.5374838	(57.49)	0.6910900	(39.60)	0.6092065	(52.47)	0.4714439	(61.87)	0.6196480	(35.50)	0.7853982	(45.00)	0.0456683
34	0.5374838	(57.49)	0.8797064	(50.40)	0.6092065	(52.47)	0.4714439	(61.87)	0.7853982	(45.00)	0.9511483	(54.50)	0.0456683
35	0.5374838	(57.49)	1.0841014	(62.11)	0.6092065	(52.47)	0.4714439	(61.87)	0.9511483	(54.50)	1.2755358	(73.08)	0.0893769
36	0.5374838	(57.49)	1.3930857	(79.82)	0.6092065	(52.47)	0.4714439	(61.87)	1.2755358	(73.08)	1.5707963	(90.00)	0.0813517
43	0.3944053	(66.77)	0.1629415	(9.34)	0.4714439	(61.87)	0.2903347	(73.12)	0.0	(0.0)	0.3388846	(19.42)	0.1227502
44	0.3944053	(66.77)	0.4436041	(25.42)	0.4714439	(61.87)	0.2903347	(73.12)	0.3388846	(19.42)	0.5137029	(29.43)	0.0633224
45	0.3944053	(66.77)	0.6247539	(35.80)	0.4714439	(61.87)	0.2903347	(73.12)	0.5137029	(29.43)	0.7604516	(43.57)	0.0893769
46	0.3944053	(66.77)	0.7853982	(45.00)	0.4714439	(61.87)	0.2903347	(73.12)	0.7604516	(43.57)	0.8103447	(46.43)	0.0180722
47	0.3944053	(66.77)	0.9460425	(54.20)	0.4714439	(61.87)	0.2903347	(73.12)	0.8103447	(46.43)	1.0570934	(60.57)	0.0893769
48	0.3944053	(66.77)	1.1271922	(64.58)	0.4714439	(61.87)	0.2903347	(73.12)	1.0570934	(60.57)	1.2319118	(70.58)	0.0633224
49	0.3944053	(66.77)	1.4078548	(80.66)	0.4714439	(61.87)	0.2903347	(73.12)	1.2319118	(70.58)	1.5707963	(90.00)	0.1227502
57	0.1490712	(81.43)	0.1513326	(8.67)	0.2903347	(73.12)	0.0	(90.00)	0.0	(0.0)	0.2940272	(16.85)	0.1707326
58	0.1490712	(81.43)	0.4102755	(23.51)	0.2903347	(73.12)	0.0	(90.00)	0.2940272	(16.85)	0.5054216	(28.96)	0.1227502
59	0.1490712	(81.43)	0.5746694	(32.93)	0.2903347	(73.12)	0.0	(90.00)	0.5054216	(28.96)	0.6455214	(36.99)	0.0813517
60	0.1490712	(81.43)	0.7170033	(41.08)	0.2903347	(73.12)	0.0	(90.00)	0.6455214	(36.99)	0.7853982	(45.00)	0.0812221
61	0.1490712	(81.43)	0.8537931	(48.92)	0.2903347	(73.12)	0.0	(90.00)	0.7853982	(45.00)	0.9252749	(53.01)	0.0812221
62	0.1490712	(81.43)	0.9961269	(57.07)	0.2903347	(73.12)	0.0	(90.00)	0.9252749	(53.01)	1.0653748	(61.04)	0.0813517
63	0.1490712	(81.43)	1.1605208	(66.49)	0.2903347	(73.12)	0.0	(90.00)	1.0653748	(61.04)	1.2767691	(73.15)	0.1227502
64	0.1490712	(81.43)	1.4194637	(81.33)	0.2903347	(73.12)	0.0	(90.00)	1.2767691	(73.15)	1.5707963	(90.00)	0.1707326
145	0.9775252	(12.17)	3.1415927	(180.00)									0.0
146	0.9067647	(24.94)	3.1415927	(180.00)									0.0
147	0.8299933	(33.90)	3.1415927	(180.00)									0.0
148	0.7453560	(41.81)	3.1415927	(180.00)									0.0
149	0.6497863	(49.47)	3.1415927	(180.00)									0.0
150	0.5374838	(57.49)	3.1415927	(180.00)									0.0
151	0.3944053	(66.77)	3.1415927	(180.00)									0.0
152	0.1490712	(81.43)	3.1415927	(180.00)									0.0

$$\Delta\psi_{n'nm'} = [2\pi\Delta\vec{\Omega}_{n'}/\sum_{L}\Delta\vec{\Omega}_{L}W^{*}_{n'Lm'}]\,W^{*}_{n'nm'}$$

3.4.3 Three-Dimensional Case

In the three-dimensional (x, y, z) geometry, we fix x, y and z directions to the front, east and north poles of the unit sphere, respectively. In this case, there exists no symmetry plane in the unit sphere and the discrete ordinates are distributed over the whole 4π area (Fig. 3.6 and Table 3.4). The points on the westmost longitude having no weights in the case of two-dimension are not necessary in this case, because interpolation of flux ϕ (x_{p-1}) with respect to φ is not necessary.

Difference from Sec. 3.4.2 is only that the contribution to $W^{*}_{n'nm'}$ from $\Delta\vec{\Omega}_{n'}$ on the back side of the unit sphere is accounted independently. Each of n', n and m' amounts to 80. The number of 80 discrete ordinates for each of (x, y, z) mesh points are too much for computers available now. The S_8 approximation is sufficient for penetration analyses, but is absolutely insufficient for streaming analyses. So, a three-dimensional calculation is now very difficult. However, we dare have constructed the source program as a base to adapt itself immediately to a computer of the next generation.

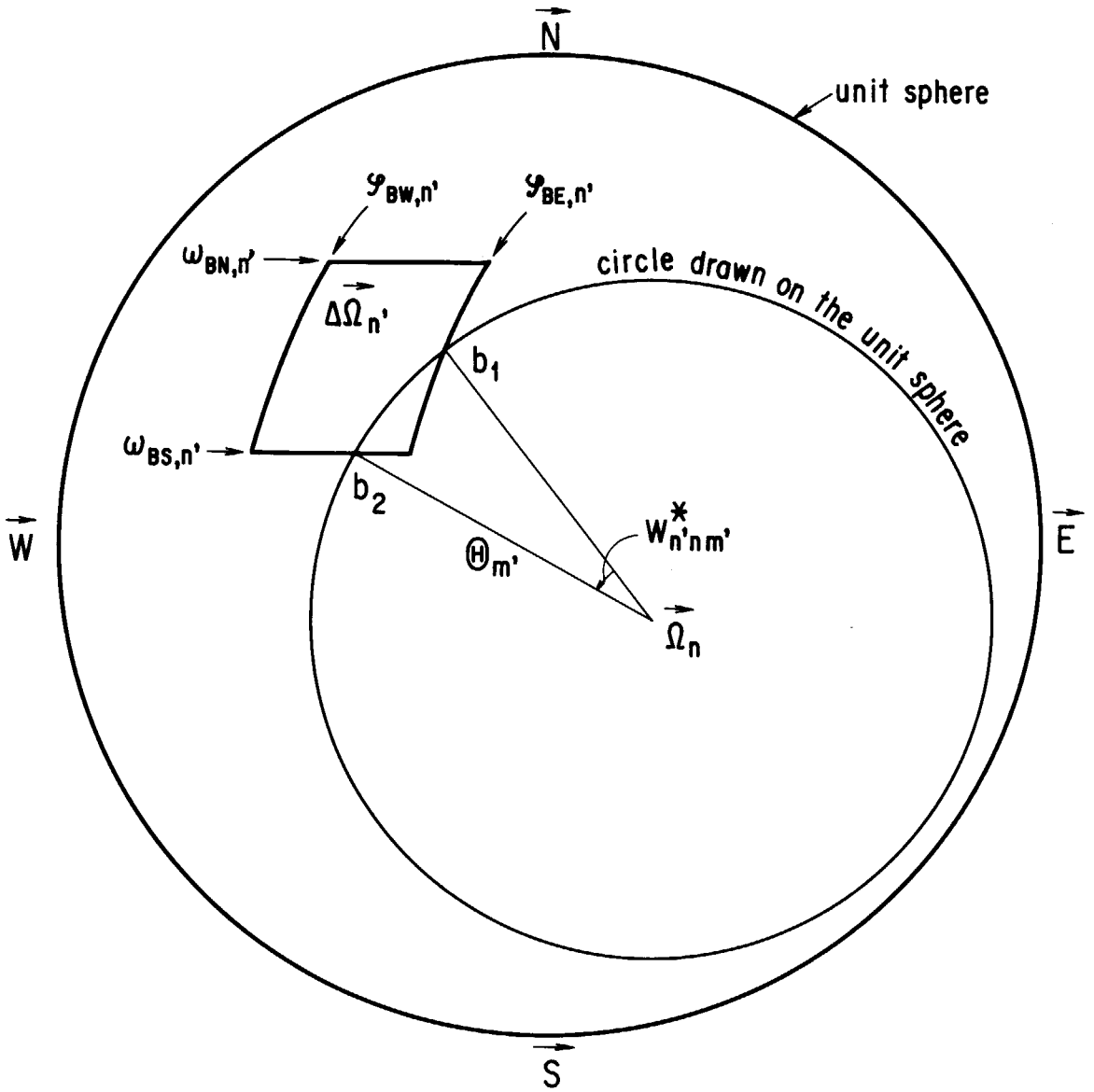

Fig. 3.5 Definition of $W^{*}_{n'nm'}$

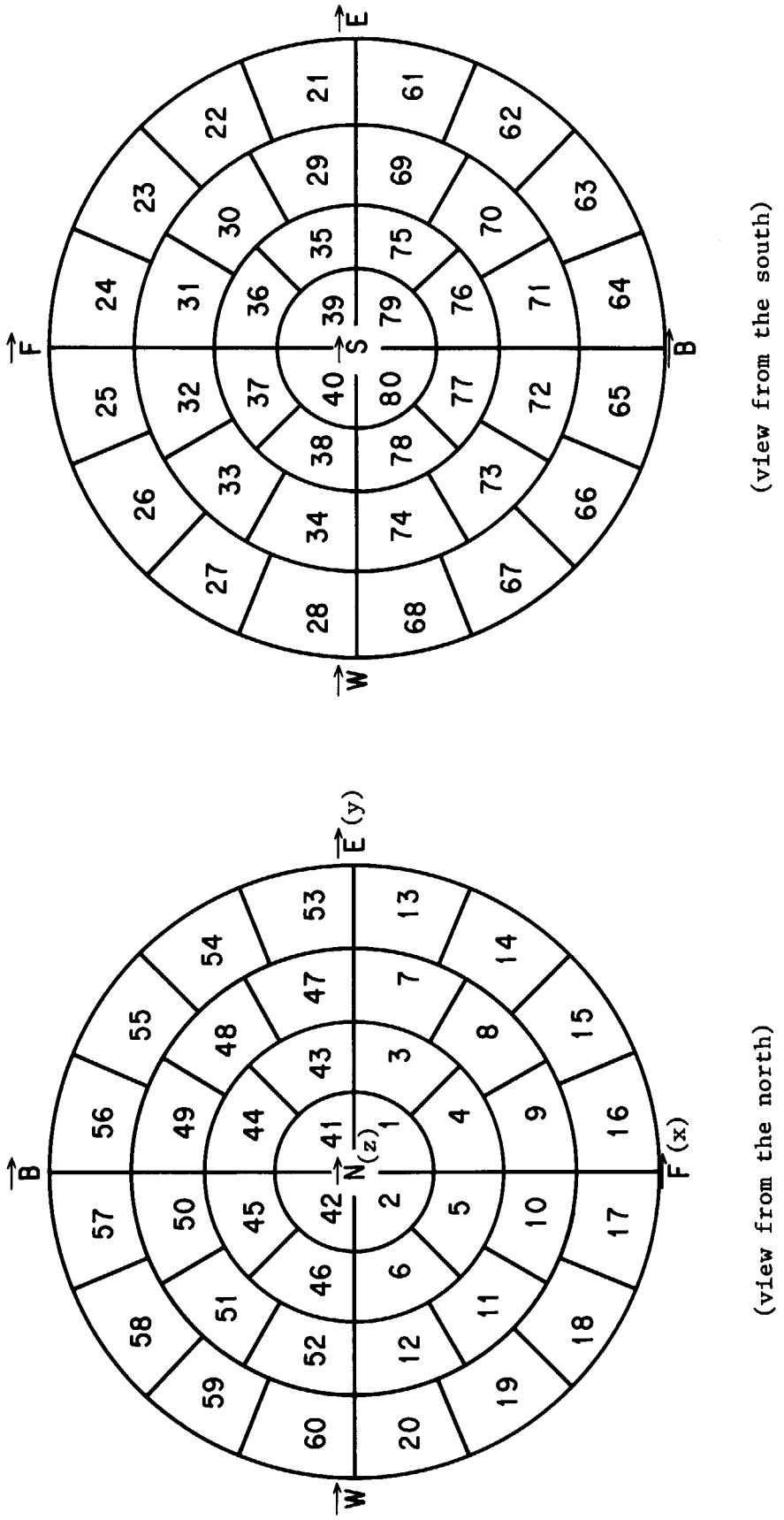

Fig. 3.6 S_8 angular ordinates and their territories on the unit sphere in case of three-dimensional (x, y, z) geometry

Table 3.4 S_8 angular discrete ordinates and their boundaries in case of three-dimensional (x, y, z) geometry

N	POLAR ANG (COS)	(DEG)	AZIMU ANG	(DEG)	NORTH BND (COS)	(DEG)	SOUTH BND (COS)	(DEG)	EAST BOUND	(DEG)	WEST BOUND	(DEG)	WEIGHT (4*PI)
1	0.9511897	(17.98)	0.7853982	(45.00)	1.0000000	(0.0)	0.8790123	(28.48)	0.0	(0.0)	1.5707963	(90.00)	0.1900470
2	0.9511897	(17.98)	2.3561945	(135.00)	1.0000000	(0.0)	0.8790123	(28.48)	1.5707963	(90.00)	3.1415927	(180.00)	0.1900470
3	0.7867958	(38.11)	0.3613671	(20.70)	0.8790123	(28.48)	0.6975309	(45.77)	0.0	(0.0)	0.7853982	(45.00)	0.1425352
4	0.7867958	(38.11)	1.2094292	(69.30)	0.8790123	(28.48)	0.6975309	(45.77)	0.7853982	(45.00)	1.5707963	(90.00)	0.1425352
5	0.7867958	(38.11)	1.9321635	(110.70)	0.8790123	(28.48)	0.6975309	(45.77)	1.5707963	(90.00)	2.3561945	(135.00)	0.1425352
6	0.7867958	(38.11)	2.7802255	(159.30)	0.8790123	(28.48)	0.6975309	(45.77)	2.3561945	(135.00)	3.1415927	(180.00)	0.1425352
7	0.5773503	(54.74)	0.2705498	(15.50)	0.6975309	(45.77)	0.4234568	(64.95)	0.0	(0.0)	0.5200610	(29.80)	0.1425352
8	0.5773503	(54.74)	0.7853982	(45.00)	0.6975309	(45.77)	0.4234568	(64.95)	0.5200610	(29.80)	1.0507353	(60.20)	0.1454441
9	0.5773503	(54.74)	1.3002466	(74.50)	0.6975309	(45.77)	0.4234568	(64.95)	1.0507353	(60.20)	1.5707963	(90.00)	0.1425352
10	0.5773503	(54.74)	1.8413461	(105.50)	0.6975309	(45.77)	0.4234568	(64.95)	1.5707963	(90.00)	2.0908573	(119.80)	0.1425352
11	0.5773503	(54.74)	2.3561945	(135.00)	0.6975309	(45.77)	0.4234568	(64.95)	2.0908573	(119.80)	2.6215317	(150.20)	0.1454441
12	0.5773503	(54.74)	2.8710429	(164.50)	0.6975309	(45.77)	0.4234568	(64.95)	2.6215317	(150.20)	3.1415927	(180.00)	0.1425352
13	0.2182179	(77.40)	0.2255134	(12.92)	0.4234568	(64.95)	0.0	(90.00)	0.0	(0.0)	0.4487990	(25.71)	0.1900470
14	0.2182179	(77.40)	0.6330518	(36.27)	0.4234568	(64.95)	0.0	(90.00)	0.4487990	(25.71)	0.7853982	(45.00)	0.1425352
15	0.2182179	(77.40)	0.9377445	(53.73)	0.4234568	(64.95)	0.0	(90.00)	0.7853982	(45.00)	1.1219974	(64.29)	0.1425352
16	0.2182179	(77.40)	1.3452829	(77.08)	0.4234568	(64.95)	0.0	(90.00)	1.1219974	(64.29)	1.5707963	(90.00)	0.1900470
17	0.2182179	(77.40)	1.7963097	(102.92)	0.4234568	(64.95)	0.0	(90.00)	1.5707963	(90.00)	2.0195953	(115.71)	0.1900470
18	0.2182179	(77.40)	2.2038482	(126.27)	0.4234568	(64.95)	0.0	(90.00)	2.0195953	(115.71)	2.3561945	(135.00)	0.1425352
19	0.2182179	(77.40)	2.5085408	(143.73)	0.4234568	(64.95)	0.0	(90.00)	2.3561945	(135.00)	2.6927937	(154.29)	0.1425352
20	0.2182179	(77.40)	2.9160792	(167.08)	0.4234568	(64.95)	0.0	(90.00)	2.6927937	(154.29)	3.1415927	(180.00)	0.1900470
21	-0.2182179	(102.60)	0.2255134	(12.92)	0.0	(90.00)	-0.4234568	(115.05)	0.0	(0.0)	0.4487990	(25.71)	0.1900470
22	-0.2182179	(102.60)	0.6330518	(36.27)	0.0	(90.00)	-0.4234568	(115.05)	0.4487990	(25.71)	0.7853982	(45.00)	0.1425352
23	-0.2182179	(102.60)	0.9377445	(53.73)	0.0	(90.00)	-0.4234568	(115.05)	0.7853982	(45.00)	1.1219974	(64.29)	0.1425352
24	-0.2182179	(102.60)	1.3452829	(77.08)	0.0	(90.00)	-0.4234568	(115.05)	1.1219974	(64.29)	1.5707963	(90.00)	0.1900470
25	-0.2182179	(102.60)	1.7963097	(102.92)	0.0	(90.00)	-0.4234568	(115.05)	1.5707963	(90.00)	2.0195953	(115.71)	0.1900470
26	-0.2182179	(102.60)	2.2038482	(126.27)	0.0	(90.00)	-0.4234568	(115.05)	2.0195953	(115.71)	2.3561945	(135.00)	0.1425352
27	-0.2182179	(102.60)	2.5085408	(143.73)	0.0	(90.00)	-0.4234568	(115.05)	2.3561945	(135.00)	2.6927937	(154.29)	0.1425352
28	-0.2182179	(102.60)	2.9160792	(167.08)	0.0	(90.00)	-0.4234568	(115.05)	2.6927937	(154.29)	3.1415927	(180.00)	0.1900470
29	-0.5773503	(125.26)	0.2705498	(15.50)	-0.4234568	(115.05)	-0.6975309	(134.23)	0.0	(0.0)	0.5200610	(29.80)	0.1425352
30	-0.5773503	(125.26)	0.7853982	(45.00)	-0.4234568	(115.05)	-0.6975309	(134.23)	0.5200610	(29.80)	1.0507353	(60.20)	0.1454441
31	-0.5773503	(125.26)	1.3002466	(74.50)	-0.4234568	(115.05)	-0.6975309	(134.23)	1.0507353	(60.20)	1.5707963	(90.00)	0.1425352
32	-0.5773503	(125.26)	1.8413461	(105.50)	-0.4234568	(115.05)	-0.6975309	(134.23)	1.5707963	(90.00)	2.0908573	(119.80)	0.1425352
33	-0.5773503	(125.26)	2.3561945	(135.00)	-0.4234568	(115.05)	-0.6975309	(134.23)	2.0908573	(119.80)	2.6215317	(150.20)	0.1454441
34	-0.5773503	(125.26)	2.8710429	(164.50)	-0.4234568	(115.05)	-0.6975309	(134.23)	2.6215317	(150.20)	3.1415927	(180.00)	0.1425352
35	-0.7867958	(141.89)	0.3613671	(20.70)	-0.6975309	(134.23)	-0.8790123	(151.52)	0.0	(0.0)	0.7853982	(45.00)	0.1425352
36	-0.7867958	(141.89)	1.2094292	(69.30)	-0.6975309	(134.23)	-0.8790123	(151.52)	0.7853982	(45.00)	1.5707963	(90.00)	0.1425352
37	-0.7867958	(141.89)	1.9321635	(110.70)	-0.6975309	(134.23)	-0.8790123	(151.52)	1.5707963	(90.00)	2.3561945	(135.00)	0.1425352
38	-0.7867958	(141.89)	2.7802255	(159.30)	-0.6975309	(134.23)	-0.8790123	(151.52)	2.3561945	(135.00)	3.1415927	(180.00)	0.1425352
39	-0.9511897	(162.02)	0.7853982	(45.00)	-0.8790123	(151.52)	-1.0000000	(180.00)	0.0	(0.0)	1.5707963	(90.00)	0.1900470
40	-0.9511897	(162.02)	2.3561945	(135.00)	-0.8790123	(151.52)	-1.0000000	(180.00)	1.5707963	(90.00)	3.1415927	(180.00)	0.1900470

Table 3.4 S_8 angular discrete ordinates and their boundaries in case of three-dimensional (x, y, z) geometry (cotinued)

N	POLAR ANG (COS)	(DEG)	AZIMU ANG	(DEG)	NORTH BND (COS)	(DEG)	SOUTH BND (COS)	(DEG)	EAST BOUND	(DEG)	WEST BOUND	(DEG)	WEIGHT (4*PI)
41	0.9511897	(17.98)	-0.7853982	(-45.00)	1.0000000	(0.0)	0.8790123	(28.48)	0.0	(0.0)	-1.5707963	(-90.00)	0.1900470
42	0.9511897	(17.98)	-2.3561945	(-135.00)	1.0000000	(0.0)	0.8790123	(28.48)	-1.5707963	(-90.00)	-3.1415927	(-180.00)	0.1900470
43	0.7867958	(38.11)	-0.3613671	(-20.70)	0.8790123	(28.48)	0.6975309	(45.77)	0.0	(0.0)	-0.7853982	(-45.00)	0.1425352
44	0.7867958	(38.11)	-1.2094292	(-69.30)	0.8790123	(28.48)	0.6975309	(45.77)	-0.7853982	(-45.00)	-1.5707963	(-90.00)	0.1425352
45	0.7867958	(38.11)	-1.9321635	(-110.70)	0.8790123	(28.48)	0.6975309	(45.77)	-1.5707963	(-90.00)	-2.3561945	(-135.00)	0.1425352
46	0.7867958	(38.11)	-2.7802255	(-159.30)	0.8790123	(28.48)	0.6975309	(45.77)	-2.3561945	(-135.00)	-3.1415927	(-180.00)	0.1425352
47	0.5773503	(54.74)	-0.2705498	(-15.50)	0.6975309	(45.77)	0.4234568	(64.95)	0.0	(0.0)	-0.5200610	(-29.80)	0.1425352
48	0.5773503	(54.74)	-0.7853982	(-45.00)	0.6975309	(45.77)	0.4234568	(64.95)	-0.5200610	(-29.80)	-1.0507353	(-60.20)	0.1454441
49	0.5773503	(54.74)	-1.3002466	(-74.50)	0.6975309	(45.77)	0.4234568	(64.95)	-1.0507353	(-60.20)	-1.5707963	(-90.00)	0.1425352
50	0.5773503	(54.74)	-1.8413461	(-105.50)	0.6975309	(45.77)	0.4234568	(64.95)	-1.5707963	(-90.00)	-2.0908573	(-119.80)	0.1425352
51	0.5773503	(54.74)	-2.3561945	(-135.00)	0.6975309	(45.77)	0.4234568	(64.95)	-2.0908573	(-119.80)	-2.6215317	(-150.20)	0.1454441
52	0.5773503	(54.74)	-2.8710429	(-164.50)	0.6975309	(45.77)	0.4234568	(64.95)	-2.6215317	(-150.20)	-3.1415927	(-180.00)	0.1425352
53	0.2182179	(77.40)	-0.2255134	(-12.92)	0.4234568	(64.95)	0.0	(90.00)	0.0	(0.0)	-0.4487990	(-25.71)	0.1900470
54	0.2182179	(77.40)	-0.6330518	(-36.27)	0.4234568	(64.95)	0.0	(90.00)	-0.4487990	(-25.71)	-0.7853982	(-45.00)	0.1425352
55	0.2182179	(77.40)	-0.9377445	(-53.73)	0.4234568	(64.95)	0.0	(90.00)	-0.7853982	(-45.00)	-1.1219974	(-64.29)	0.1425352
56	0.2182179	(77.40)	-1.3452829	(-77.08)	0.4234568	(64.95)	0.0	(90.00)	-1.1219974	(-64.29)	-1.5707963	(-90.00)	0.1900470
57	0.2182179	(77.40)	-1.7963097	(-102.92)	0.4234568	(64.95)	0.0	(90.00)	-1.5707963	(-90.00)	-2.0195953	(-115.71)	0.1900470
58	0.2182179	(77.40)	-2.2038482	(-126.27)	0.4234568	(64.95)	0.0	(90.00)	-2.0195953	(-115.71)	-2.3561945	(-135.00)	0.1425352
59	0.2182179	(77.40)	-2.5085408	(-143.73)	0.4234568	(64.95)	0.0	(90.00)	-2.3561945	(-135.00)	-2.6927937	(-154.29)	0.1425352
60	0.2182179	(77.40)	-2.9160792	(-167.08)	0.4234568	(64.95)	0.0	(90.00)	-2.6927937	(-154.29)	-3.1415927	(-180.00)	0.1900470
61	-0.2182179	(102.60)	-0.2255134	(-12.92)	0.0	(90.00)	-0.4234568	(115.05)	0.0	(0.0)	-0.4487990	(-25.71)	0.1900470
62	-0.2182179	(102.60)	-0.6330518	(-36.27)	0.0	(90.00)	-0.4234568	(115.05)	-0.4487990	(-25.71)	-0.7853982	(-45.00)	0.1425352
63	-0.2182179	(102.60)	-0.9377445	(-53.73)	0.0	(90.00)	-0.4234568	(115.05)	-0.7853982	(-45.00)	-1.1219974	(-64.29)	0.1425352
64	-0.2182179	(102.60)	-1.3452829	(-77.08)	0.0	(90.00)	-0.4234568	(115.05)	-1.1219974	(-64.29)	-1.5707963	(-90.00)	0.1900470
65	-0.2182179	(102.60)	-1.7963097	(-102.92)	0.0	(90.00)	-0.4234568	(115.05)	-1.5707963	(-90.00)	-2.0195953	(-115.71)	0.1900470
66	-0.2182179	(102.60)	-2.2038482	(-126.27)	0.0	(90.00)	-0.4234568	(115.05)	-2.0195953	(-115.71)	-2.3561945	(-135.00)	0.1425352
67	-0.2182179	(102.60)	-2.5085408	(-143.73)	0.0	(90.00)	-0.4234568	(115.05)	-2.3561945	(-135.00)	-2.6927937	(-154.29)	0.1425352
68	-0.2182179	(102.60)	-2.9160792	(-167.08)	0.0	(90.00)	-0.4234568	(115.05)	-2.6927937	(-154.29)	-3.1415927	(-180.00)	0.1900470
69	-0.5773503	(125.26)	-0.2705498	(-15.50)	-0.4234568	(115.05)	-0.6975309	(134.23)	0.0	(0.0)	-0.5200610	(-29.80)	0.1425352
70	-0.5773503	(125.26)	-0.7853982	(-45.00)	-0.4234568	(115.05)	-0.6975309	(134.23)	-0.5200610	(-29.80)	-1.0507353	(-60.20)	0.1454441
71	-0.5773503	(125.26)	-1.3002466	(-74.50)	-0.4234568	(115.05)	-0.6975309	(134.23)	-1.0507353	(-60.20)	-1.5707963	(-90.00)	0.1425352
72	-0.5773503	(125.26)	-1.8413461	(-105.50)	-0.4234568	(115.05)	-0.6975309	(134.23)	-1.5707963	(-90.00)	-2.0908573	(-119.80)	0.1425352
73	-0.5773503	(125.26)	-2.3561945	(-135.00)	-0.4234568	(115.05)	-0.6975309	(134.23)	-2.0908573	(-119.80)	-2.6215317	(-150.20)	0.1454441
74	-0.5773503	(125.26)	-2.8710429	(-164.50)	-0.4234568	(115.05)	-0.6975309	(134.23)	-2.6215317	(-150.20)	-3.1415927	(-180.00)	0.1425352
75	-0.7867958	(141.89)	-0.3613671	(-20.70)	-0.6975309	(134.23)	-0.8790123	(151.52)	0.0	(0.0)	-0.7853982	(-45.00)	0.1425352
76	-0.7867958	(141.89)	-1.2094292	(-69.30)	-0.6975309	(134.23)	-0.8790123	(151.52)	-0.7853982	(-45.00)	-1.5707963	(-90.00)	0.1425352
77	-0.7867958	(141.89)	-1.9321635	(-110.70)	-0.6975309	(134.23)	-0.8790123	(151.52)	-1.5707963	(-90.00)	-2.3561945	(-135.00)	0.1425352
78	-0.7867958	(141.89)	-2.7802255	(-159.30)	-0.6975309	(134.23)	-0.8790123	(151.52)	-2.3561945	(-135.00)	-3.1415927	(-180.00)	0.1425352
79	-0.9511897	(162.02)	-0.7853982	(-45.00)	-0.8790123	(151.52)	-1.0000000	(180.00)	0.0	(0.0)	-1.5707963	(-90.00)	0.1900470
80	-0.9511897	(162.02)	-2.3561945	(-135.00)	-0.8790123	(151.52)	-1.0000000	(180.00)	-1.5707963	(-90.00)	-3.1415927	(-180.00)	0.1900470

3.5 Uncollided Flux from Point Source and First Collision Source

In the present version of BERMUDA, a fixed independent source can be given as a point source or a distributed source. The point source can be given only for the following three cases:

(1) Center of a sphere (one–dimensional),
(2) One mesh point on axis of a cylinder (two–dimensional) and
(3) One mesh point on y–axis (0, y, 0) of a rectangular parallelpiped (three–dimensional).

The uncollided flux is analytically obtained in the point kernel model. For simplicity, let us assume that the source point is located on the origin of the coordinates and the source S_0^i is isotropic. Then we have

$$\Phi_0{}^i(\vec{r}) = [S_0^i/4\pi|\vec{r}|^2] exp\{-\lambda^i(0, \vec{r})\},$$

where $\lambda^i(0, \vec{r})$ is the optical distance between the origin and $\vec{r}$: the linear integral of the i–th group macroscopic total cross section $\Sigma_t^i(\vec{r'})$, over the straight line from the origin to the mesh point $\vec{r}$. Dimension of Φ_0^i is that of a scalar flux, so that a factor $1/\Delta\vec{\Omega}_n$ (n is determined by the direction $\vec{r}$ from the origin) is necessary to be multiplied to the $\Phi_0^i(\vec{r})$ in order to obtain $\phi_0^i(\vec{r}, \vec{\Omega}_n)$ having the same dimension of an angular flux $\phi^i(\vec{r}, \vec{\Omega}_n)$. However, this $\phi_0^i(\vec{r}, \vec{\Omega}_n)$ is directed approximately to $\vec{\Omega}_n$.

Only in the three–dimensional case, this approximated uncollided flux ϕ_0^i is used to obtain the first collision source (FCS) distribution as the product of ϕ_0^i and the group–angle transfer matrices $K^{i\to j,\, n\to n'}$ prepared in Sec. 3.3 (here K contains also the isotropic component from the term of $\Sigma_{iso}{}^{i\to j}$). We use this approximate FCS because the kernel K_0 as in the next paragraph is difficult to be calculated in the three–dimensional case.

In the one– and two–dimensional cases, the uncollided scalar flux Φ_0^i is used, which is defined only on the north pole of the unit sphere for one–dimensional sphere case, and on the eastmost longitude for two–dimensional cylinder case (either S_8 or S_{16}). In these cases, another set of group–angle transfer matrices $K_0^{i\to j,\, n_0\to n}$ is separately prepared to account accurately the direction of the uncollided flux. Forty points of $\vec{\Omega}_{n_0}$ are uniformly distributed on the eastmost longitude as $\theta_{n_0} = (\pi/40)(n_0 - 1/2)$, $\varphi_{n_0} = 0$ for matrices K_0 of the two–dimensional case. The K_0 for $n_0 = 21, \cdots, 40$ are used when the point source is located not on the origin but on a point (0, z) where $z > 0$. The 40 points are considered to be sufficient to account accurately the direction of Φ_0 because they are equivalent to S_{40} approximation and φ_{n_0} is just 0.

The first collision source (FCS) distribution thus obtained is used in place of the independent volume source in Eq. (3.2), so that the ray–effect is remarkably mitigated. In this case, the flux as the solution of Eq. (3.1) is obtained without the uncollided component, which is usually added to the scalar flux (one– or two–dimensional) or to the angular flux (three–dimensional) of the solution.

3.6 Iteration and Energy Grid Model

3.6.1 Iteration Procedure

Now it is possible to calculate the source term for group i in Eq. (3.2). The isotropic scattering matrices

$$K_{iso}{}^{j\to i,\, n'\to n}(\vec{r}) = [\Delta\vec{\Omega}_{n'}/4\pi]\Sigma_{iso}{}^{j\to i}(\vec{r})$$

can be contained into the group–angle matrices $K^{j\to i,\, n'\to n}$ by adding them to $K_{aniso}{}^{j\to i, n'\to n}$,

$$K^{j\to i,\, n'\to n}(\vec{r}) = K_{aniso}{}^{j\to i,\, n'\to n}(\vec{r}) + K_{iso}{}^{j\to i,\, n'\to n}(\vec{r}).$$

So, the fixed component of the i–th group source (SD^i) is obtained as the sum of slowing down source from upper groups and first collision source FCS^i or input distributed source. In the source term, the self–group scattering of $\phi^i(\vec{r}, \vec{\Omega}_n)$ is excluded.

(1) Case of a point source (one or two–dimensional)

$$SD^i(\vec{r}, \vec{\Omega}_n) = \sum_{j=1}^{i-1} \sum_{n'} K^{j\to i,\, n'\to n}(\vec{r})\, \phi^j(\vec{r}, \vec{\Omega}_{n'}) + \sum_{j=1}^{i} K_0^{j\to i,\, n_0\to n}(\vec{r})\, \Phi_0^j(\vec{r}), \tag{3.23}$$

(2) Case of a point source (three–dimensional)

$$SD^i(\vec{r}, \vec{\Omega}_n) = \sum_{j=1}^{i-1} \sum_{n'} K^{j\to i,\, n'\to n}(\vec{r})\, \phi^j(\vec{r}, \vec{\Omega}_{n'}) + \sum_{j=1}^{i} \sum_{n'} K^{j\to i,\, n'\to n}(\vec{r})\, \phi_0^j(\vec{r}, \vec{\Omega}_{n'}) \text{ and} \tag{3.24}$$

(3) Case of a distributed source

$$SD^i(\vec{r}, \vec{\Omega}_n) = \sum_{j=1}^{i-1} \sum_{n'} K^{j\to i, n'\to n}(\vec{r})\, \phi^j(\vec{r}, \vec{\Omega}_{n'}) + S^i(\vec{r}, \vec{\Omega}_n).$$

Then, Eq. (3.1) is written as,

$$\vec{\Omega}_n \cdot grad\, \phi^i(\vec{r}, \vec{\Omega}_n) + \Sigma_t^i(\vec{r})\, \phi^i(\vec{r}, \vec{\Omega}_n) = \sum_{n'} K^{i\to i,\, n'\to n}(\vec{r})\, \phi^i(\vec{r}, \vec{\Omega}_{n'}) + SD^i(\vec{r}, \vec{\Omega}_n) = q^i(\vec{r}, \vec{\Omega}_n). \tag{3.25}$$

For the special cases of one–dimensional slab and three–dimensional rectangular parallelpiped, no curvilinear coordinate exists. In these cases, the term $K^{i\to i,\, n\to n}(\vec{r})\, \phi^i(\vec{r}, \vec{\Omega}_n)$ can be subtracted from the both sides of Eq. (3.25). Then we have an equation given as,

$$\vec{\Omega}_n \cdot grad\phi^i(\vec{r}, \vec{\Omega}_n) + \Sigma_T^i(\vec{r})\, \phi^i(\vec{r}, \vec{\Omega}_n) = Q^i(\vec{r}, \vec{\Omega}_n). \tag{3.26}$$

where $\Sigma_T^i(\vec{r}) = \Sigma_t^i(\vec{r}) - K^{i\to i,\, n\to n}(\vec{r})$ *and*

$$Q^i(\vec{r}, \vec{\Omega}_n) = \sum_{n'\neq n} K^{i\to i,\, n'\to n}(\vec{r})\, \phi^i(\vec{r}, \vec{\Omega}_{n'}) + SD^i(\vec{r}, \vec{\Omega}_n).$$

The ϕ^i in the right hand side of Eqs. (3.25) and (3.26) is unknown at this moment. So, the equation is solved by iteration, starting with an initial guess value of ϕ^i which is set equal to ϕ^{i-1} (0 for group 1). Each stage of the iteration consists of calculational sweeping for all $(\vec{r}, \vec{\Omega})$ points, performing the direct integration method as Eq. (3.5) for Eq. (3.4). Interpolation of $\phi(x_{p-1})$ and $q(x_{p-1})$ is necessary with respect to polar angle for sphere, azimuthal angle and either r or z for cylinder and two variables out of (x, y, z) for rectangular parallelpiped. Usually an exponential function is used for the interpolation, while linear interpolation is adopted for regions such as $\Sigma_t < 10^{-3}$ or $\nu\Sigma_f > 0$. This is the same as for the interpolation of q (x) in the integrand of Eq. (3.5).

The sweeping flow is as follows:

(1) One-dimensional case

The direction number n is defined in Table 3.1 for this case.

(a) In the order of n=20, ···, 11 from the outermost mesh of r or z consecutively to the origin and

(b) In the order of n=10, ···, 1 from the origin to the outermost.

(2) Two-dimensional S_8 case

The direction number n is defined in Fig. 3.3.

First, the set of procedures (a) and (b) given below is performed from the radially outermost mesh consecutively to the axis of the cylinder.

(a) In the order of n=48, 40, 47, 38, 37, 46, 34, 33, 32, 45, 28, 27, 26, 25 from the top (maximum z) to the bottom (minimum z) and

(b) In the order of n=44, 20, 19, 18, 17, 43, 12, 11, 10, 42, 6, 5, 41, 2 from the bottom to the top.

Secondly, the set of procedures (c) and (d) given below is performed from the axis to the radially outermost.

(c) In the order of n=39, 36, 35, 31, 30, 29, 24, 23, 22, 21 from the top to the bottom and

(d) In the order of n=16, 15, 14, 13, 9, 8, 7, 4, 3, 1 from the bottom to the top.

The angular fluxes of the eight westmost points n=41, ···, 48 are used only to obtain $\phi\ (x_{p-1})$ and $q\ (x_{p-1})$ for n=2, 6, 12, 20, 28, 34, 38, 40, respectively, by interpolation with respect to azimuthal angle φ from the flux values of adjacent mesh points. This ordering has been optimally decided so as to use the newest flux values through the iteration.

(3) Two-dimensional S_{16} case

This case is analogous to that of S_8. The direction number n is defined in Fig. 3.4.

(4) Three-dimensional case

The direction number n is defined in Fig. 3.6.

First, the set of procedures (a)···(d) given below is performed from the front (maximum x) consecutively to the back (minimum x).

(a) In the order of n=80, 78, 77, 74, 73, 72, 68, 67, 66, 65 from the top (maximum z) to the bottom (minimum z) and

(b) In the order of n=60, 59, 58, 57, 52, 51, 50, 46, 45, 42 from the bottom to the top.

The set of (a) and (b) is performed from the right (maximum y) to the left (minimum y).

(c) In the order of n=79, 76, 75, 71, 70, 69, 64, 63, 62, 61 from the top to the bottom and

(d) In the order of n=56, 55, 54, 53, 49, 48, 47, 44, 43, 41 from the bottom to the top.

The set of (c) and (d) is performed from the left to the right.

Secondly, the set of procedures (e)···(h) given below is performed from the back to the front.

(e) In the order of n=40, 38, 37, 34, 33, 32, 28, 27, 26, 25 from the top to the bottom and

(f) In the order of n=20, 19, 18, 17, 12, 11, 10, 6, 5, 2 from the bottom to the top.

The set of (e) and (f) is performed from the right to the left.

(g) In the order of n=39, 36, 35, 31, 30, 29, 24, 23, 22, 21 from the top to the bottom and

(h) In the order of n=16, 15, 14, 13, 9, 8, 7, 4, 3, 1 from the bottom to the top.

The set of (g) and (h) is performed from the left to the right.

After each stage (one set of the whole sweep) of iteration above, the obtained angular flux is normalized so as to maintain neutron balance in the energy group and also in the spatial regions. The total gain by independent source or FCS and slowing down source from upper groups is equal to the total loss

by absorption, leakage and slowing down into lower groups. The neutron balance is described in Sec. 3.7. We denote the normalized flux after "t" times' iteration as $\phi^{i\,(t)}(\vec{r}, \vec{\Omega}_n)$. Then the convergence is checked for the criterion ε (ε is given as an input parameter) as

$$|\phi^{i\,(t-1)}(\vec{r}, \vec{\Omega}_n)/\phi^{i\,(t)}(\vec{r}, \vec{\Omega}_n)-1|<\varepsilon \tag{3.27}$$

for all the spatial and angular mesh points except those $\phi^{i\,(t)}=0$. If Eq. (3.27) is not satisfied for the all mesh points, the procedures Eq. (3.25) or (3.26) and the followings are repeated until Eq. (3.27) is satisfied. Thus the i-th group angular flux distribution is obtained.

3.6.2 Restart and Bootstrap Options

The calculation requires a fairly long computation time except one-dimensional case, so that often it is not completed in a single run. So, to continue the calculation from the previous run, we programmed a restart option for energy group continuation. Input parameter TMAX (see Chapter 5) controls to stop a calculation where the convergence of some group (i_R) is attained before permitted CPU time is exhausted. Then the angular fluxes of groups 1 to i_R and the other necessary data are stored on the disk files for continuing the calcualtion for the next batch where i_R+1 is input as the starting group number as well as the data on the disk files.

Another option is a so-called bootstrap method for spatial region continuation in the z direction. The first bootstrap step deals mainly with the region nearest to the source. The second bootstrap step is for the region adjacent to the region of the first step in the z-direction. The second step is started after the calculation from group i to group IMAX finished in the first bootstrap. A fictitious interface of z-plane ($z>0$) is set as an interface between the regions of the two steps. At the first step, the angular flux on the plane (only the component for $\theta<\pi/2$) is stored on a disk file to be used as the boundary condition for the second step.

In case of a point source, the point source must be placed exactly on the corresponding position for each bootstrap step. Only mesh sizes (Δz) can be coarser except for the z region under calculation. This is because the first collision source FCS^i must be obtained for each spatial mesh point of the region under calculation.

3.6.3 Energy Grid Model

In the course of developing the present code system, we have been in trouble for three years for an overestimation of flux in a deep penetration analysis. We have found that this is mainly because of the overestimation of elastic self-group scattering source especially in the group having a peak of source spectrum. The cause of error is considered to exist in assuming the flux distribution flat with respect to lethargy within a group.

Let us assume that the source is of mono-energy or is given only in the first group. The neutron spectrum will shift to lower energy side in the group with suffering scattering in due course of penetration. The flat flux approximation cannot account this spectral shift within the group. This means that elastic removal from this group is underestimated. The spectral shift occurs also because the group does not accept the elastic slowing down source from upper groups if it is the first group. Then the neutrons can reach in the calculation too deep without losing energy. The overestimation of the flux for the first group in the deep region will also cause overestimation of the fluxes for every group of lower energy.

The problem has been solved by making energy group structure fine enough. It will be explained as follows: at every collision of elastic scattering, neutron loses energy though it remains within the same energy group as before collision. According to increase of penetration distance, neutron flux itself attenuates exponentially. Moreover the scattering components shift neutron spectrum in the group to lower energy side or goes down to the lower groups as neutron suffers more collisions in due course of

penetration as illustrated in the upper part of Fig.3.7. However, the scattering kernel into the self group $K^{i\to i,n'\to n}(\vec{r})$ is not represented with respect to penetration distance. The $\vec{r}$ means only the composition at the point $\vec{r}$. And the group model treats the neutron flux always as flat with respect to lethargy within a group. So the spectral shift within a group is always raised back to the upper energy side and

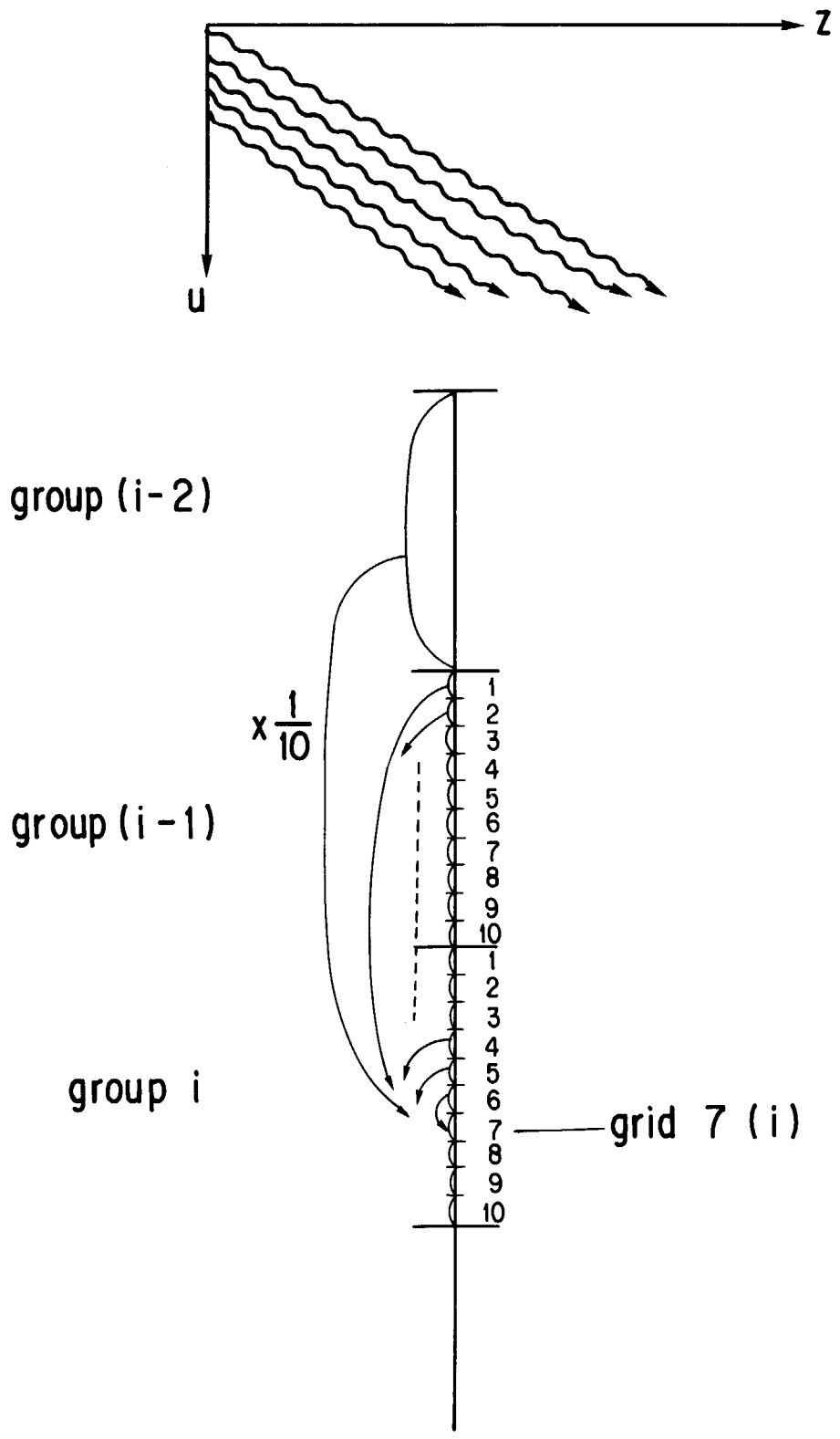

Fig. 3.7 Illustration of slowing down and penetration procedures and calculation of slowing down source into a grid

overestimation occurs at deep penetration.

In the scope given above, we find a definite improvement in the overestimation by dividing each energy group into several fine groups (grids) of equal lethargy widths.[9] The scattering source is calculated precisely between grids with the transfer matrices $K^{g'\to g,\, n'\to n}$. After a survey about the number of divisions, it has been confirmed that ten grids in a group are sufficient for almost compositions of nuclides for the present 125-group structure. The lethargy width of a grid is 0.00156 in the high energy region above 10MeV. Energy group structure of the group constants library is already fine enough to represent the 14MeV source spectrum and resonance cross sections of iron etc. Since the grid is rather an artificial division for elastic removal calculation in relation with penetration distance, the group constants can be used commonly for ten grids in a group. Usually iteration procedure is not necessary for a grid, or, at most two or three times of iteration are sufficient even for composition of heavy nuclides. This means that computation time is equivalent to that of the case where ten or more times of iteration are performed for a group without grids.

For the thermal group where up-scattering exists, we do not apply this energy-grid method but perform the usual iteration procedure until the Condition(3.27) is fulfilled, though it often exceeds a hundred times of iteration to satisfy a convergence for compositions like concrete which contain hydrogen.

To save magnetic disk area for storing angular flux, the flux for each grid is condensed (summed up) for the group. But the ten-grid fluxes in the just upper group ((i−1)th group) are kept as well as the ten-grid fluxes in the i-th group for calculating slowing down source into a grid from the grids in the (i−1)th and the i-th groups precisely. The slowing down source from the (i−2)th or upper groups are equally distributed into the ten grids (Fig. 3.7).

Thus the relation between elastic slowing down process and penetration distance can be dealt with more precisely. This proves that the flux distribution function is very hard to treat in the form of separation of variables, that is, the variables of energy E and penetration distance $\vec{r}$. An example of deep penetration calculation into a stainless steel assembly is given in Sec. 4.1.

3.7 Coarse Mesh Rebalance

Equation (3.1) is a balance equation concerning the number of neutrons in a subspace of $(\vec{r}, \vec{\Omega})$. However, Eq. (3.4) has no attribute as balance equation. So it is necessary to renormalize the calculated $\phi^i(\vec{r}, \vec{\Omega})$ after sweeping over all $(\vec{r}, \vec{\Omega})$ points. This is applied for each time of iteration in either a group or a grid. The $\vec{r}$ space is divided into some number of regions (volumes) each of which is called a coarse mesh. In each of them, the ϕ^i is renormalized to maintain a relation given as,

$$\int_{V_c} d\vec{r} \int d\vec{\Omega}\, [S^i + \sum_{j=1}^{i-1} \int d\vec{\Omega}' K^{j\to i} \phi^j]$$

$$= \int_{V_c} d\vec{r} \int d\vec{\Omega}\, [\Sigma_t^i \phi^i - \int d\vec{\Omega}' K^{i\to i} \phi^i]$$

$$+ [\textit{net leakage from a coarse mesh}],$$

where V_c is the volume of a coarse mesh. The coarse meshes are defined by input parameters INTERX etc. (see Chapter 5) for the two-and three-dimensional cases. In the one-dimensional sphere and slab cases, the whole volume is treated as one coarse mesh. In the one-dimensional slab, only z direction is considered so that the cross section of $1cm^2$ is assumed in the (x, y) plane.

For the two- and three-dimensional cases, the whole volume is divided into plural number of coarse

mesh regions. In the two-dimensional (r, z) case, a rectangular region in the (r, z) plane stands for a ring-shaped volume made by rotating the rectangle around the axis of the cylinder (0, z). In the three-dimensional (x, y, z) case, a rectangular parallelpiped region is considered as a coarse mesh in the whole volume.

A rough estimation is performed for the net leakage from each coarse mesh, and one coarse mesh is selected as of the largest leakage. Coarse mesh rebalance is performed for this region. At the mesh points on surfaces, edge-lines or corners, only the outgoing angular fluxes are normalized, while at the inner mesh points, the angular fluxes are renormalized for all directions of the discrete ordinates.

A rough estimation is again performed for the net leakage from each of the remaining coarse meshes, and the one coarse mesh is selected as of the largest leakage. At this step, the current incoming from the adjacent normalized coarse meshes is assumed to be zero in the meaning of minus leakage. This current is considered as a fixed source in an accepting coarse mesh. This flow is essential to keep the coarse mesh rebalance. Otherwise, the order of renormalized regions would fall in an absurdity in the next iteration stage. Thus the procedure continues until all the coarse meshes are renormalized.

The renormalization factor F to be multipiled to $\phi^i(\vec{r}, \vec{\Omega})$ in a coarse mesh is obtained as

$$F = \mathrm{GAIN}/(\mathrm{ABBS}-\mathrm{SELF}+\mathrm{XLEK}),$$

where

$$\mathrm{GAIN} = \int_{V_c} d\vec{r} \sum_n \Delta\vec{\Omega}_n SD^i(\vec{r}, \vec{\Omega}_n),$$

$$\mathrm{ABBS} = \int_{V_c} d\vec{r}\, \Sigma_t^i(\vec{r}) \sum_n \Delta\vec{\Omega}_n \phi^i(\vec{r}, \vec{\Omega}_n),$$

$$\mathrm{SELF} = \int_{V_c} d\vec{r} \sum_n \Delta\vec{\Omega}_n \sum_{n'} K^{i\to i, n'\to n}(\vec{r})\, \phi^i(\vec{r}, \vec{\Omega}_{n'}),$$

$$\mathrm{XLEK} = \int_{S_c} d\vec{s} \sum_n (\vec{n}\cdot\vec{\Omega}_n)\, \phi^i(\vec{s}, \vec{\Omega}_n),$$

S_c :surface of a coarse mesh,

$\int d\vec{s}$:surface integral and

$\vec{n}$:outward normal unit vector at $\vec{s}$.

4. Validity Tests of Code System

4.1 Deep Penetration

Nakashima et al.[10] have made a benchmark experiment concerning neutron deep penetration to assess the multigroup neutron cross section libraries and the calculational methods for fusion neutronics. Here, a validity test of the BERMUDA-2DN is made by analyzing the benchmark experiment of DT neutrons into an assembly of type 316L stainless steel with thickness 120cm which is composed of two cylinders of 45cm diam. × 60cm long and 50cm diam. × 60cm long. Neutron spectra are measured in the cylindrical assembly for DT neutrons of the FNS[21] in JAERI. The DT neutrons are injected to one side of the flat surface of the cylinder as illustrated in Fig.4.1. Energy spectra of scalar flux above 0.8MeV have been measured at five positions of 8, 28, 48, 68 and 88cm in depth along the axis of the cylinder in the experimental arrangement shown in Fig.4.2, using a small spherical NE213 liquid scintillator with an unfolding code FORIST.[11]

For analyzing the experiments with the BERMUDA-2DN, the target room shown in Fig.4.1 is modelled as a cylinder so that its axis coincides with that of the test port loading the stainless steel assembly. A DT point source is located at the origin, and the spectrum is given as input data prepared by a Monte Carlo calculation[22] with the MORSE-DD code[20] taking account of the detail of the rotating target structure. Symmetry condition is imposed with respect to the $z=0$ plane.

Then the bootstrap method described in Sec.3.6.2 is used. As the first step of bootstrap, axial mesh sizes in the target room are made rather smaller than in the assembly. Thus the angular flux for each energy group is obtained as the boundary flux over the z-plane corresponding to the surface of the stainless steel assembly. At the second step, the angular flux in the assembly is calculated from the boundary flux plus the first collision source, setting axial meshes fine enough and radial meshes common to the first step calculation. Scalar flux is estimated as the sum of Φ and Φ_0.

A calculation with BERMUDA-2DN was at first made for the present benchmark experiment without the energy grid method. There an overestimation was observed larger than that with DOT3.5. After trials which were repeated many times, we have attained the energy grid model described in Sec. 3.6.3.

The calculated results with the improved BERMUDA-2DN are compared with the experiments in Fig.4.3, in which the small circles with error bar show the measured values. For a comparison, the calculations with the DOT3.5 code[2] are shown in Fig.4.4. The both calculations are made using the same group cross sections: BERM125X for BERMUDA-2DN and JACKEX[26] for DOT3.5 processed from the JENDL files with the same energy group structure. Nevertheless, BERMUDA-2DN reproduces better the measured spectra, especially at the deep penetrations, than the DOT3.5 code. These results prove the necessity and the usefulness of the energy grid method in the BERMUDA-2DN.

The required computer resources are shown in Table 4.1 for the present code, and in Table 4.2 for the DOT3.5. In Table 4.1, VU time represents the CPU time performed as vector computation, that is, the figures for CPU time contains those of VU time. These tables show that the BERMUDA-2DN code requires a large computer resource comparing with the DOT3.5 code.

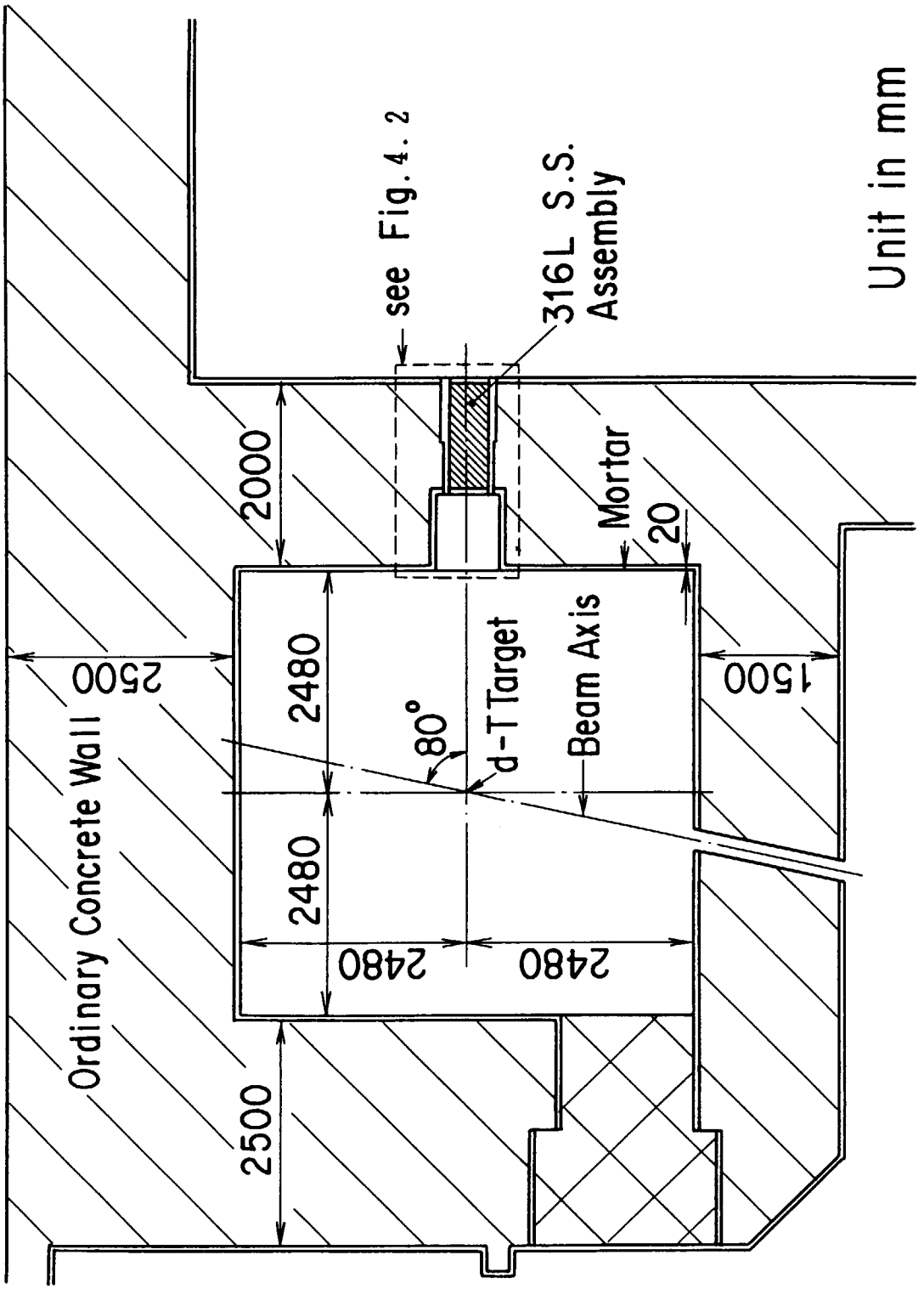

Fig. 4.1 Horizontal section of the experimental room, the experimental port and a Type 316L stainless steel assembly

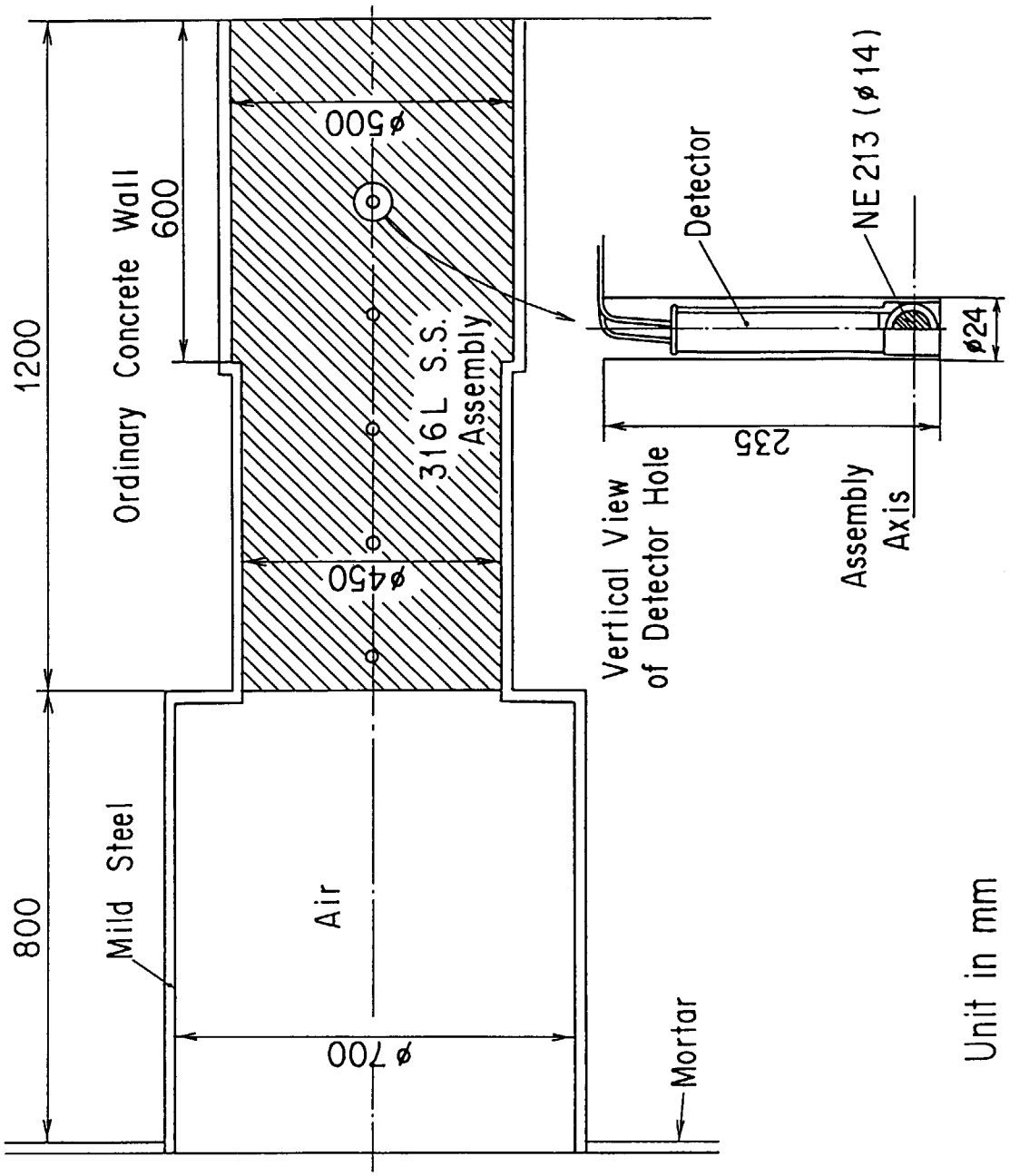

Fig. 4.2 Arrangement of the experimental configuration and the detector hole for a neutron spectrometer

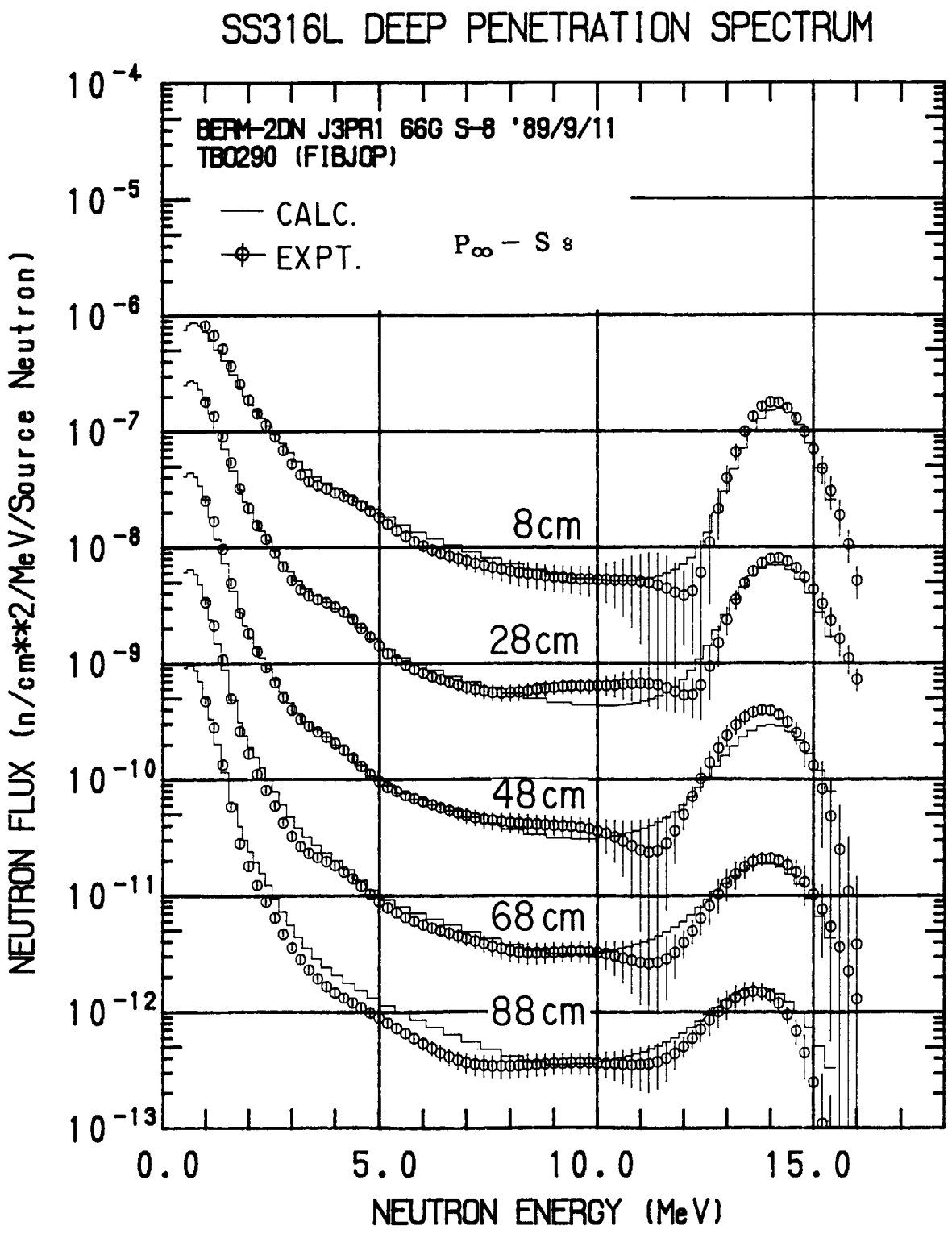

Fig. 4.3 Comparison between the calculated spectra with the BERMUDA–2DN code and the measured spectra in the Type 316L stainless steel assembly

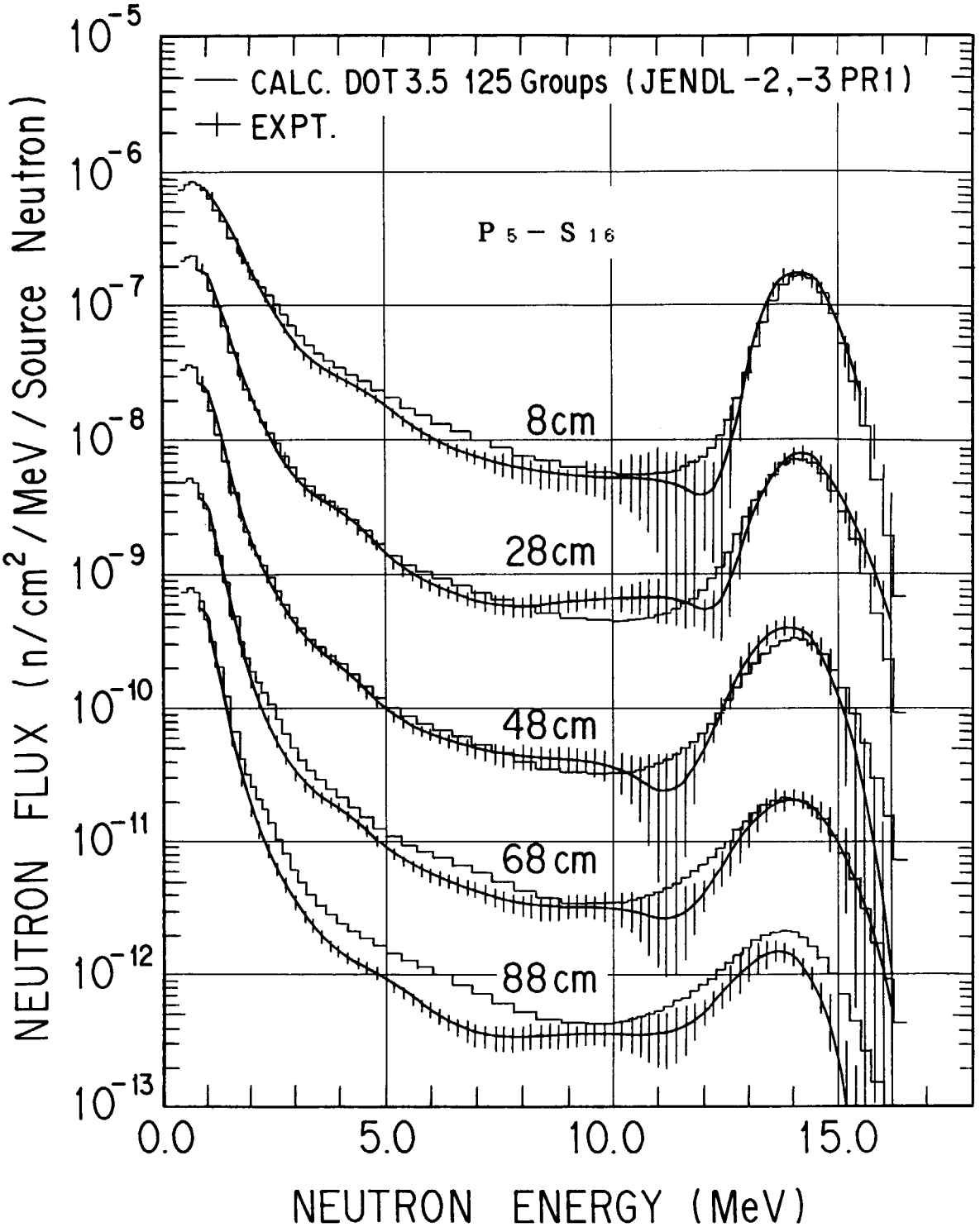

Fig. 4.4 Comparison between the calculated spectra with the DOT3.5 code and the measured spectra in the Type 316L stainless steel assembly

Table 4.1 Problem dimensions and required computer resources for BERMUDA-2DN on FACOM/VP100

	step1	step2
energy groups	66	66
radial meshes	50	50
axial meshes	50	42
angular ordinates	48 (S_8)	48 (S_8)
memory (MB)	41	41
CPU (min)	142	129
VU (min)	50	42
disk (MB)	~200	~200
I/O times (EXCP)	~40,000	~40,000

Table 4.2 Problem dimensions and required computer resources for DOT3.5 on FACOM/M380

energy groups	66
radial meshes	50
axial meshes	90
angular ordinates	160 (S_{16})
order of spherical harmonics	P_5
memory (MB)	5
CPU (min)	80
disk (MB)	~100
I/O times (EXCP)	~55,000

4.2 Spectrum in a Cavity

An experiment has been carried out to study the behavior of 14MeV neutrons incident to a large cavity.[12] The cavity is composed of mortar wall, whose inner surface is coated with stainless steel. It simulates a shielding box of a neutral beam injector (NBI) in a tokamak fusion reactor, where 14MeV neutrons are considered to be injected from the core plasma in the opposite direction to the neutral beam. Fast neutron spectra have been measured inside the cavity with a 5.06cm diam. × 5.06cm long cylindrical NE213 scintillator with the FORIST code.[11]

The experimental arrangement and the vertical cross-sectional view are shown in Figs.4.5 and 4.6, respectively. The DT neutrons travel through a cylindrical hole in the concrete shield and a rectangular transport of stainless steel before arriving at the cavity. The inner surface of the duct is completely lined with stainless steel: therefore, it is expected that neutrons uncollided and shallowly scattered within the stainless steel layer are mainly able to enter the cavity.

The measured results have been analyzed with the MCNP-3,[13] DOT3.5[2] and BERMUDA-2DN-S16 codes using the group constants based on the ENDF/B-IV,[14] JENDL-2[15] and JENDL-3PR1.[16] In the analyses, the experimental configuration having the rectangular transport and the cavity is approximated with a two-dimensional (r,z) geometry: the rectangular transport with a cylinder having the same

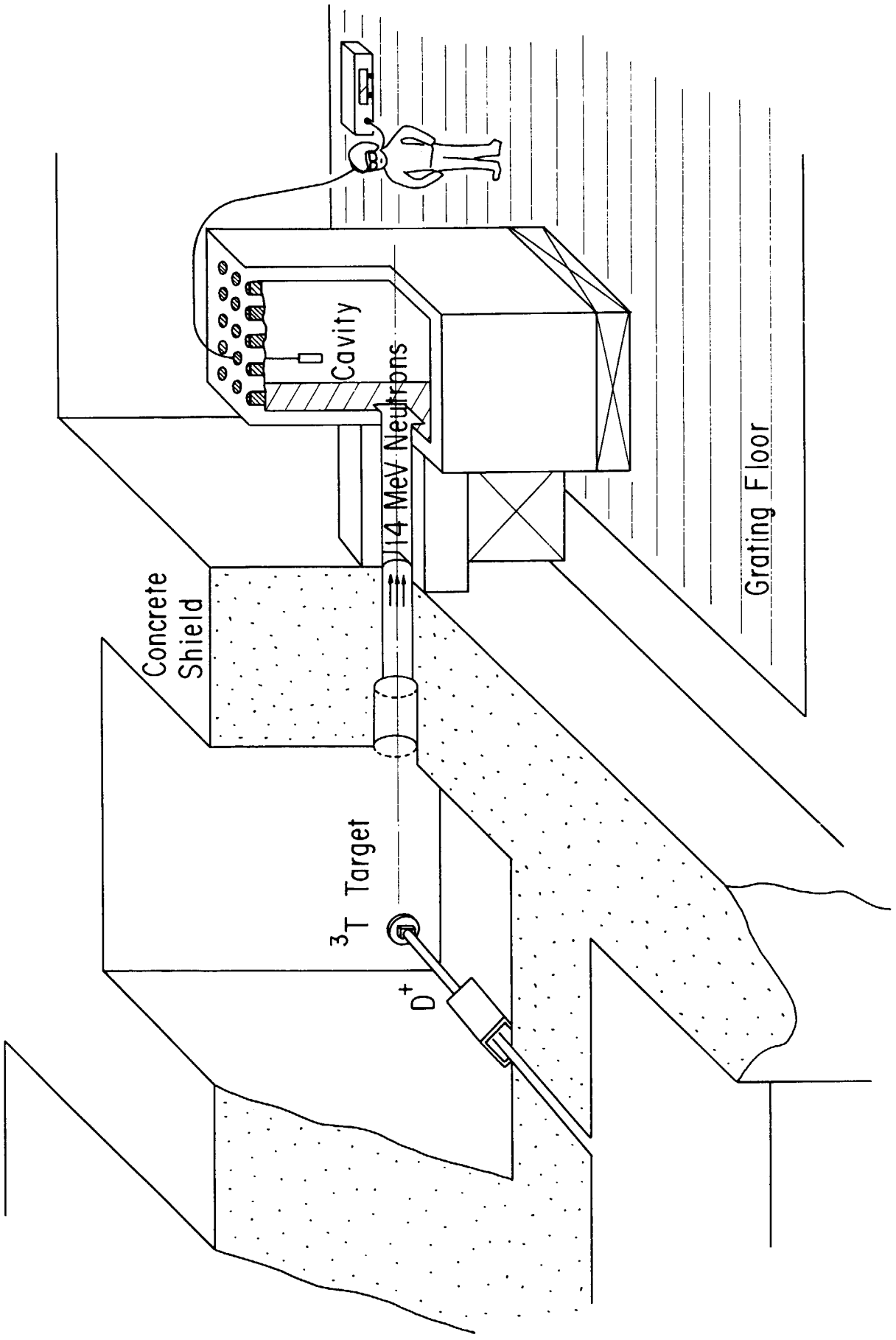

Fig. 4.5 Arrangement of duct-cavity experiment

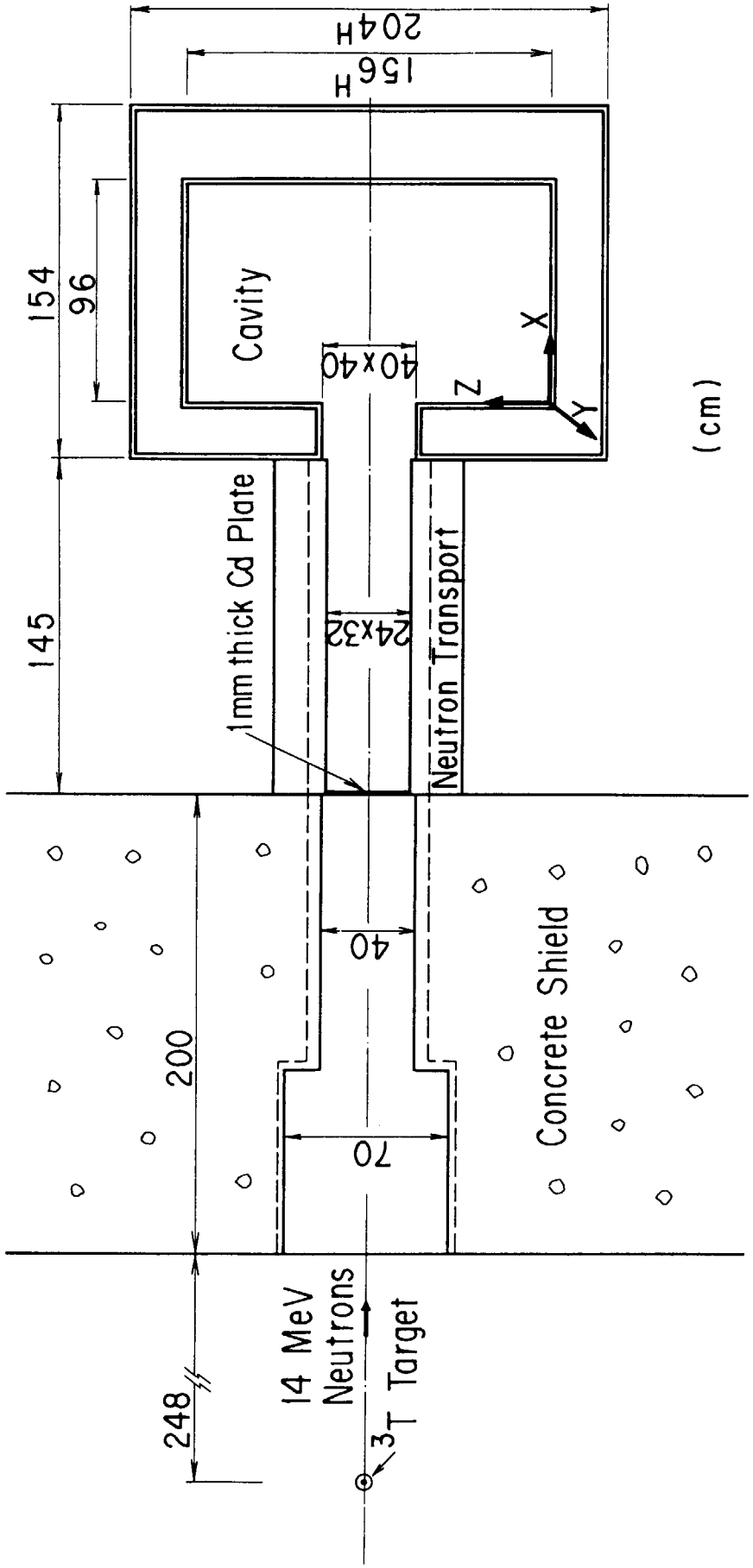

Fig. 4.6 Vertical cross section of experimental configuration

cross section and the cavity with a cylinder of 156cm inner diameter. Table 4.3 gives the material composition used for the calculations. To make the comparison rigorously between the results of calculations and measurements, the calculated fast neutron spectra are smeared with a Gaussian distribution function having the same resolution as that determined in unfolding the measured data using the FORIST code. In several figures (Figs.4.8(a) to 4.12), the positions of interest inside the cavity are referred with the Cartesian coordinates (x,y,z) as defined in Fig.4.7, where the origin is fixed at the center of the front inner surface of the cavity and the x-axis corresponds to the z-axis in the (r,z) geometry.

In Figs.4.8(a) and 4.8(b), the results of BERMUDA-2DN-S16 are compared with those of the experiments. In these figures, the spectra calculated with the MCNP-3 code and FSXLIB[27] library in the same (r,z) geometry are also given. They also show a similar difference above 12MeV to those of BERMUDA-2DN-S16. As the spectra are possibly dominated by single scattering of source neutrons, the difference between the experiments and the calculations can be attributed to the geometrical approximation, especially the cylindrical presentation for the rectangular inlet of the cavity. Except for the above difference, the BERMUDA-2DN-S16 calculations are in good agreement with the experiments, in particular, compared with the DOT3.5 calculations at the position (88,0,60) represented in Fig.4.9.

The contour map in Fig.4.10 shows the shortcoming of the Legendre expansion in the high energy region. Serious spatial fluctuations are observed in the flux obtained with the DOT3.5 code. In addition, a large discrepancy is also seen between the P_5 and P_7 approximations. Although it is not shown in Fig.

Table 4.3 Atomic densities of the structural materials

Element	Ordinary concrete	Mortar	Type 304 stainless steel	Air
Hydrogen	7.94−3[a]	1.82−2		
Cardon	5.41−4	3.80−4	3.17−4	
Nitrogen				4.20−5
Oxygen	4.32−2	4.39−2		1.13−5
Sodium	7.86−4	1.02−3		
Magnesium[b]	3.82−4	3.14−4		
Aluminium	2.64−3	3.44−3		
Silicon	1.48−2	1.59−2	1.70−3	
Phosphorus[b]			6.92−5	
Sulfur[b]	5.15−5	6.52−5	4.46−5	
Potassium[b]	5.29−4	7.35−4		
Calcium	2.56−3	1.74−3		
Chromium			1.74−2	
Manganese			1.73−3	
Iron	5.86−4	5.05−4	5.79−2	
Nickel			8.11−3	

[a]Read as 7.94×10^{-3}/barn • cm.

[b]Element not existing in the group constants library was treated in the manner that its number density was added to another appropriate element (*) having almost the same atomic weight as if it was (*).

4.10, even the negative flux appears in P_5 calculations in spite of the use of first collision source option. These dreadful features are originated from that the distribution in the cavity is dominated by the neutrons backscattered with the rear wall. But the backscattering distribution is unable to approximate with P_5 and P_7 expansions. Contrary, the BERMUDA-2DN-S16 with P_∞ model gives a smooth distribution and reveals the neutron flow from the inlet into the cavity. These results demonstrate the superiority of the BERMUDA code considering exactly the relationship between the energy and angle.

Next, the BERMUDA-3DN code is also tested using a supercomputer FACOM/VP2600 in a three-dimensional geometry, although only the S_8 approximation is applicable because of the limitation of memory size available on the computer. The calculated results are shown in Figs.4.11 and 4.12 with the measured spectra, for which required are almost one day of CPU+VU time with a memory of 440MB taking (30,30,60,80) points for $(x,y,z,\vec{\Omega})$, respectively and 70 energy groups. At least, the three-dimensional geometry is exactly described to represent the experimental configuration, whereas the S_8 approximation is very poor for calculating the streaming and backscattered neutrons.

Moreover, the usage of Eq.(3.24) in the three-dimensional case instead of Eq.(3.23) makes a cause

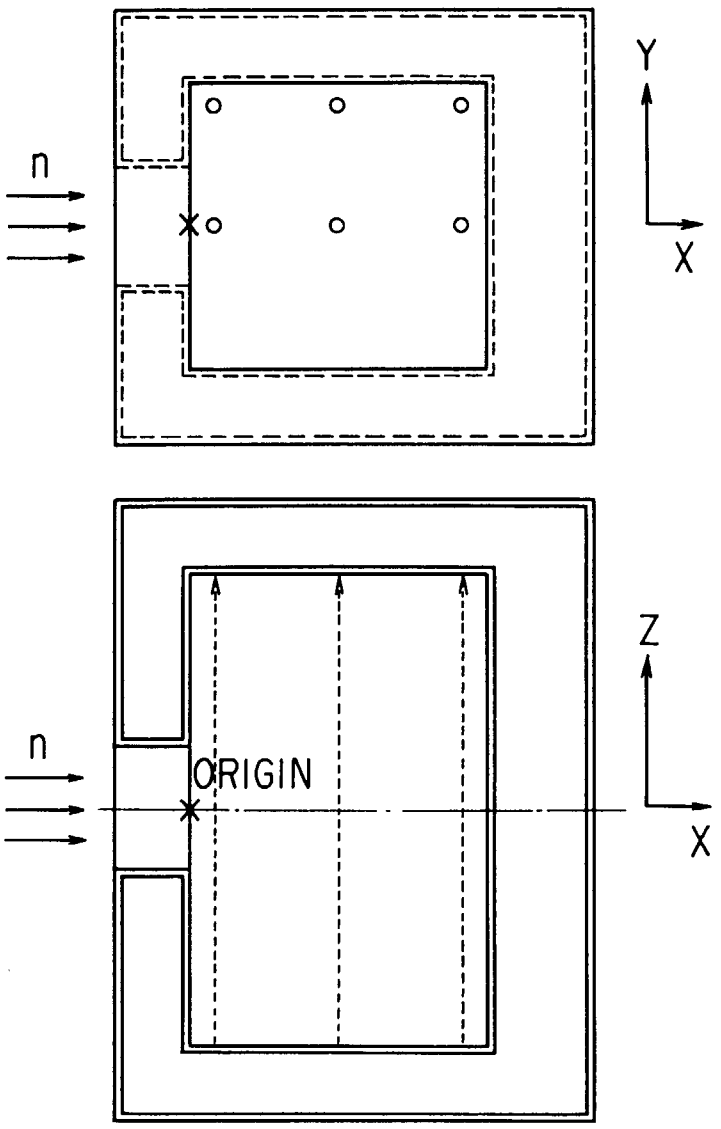

Fig. 4.7 Cartesian coordinates representing a measured positions : horizontal (x, y) and vertical (x, z) cross sections

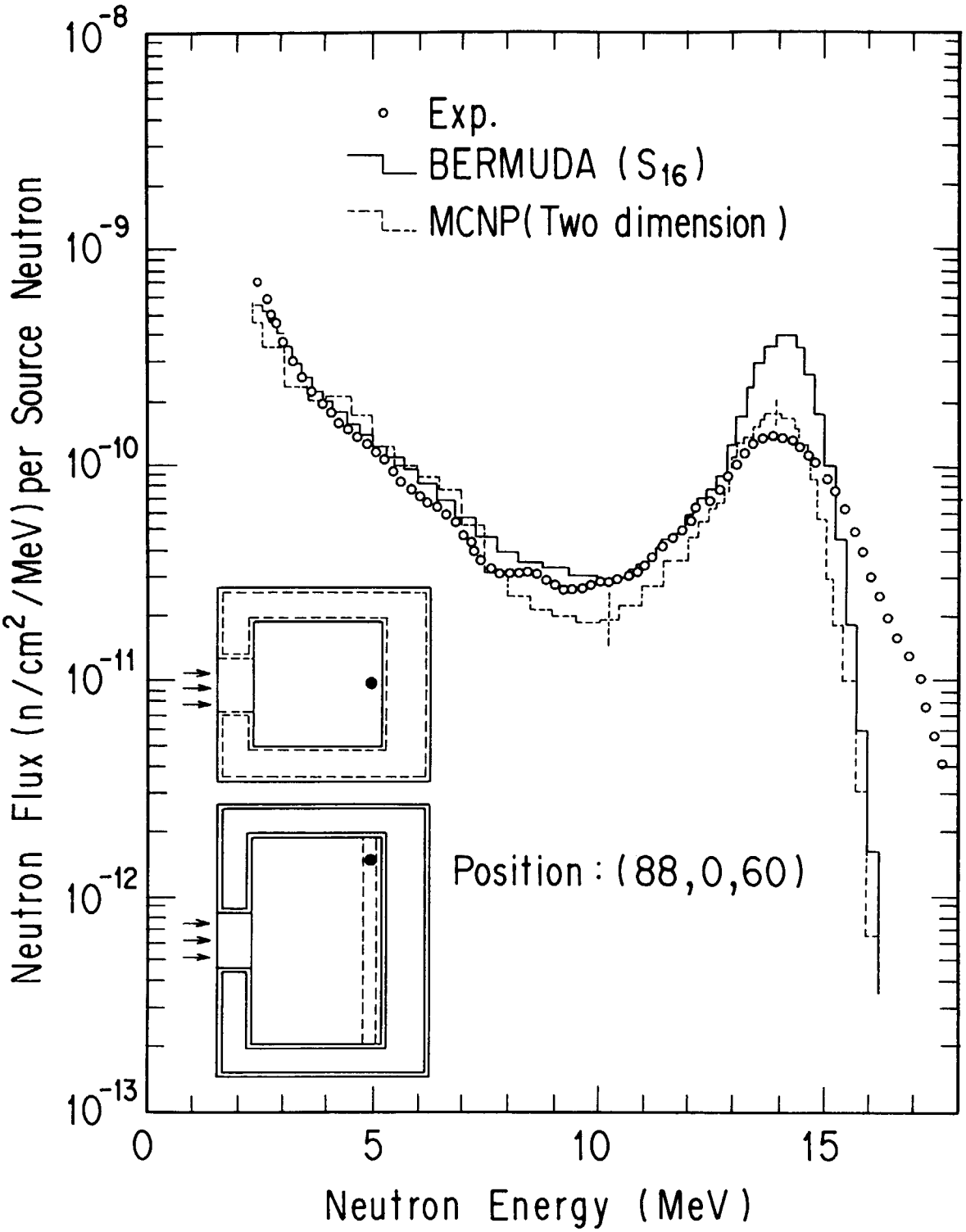

Fig. 4.8 (a) Fast neutron spectra measured and calculated using the BERMUDA-2DN-S16 and the MCNP codes with the two-dimensional geometry approximation at the (88, 0, 60) position

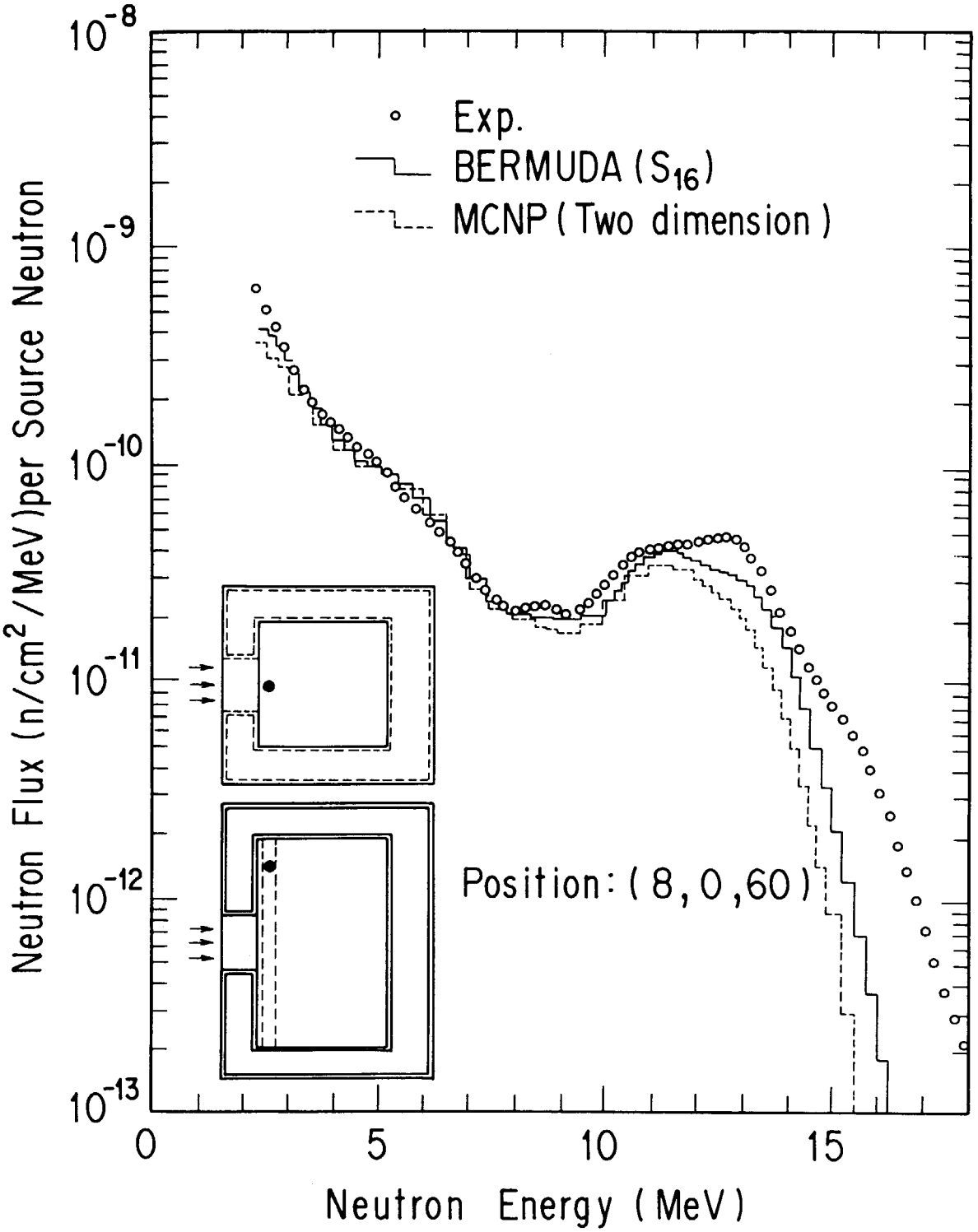

Fig. 4.8 (b) Fast neutron spectra measured and calculated using the BERMUDA-2DN-S16 and the MCNP codes with the two-dimensional geometry approximation at the (8, 0, 60) position

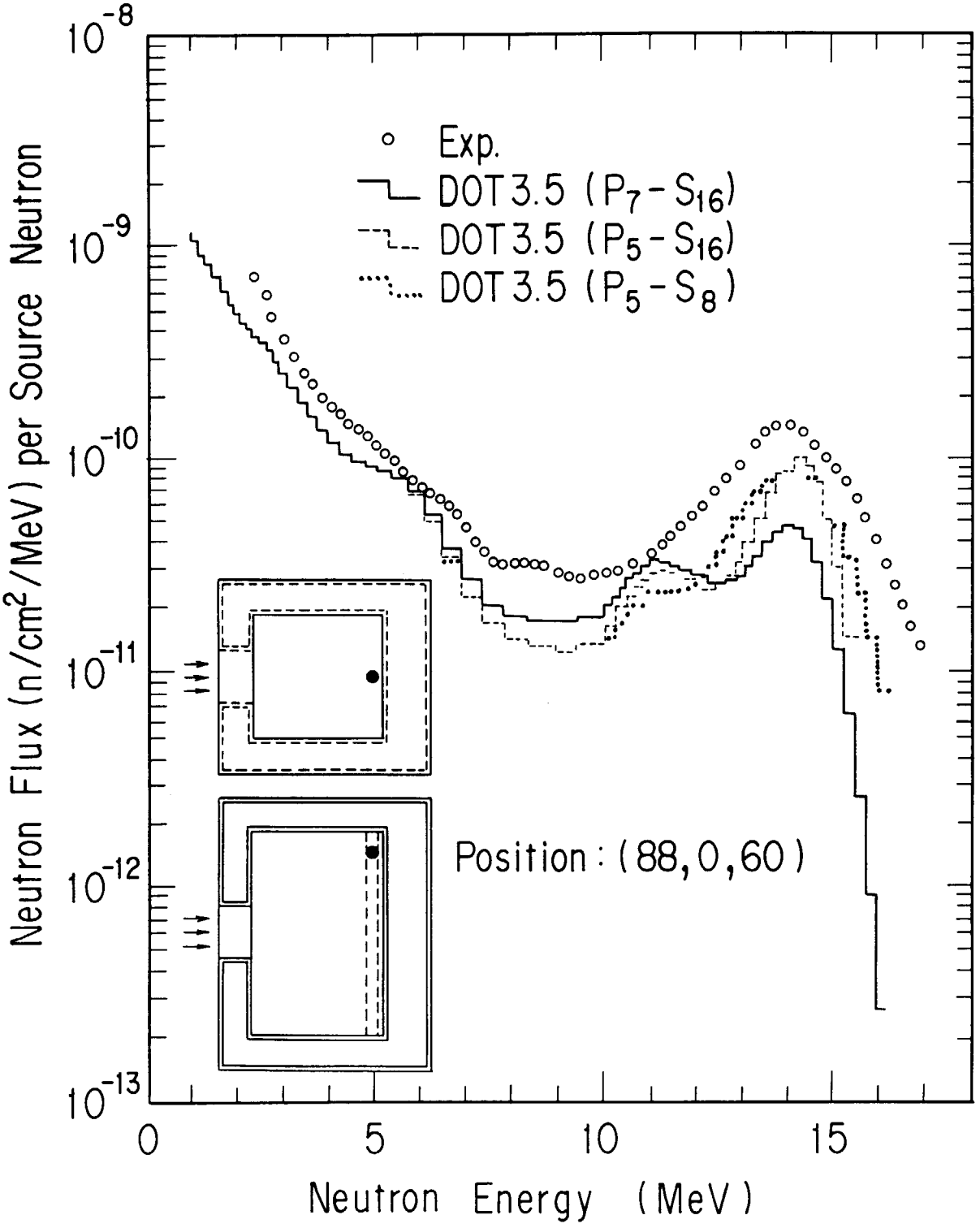

Fig. 4.9 Fast neutron spectra measured and calculated using the DOT3.5 code with the P_7–S_{16}, P_5–S_{16} and P_5–S_8 sets at the (88, 0, 60) position

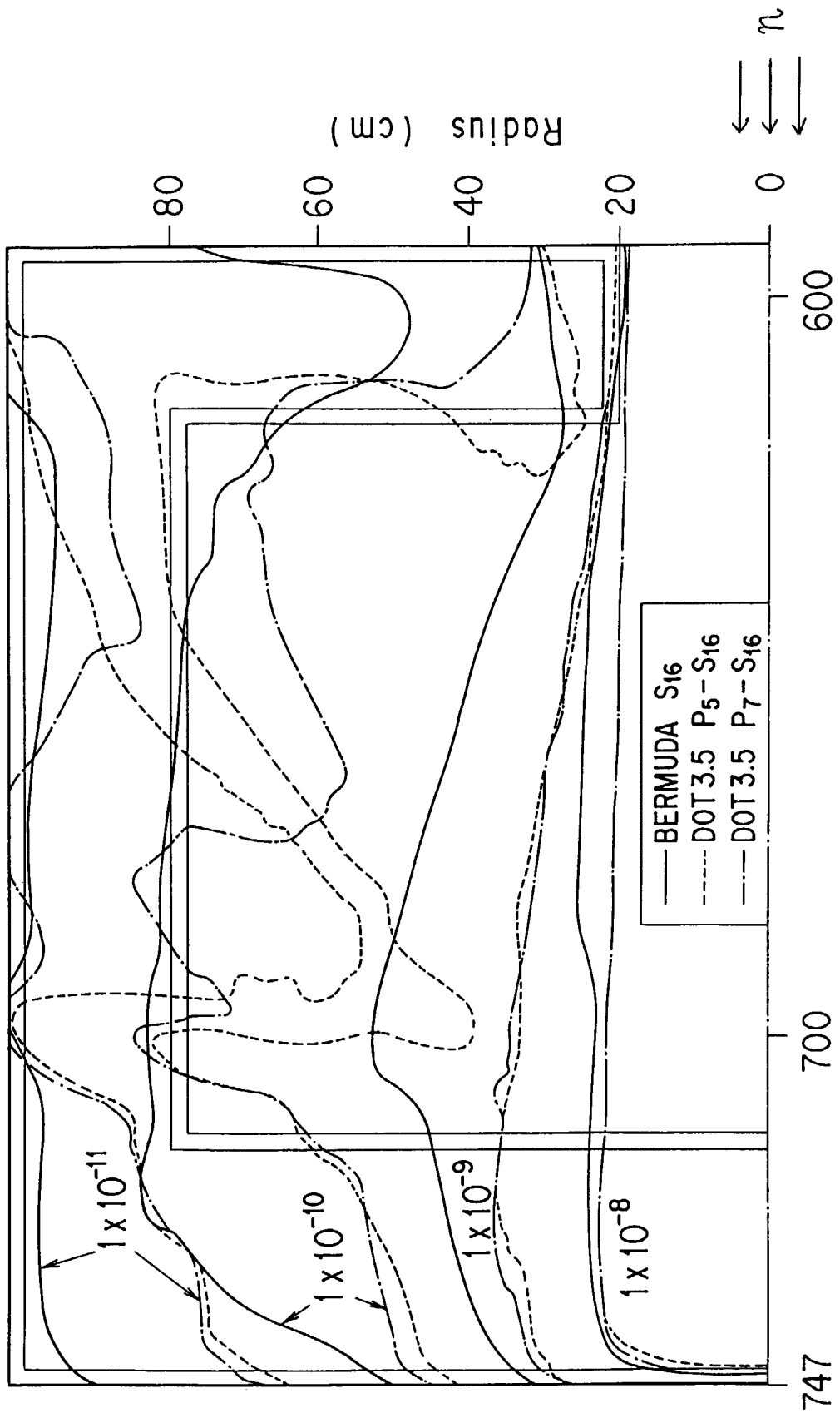

Fig. 4.10 Contour of the neutron scalar flux integrated above 10MeV in the cavity calculated using the BERMUDA-2DN-S16 code and the DOT3.5 code with the P_5-S_{16} and P_7-S_{16} approximations

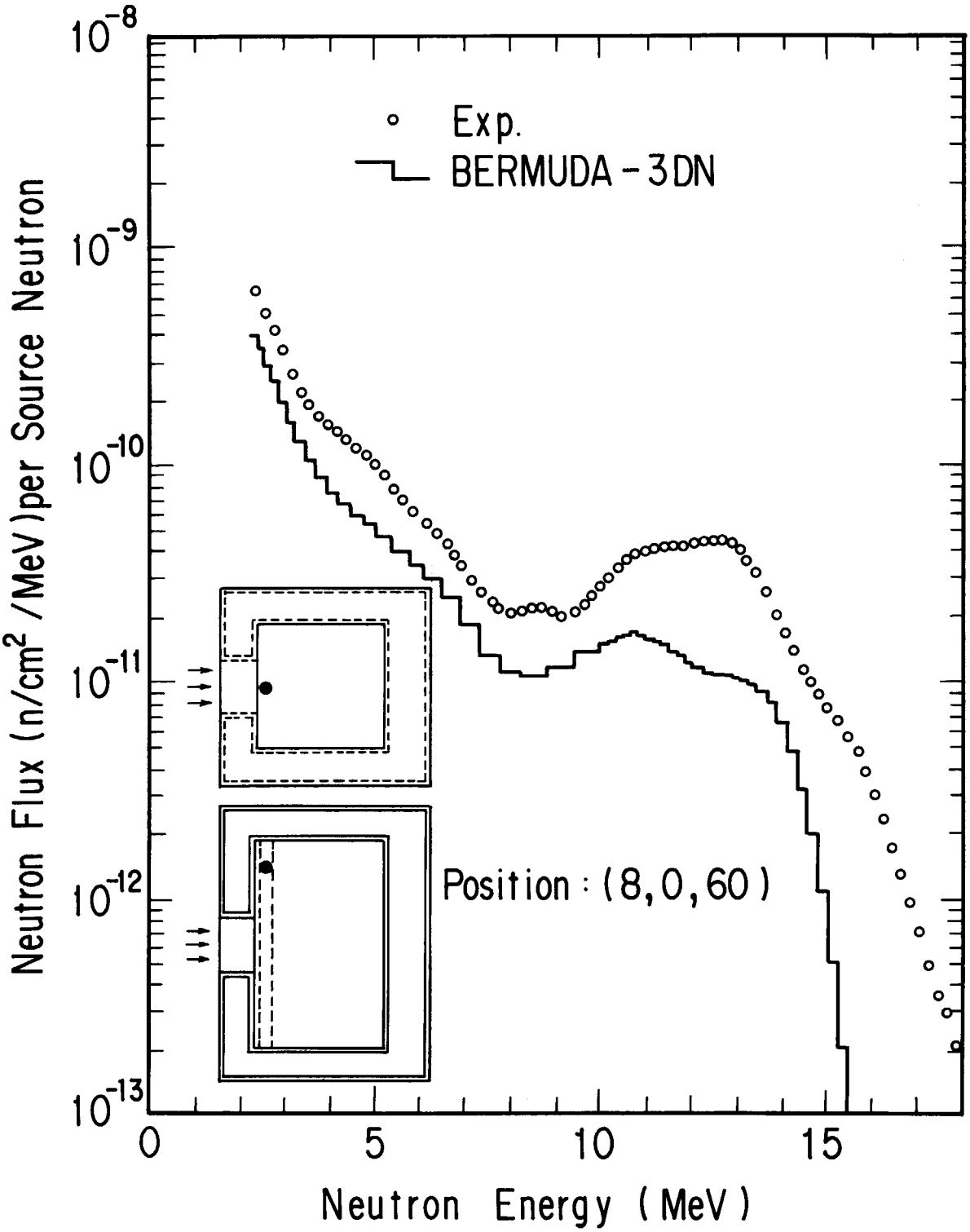

Fig. 4.11 Fast neutron spectra measured and calculated with the BERMUDA-3DN at the (8, 0, 60) position

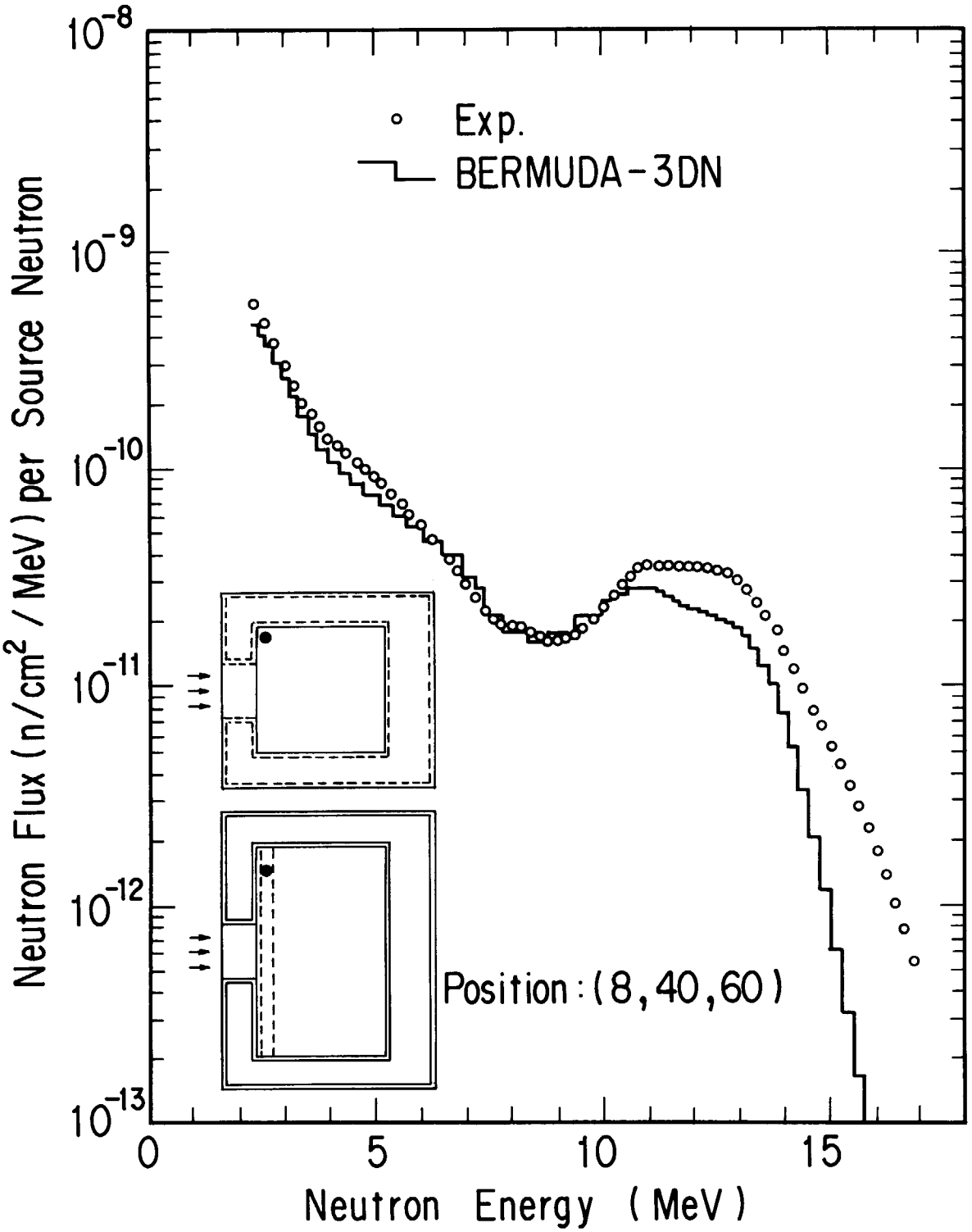

Fig. 4.12 Fast neutron spectra measured and calculated with the BERMUDA-3DN at the (8, 40, 60) position

of error to some extent because the direction of the uncollided flux ϕ_0^j is not so exactly taken into account as in the n_0 in Eq.(3.23) which is also a difficulty of the available memory. So far, a few three-dimensional discrete ordinates transport codes[23),24),25)] have been developed and employed as only an auxiliary tool to two-dimensional codes under the limited conditions without any validity test with the experiments. The present validity test suggests that the BERMUDA-3DN code will become more practical in use with the great development of the computer.

4.3 Offset Slits Streaming

Another validity test of the BERMUDA-2DN-S16 and BERMUDA-3DN codes have been made using an experiment of DT neutrons streaming through slits in type 304 stainless steel.[19)] The experimental arrangement and the cross-sectional view are shown in Figs.4.13 and 4.14. Reaction rates of a NE213 detector have been measured for fast neutrons at eleven points inside the slits and the stainless steel as indicated in Fig.4.15. The reaction rates are obtained by integrating the pulse height distribution of the small spherical NE213 scintillator produced by fast neutrons above some threshold energy. Three kinds of reaction rates covering 15MeV neutrons have been measured for different threshold energies of 2MeV, 5 MeV and 10MeV.[18)]

The results of the measurement and a calculation with the BERMUDA-3DN code are summarized in Table 4.4, in which the measured values are given as the reaction rates [reactions/(10^{24} detector atoms) /(1 source neutron)] and the calculated values in the ratios (C/E) to the measured values. The calculations are in good agreement with the measurements inside the first slit seeing the DT source directly, while they are considerably different at other positions. Streaming neutrons through the narrow

Table 4.4 The measured neutron reaction rates in the offset slits assembly and the ratios of the calculated values with the BERMUDA-3DN to the measured values (C/E)

position (cm)				neutron reaction rates[a]					
				a) E>2MeV		b) E>5MeV		c) E>10MeV	
	X	Y	Z	measured	C/E	measured	C/E	measured	C/E
Air line	s	①	5 0 0	2.48−08[b]	1.25	1.01−08	1.18	4.09−09	1.14
	1	②	20 0 0	1.79−08	1.27	9.60−09	1.08	3.94−09	1.08
	i	③	35 0 0	1.45−08	1.26	8.14−09	1.13	3.39−09	1.15
	t								
	s[c]	④	45 0 0	8.78−09	1.59	4.47−09	1.41	1.78−09	1.45
	s	⑤	65 0 0	2.99−10	2.10	1.24−10	1.91	4.69−11	2.04
		⑥	85 0 0	1.48−11	4.04	4.10−12	3.55	1.35−12	3.84
Bi line	s	⑦	5 4 0	1.62−08	1.90	6.62−09	1.73	2.51−09	1.77
	s	⑧	35 4 0	7.15−10	2.52	1.80−10	2.00	5.97−11	1.95
	s								
	1	⑨	45 4 0	1.14−09	1.65	2.40−10	1.54	7.23−11	1.58
	i	⑩	65 4 0	3.31−10	1.72	1.27−10	1.36	4.82−11	1.34
	t	⑪	85 4 0	5.68−11	1.13	2.19−11	0.694	8.29−12	0.641

[a] reactions/10^{24} detector atoms) / (1 source neutron)

[b] Read as 2.48×10^{-8}

[c] Type 304 stainless steel

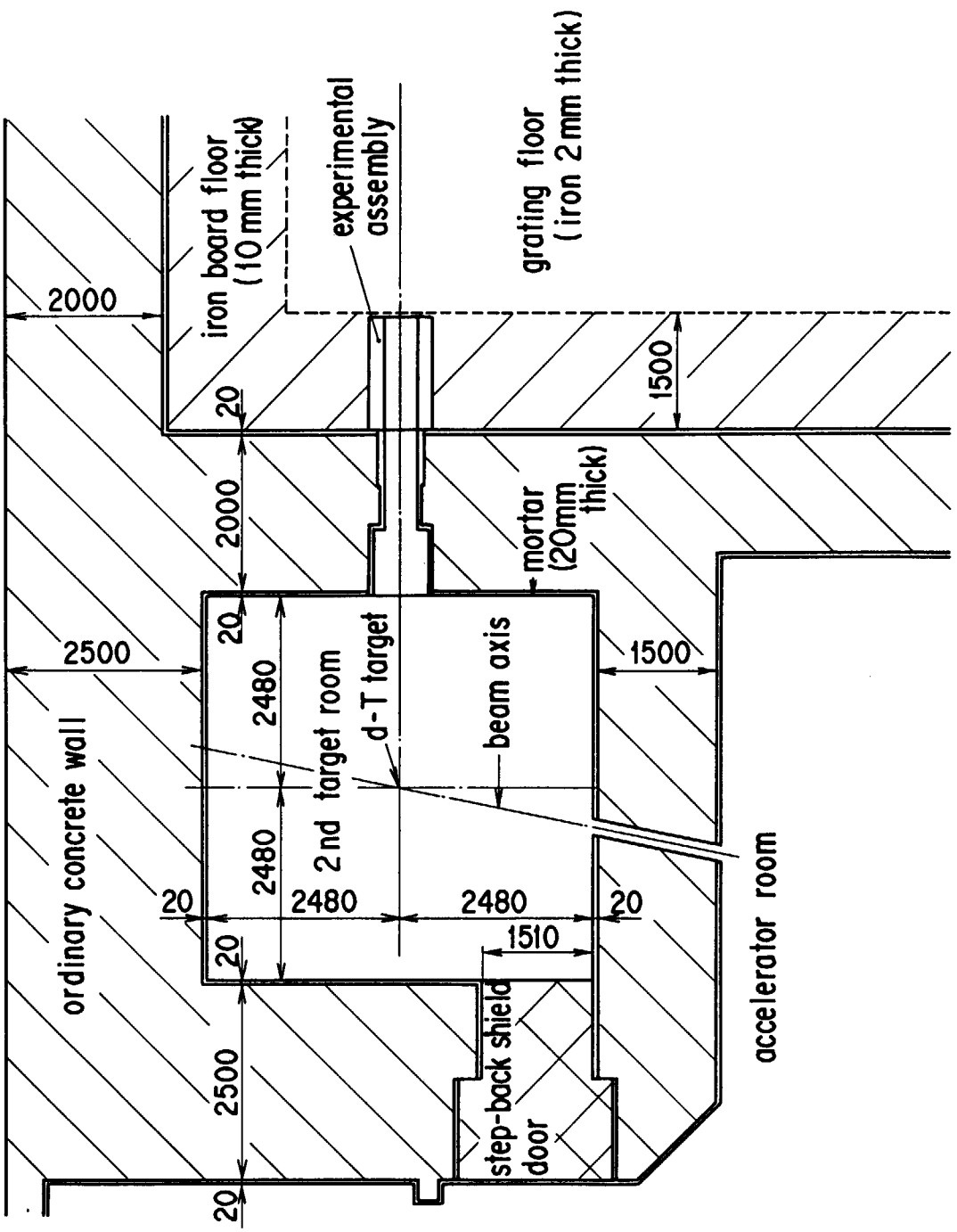

Fig. 4.13 Horizontal section of the accelerator room, the experimental port and the Type 304 stainless steel assembly (unit in mm)

gaps are strongly directive, and their behaviour is traced accurately only when the angular quadrature is matching with the direction. The S_8 approximation is insufficient for tracing the directive neutrons. More quadrature points, however, are unavailable, because about 22 hours of CPU+VU time and 440MB memory have been required for the present analysis. Besides, another difficulty has been made clear concerning to the coarse mesh rebalance. The coarse meshes in the present calculation are defined so that each of the slits is treated as a single coarse mesh, while the intensity and spectrum of neutrons are significantly different inside each slit and in the surrounding shield. Another systematic survey with the BERMUDA-2DN-S16 code suggests that an inappropriate setting of coarse meshes will introduce wrong results: the coarse meshes have to be given with consideration of the behaviour of neutrons.[19]

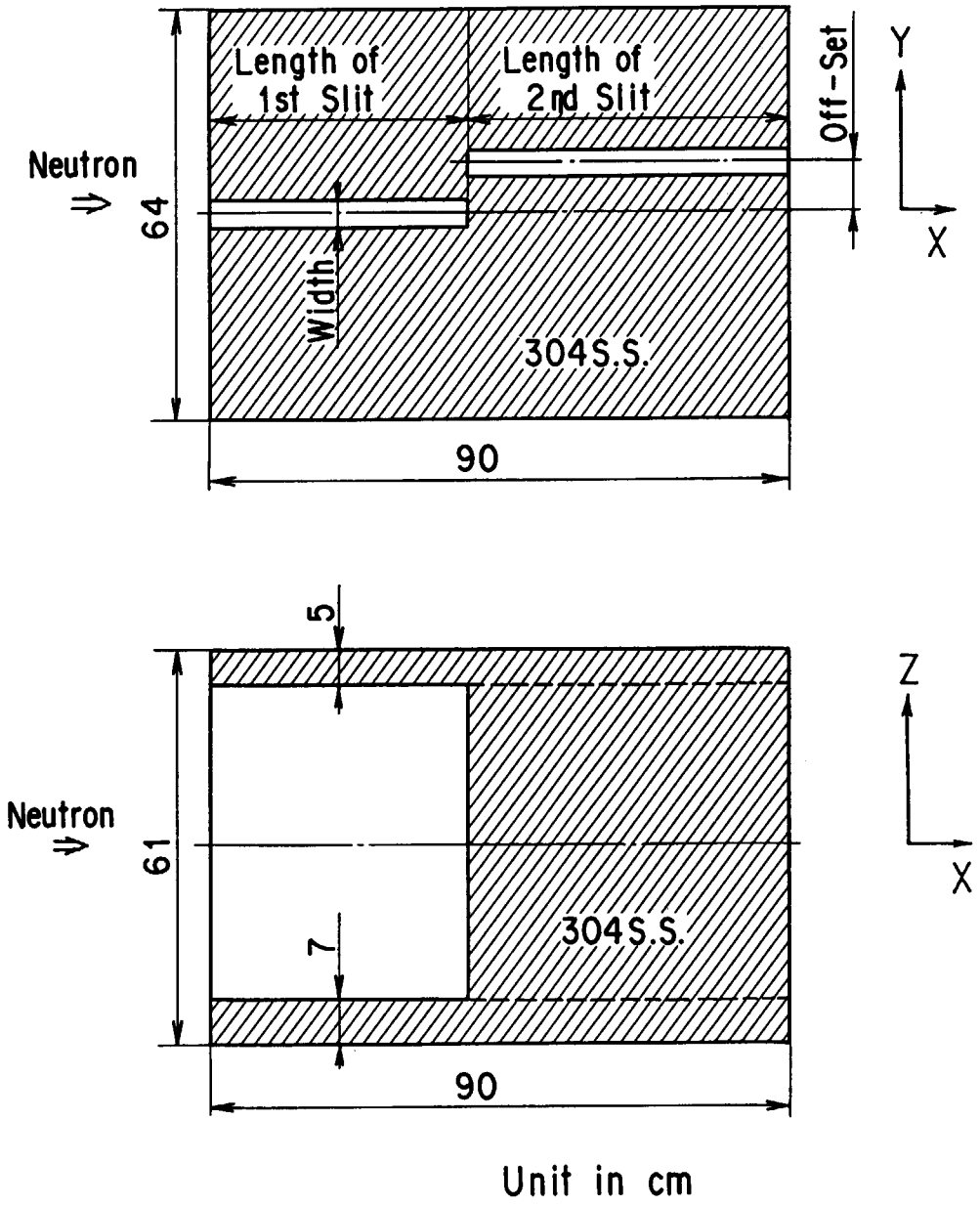

Fig. 4.14 Horizontal (x, y) and vertical (x, z) cross-section views of the experimental assembly

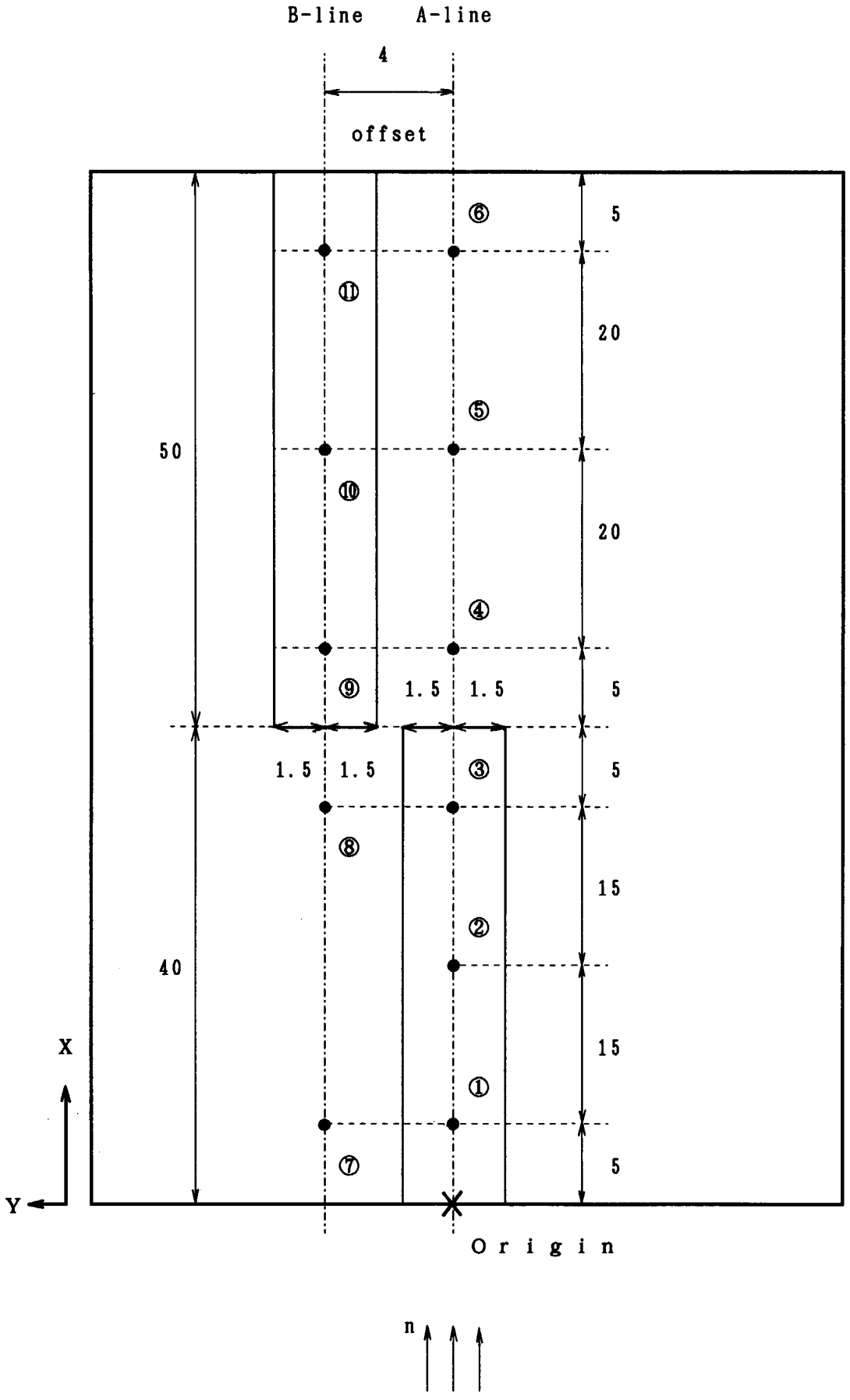

Fig. 4.15 The Positions of reaction rates measurement (unit in cm)

4.4 Summary

The validity tests of the neutron transport codes in the BERMUDA code system have been carried out using three kinds of shielding benchmark experiments for DT neutrons: deep penetration, cavity and slits streaming. The state-of-art of the present codes are summarized in the followings:

1) Fine energy meshes are essential for deep penetration problems, and the energy grid model used in the BERMUDA code is very effective.
2) The behaviour of neutrons in a cavity is dominated by backscattered neutrons. Therefore, the exact description of the angular dependence of scattering cross section is definitely important. In this point of view, the BERMUDA code using the P_∞ approximation is superior to other discrete ordinates codes such as DOT3.5. On the other hand, the usual energy model with iterations is sufficient, because the penetrated neutrons are negligible: the distribution is determined by neutrons with small number of scatterings.
3) The cavity problem has made clear the importance of the shallowly scattered neutrons in the vicinity of the cavity inlet. In order to obtain exactly the figure of distribution, exact angular scattering, higher order of Sn quadratures and exact treatment of the geometry are required. The BERMUDA-2DN and BERMUDA-2DN-S16 have a drawback in the description of the rectangular geometry, while BERMUDA-3DN has a difficulty in the applicable Sn quadratures because of the limitatiion of the computer available.
4) As for the offset slits streaming, the approximation of the geometry is very important and the BERMUDA-3DN code is essentially suitable. Nevertheless, it might be said that the BERMUDA-3DN code is not so practical for the streaming problems on the computer at the present, except for the cases where an accurate solution is needed in a localized region, because all variables of $(\vec{r},E,\vec{\Omega})$ are necessary to be dealt with very minutely in the problem.

5. User's Manual

5.1 BERMUDA-1DN

5.1.1 JCL

The JCL (a set of job control languages) for the BERMUDA-1DN execution on the FACOM/VP2600 computer in JAERI is as follows:

```
//JCLG JOB
// EXEC JCLG
//SYSIN DD DATA,DLM='++'
// JUSER xxxxxxxx, xx. xxxxxxxx, xxxx. xx
      T.05 W.03 C.00 I.02 E.01 SRP
      OPTP MSGCLASS=X,MSGLEVEL=(1, 1, 2), CLASS=0,NOTIFY=Jxxxx
      OPTP PASSWORD=xxxxxxxx
//    EXEC LMGO,LM=J9091.BERMD1DN($1)
//FT01F001 DD DISP=SHR,DSN=Jxxxx.FLUX1DN.DATA($2)
//FT02F001 DD UNIT=WK10,SPACE=(TRK, (100, 50)), DISP=(NEW, DELETE, DELETE),
//    DSN=&&WORK, DCB=(RECFM=VBS, LRECL=23472, BLKSIZE=23476, DSORG=PS)
//FT03F001 DD DISP=SHR, DSN=Jxxxx. SDB1DN. DATA($3)
//FT04F001 DD DISP=SHR, DSN=J3931. BERM125X. DATA, LABEL=(,,,IN)
//SYSIN     DD DISP=SHR, DSN=Jxxxx. DATA1DN. DATA($4)
++
//
```

($1) There has already been a load module J9091. BERMD1DN. LOAD prepared for a public use in JAERI.

If necessary, a new load module is able to be created on a disk from the source module J9091. BERMUDA. FORT77 (BERMD1DN). The JCL for creating a new load module is as follows:

```
//JCLG JOB
// EXEC JCLG
//SYSIN DD DATA,DLM='++'
// JUSER xxxxxxxx, xx. xxxxxxxx, xxxx. xx
      T.01 W.01 C.02 I.02 E.00 SRP
      OPTP MSGCLASS=X, MSGLEVEL=(1, 1, 2), NOTIFY=Jxxxx, PASSWORD=xxxxxxxx
//    EXEC FORT77VE, SO=J9091. BERMUDA,
//      A='ELM (BERMD1DN), SOURCE, NOVMSG, NOVSOURCE', LCT=62
//    EXEC LKEDCT77, LM=Jxxxx. BERMD1DN, UNIT=xxxxx, MODS='07, 07, 1', A=MAP
++
//
```

These steps of compilation and linkage are executed rather rapidly on the FACOM/M780 scalar computer. The new load module is applied by replacing the above "LM=J9091.BERMD1DN"($1) with "LM=Jxxxx. BERMD1DN".

($2) The flux file Jxxxx. FLUX1DN. DATA has to be allocated beforehand as:

```
//FT01F001 DD UNIT=xxxxx,SPACE= (TRK, (70, 10)),
//     DISP= (NEW, CATLG, CATLG), DSN=Jxxxx. FLUX1DN. DATA,
//     DCB= (RECFM=VBS, LRECL=23472, BLKSIZE=23476, DSORG=PS)
```

This file contains the angular and spatial distributions of neutron flux etc. for all of the calculated energy groups, which is processed for the output data edition with the post-processing codes.[6]

($3) The grid source file Jxxxx. SDB1DN. DATA has to be allocated beforehand as:

```
//FT03F001 DD UNIT=xxxxx, SPACE=(TRK, (10, 05)),
//     DISP=(NEW, CATLG, CATLG), DSN=Jxxxx. SDB1DN. DATA,
//     DCB=(RECFM=VBS, LRECL=23472, BLKSIZE=23476, DSORG=PS)
```

This file is necessary for restarting the job (see Sec. 3. 6. 2), and can be deleted after the calculation up to the last (IMAX-th) energy group has been completed.

Usually a one-dimensional problem is rapidly completed in a batch job. So, when required CPU time for the job is sufficient for completing calculation up to the last group, the one line of the JCL($3) may be substituted with

```
//FT03F001 DD DUMMY
```

without allocating the Jxxxx. SDB1DN. DATA.

($4) The input data file Jxxxx. DATA1DN. DATA has to be allocated beforehannd as:

```
//FT05F001 DD UNIT=xxxxx, SPACE=(TRK, (01, 01)),
//     DISP=(NEW, CATLG, CATLG), DSN=Jxxxx. DATA1DN. DATA,
//     DCB=(RECFM=FB, LRECL=80, BLKSIZE=3120, DSORG=PS)
```

The content of this file is described in Sec. 5. 1. 2.
Otherwise, the one line of the JCL($4) is substituted with

```
//SYSIN     DD  *
      [input data described in Sec. 5. 1. 2]
/*
```

without allocating the Jxxxx. DATA1DN. DATA.

5.1.2 Input Data

#01 (F6.0) 1 line

- TMAX (≡300.) : CPU time (sec) to terminate the job and to prepare the disk files for restarting the next job

#02 (I3) 1 line

- KIND(≡0) : dummy

#03 (2I3) 1 line

- IRSTRT($\equiv$1) : group no. to be restarted (initially$\equiv$1)
- ITMAX : maximum number of iteration times for each energy grid
  (ITMAX=1, 2 or 3)
  (ITMAX is defined as 1, if 0 or blank is input.)

#04 (18A4) 1 line

- Problem title : any characters, numbers or blanks describing the problem on columns 1$\sim$72

#05 (9I4, 2E12.5) 1 line

- IMAX : total number of energy groups for this problem ($\leqq$125)
- IP : geometry

$$IP=\begin{cases}0 \cdots \text{slab (infinite in x- and y-directions)}\\ 2 \cdots \text{sphere}\end{cases}$$

- MMAX : number of kinds of mixture ($\leqq$20)
- KMAX : number of spatial regions (MMAX$\leqq$KMAX$\leqq$20)
  (In a region, mixture is assigned to be homogeneous and mesh sizes (Δz or Δr) are assigned to be equal to each other.)
- IMAXL : total number of groups of the group constants library used
  (for example, IMAXL=125 for J3931. BERM125X. DATA)
- I1LIB : group no. "on the group constants library" where the group 1 is to be defined
  (for example, IMAX+I1LIB$\leqq$126 for J3931. BERM125X. DATA)

In BERMUDA, the I1LIB-th group on the library is called as "group 1".

- IFIS($\equiv$0) : dummy
- IPS : type of the fixed source

$$IPS=\begin{cases}0 \cdots \text{spatially distributed source}\\ 1 \cdots \text{point source (only at the center of the sphere)}\end{cases}$$

- INTPS($\equiv$0) : dummy
- ER : upper energy (eV) for the group 1 of the problem
  EUP (I1LIB+1)$<$ER$\leqq$EUP (I1LIB)
- EPS : convergence criterion (for angular flux) to be used to terminate the thermal group iteration
  (usually 10^{-3})

#06 (20I3) 1 line

- (MM (MK), MK=1, MMAX) : number of nuclides to be included in each mixture
  (1$\leqq$MM(MK)$\leqq$10)
  (For a vacuum, assign one dummy nuclide which is contained in another mixture. Input its code number in #12 and atomic number density (0.) in #13.)

#07 (10I6) [(KMAX+9)/10] lines

The brackets [$\cdots$] means the integer discarding the fractions.

• (MR (K), K=1, KMAX) : mixture no. (≡MK defined in #06) to be assigned to each region

#08 (10I6) [(KMAX+9)/10] lines

• (INTER (K), K=1, KMAX) : number of mesh intervals between the 'origin' and the outer boundary of each region (even number only)
(2≦INTER (1)<INTER (2)<⋯<INTER (KMAX)≦260−KMAX)

#09 (10F6.3) [(KMAX+9)/10] lines

• (DR (K), K=1, KMAX) : mesh size Δz or Δr (cm) for each region
(not the region thickness)

#10 (6E12.5) 2 lines

• (BCR (L), L=11, 20) : right (outer) boundary condition (10 words)

$$\text{BCR (L)} \equiv \begin{cases} -1. \cdots \text{symmetry condition (only for IP=0)} \\ 0. \cdots \text{vacuum boundary condition (for IP=0 and 2)} \end{cases}$$

(at the present, group independent only)

#11 (6E12.5) 2 lines when IP=0, not necessary when IP=2

• (BCL (L), L=1, 10) : left (origin) boundary condition for slab (10 words)

$$\text{BCL (L)} \equiv \begin{cases} -1. \cdots \text{symmetry condition} \\ 0. \cdots \text{vacuum boundary condition} \end{cases}$$

(at the present, group independent only)

#12 (10I6) MMAX lines

• (MCODE (M, MK), M=1, MM (MK)) : code no. of each nuclide in the mixture MK defined in the group constants library to be used (for example, see Table 2.2)
(The order of nuclides in a mixture is able to be arbitrary.)

Repeat this in the order of MK=1, ⋯, MMAX renewing the line for each mixture.

#13 (6E12.5) [{MM(MK)+5} /6] lines for each mixture

• (AN (M, MK), M=1, MM (MK)) : effective number density (10^{24}cm^{-3}) of each nuclide in the mixture MK
(The order of nuclides in a mixture must be same as in #12.)

Repeat this in the order of MK=1, ⋯, MMAX renewing the line for each mixture.

#14 (2I6) 1 line

• N1 : the first mesh point no. to give spatial distribution of non-zero independent source in #15
• N2 : the last mesh point no. to give spatial distribution of non-zero independent source in #15
If IPS=1 in #1 then N1=N2=1. Otherwise, 1≦N1<N2≦NMAX.
(NMAX: see (3) below)

In BERMUDA, the numbering of the mesh points is as follows:

(1) "1" for the origin,

(2) doubly (twice) numbered as "INTER(K)+K" and "INTER(K)+K+1" for the interface between the K-th and the (K+1)-th regions where K=1, ⋯, KMAX−1 (for treating spatial discontinuity of the macroscopic cross sections and the source distribution at the interface) and

(3) "NMAX=INTER (KMAX) +KMAX" (≦260) for the outermost mesh point.

#15 (6E12.5) {[(N2−N1)/6] +1} lines

• (S1 (N), N=N1, N2) : spatial distribution of independent source

Independent source is given in the form of a function with separation of variables as S1 (N) ×S2 (I) ×S3 (L).

(Each of the S1, S2 and S3 should be normalized to its correct magnitude, respectively. However, it is also valid that the product of the S1, S2 and S3 has the correct normalized value for each energy group (*).)

#16 (2I6) 1 line

• I1 : the first energy group no. to give energy spectre of non−zero independent source in #17

• I2 : the last energy group no. to give energy spectre of non−zero independent source in #17

If the source is mono−energy (monochromatic), I1=I2=1.

Otherwise, 1≦I1<I2≦IMAX.

#17 (6E12.5) {[(I2−I1)/6] +1} lines

• (S2 (I), I=I1, I2) : energy spectre of independent source

(As BERMUDA has been programmed not in a continuous energy model but in a usual multigroup model, only the S2 (except the S1 and S3) must be given as integrated value for group i over ΔE_i.)

The S2(I) is generally normalized to be 1 integrated over energy, that is,

$$\sum_{I=I1}^{I2} S2(I)=1.$$

(However, note the proviso (*) under #15.)

#18 (2I6) 1 line

• L1 : the first ordinate no. to give angular distribution of non−zero independent source in #19 (see Table 3.1)

• L2 : the last ordinate no. to give angular distribution of non−zero independent source in #19

If the source is mono−directional, L1=L2.

Otherwise, 1≦L1<L2≦20.

#19 (6E12.5) {[(L2−L1)/6] +1} lines

• (S3 (L), L=L1, L2) : angular distribution of independent source

The S3(L) is generally normalized to be 1 integrated over the unit sphere, that is,

$$2\pi \sum_{L=L1}^{L2} W_L S3\ (L)=1. \quad (W_L : \text{see Sec. 3. 4. 1 and Table 3.1})$$

(However, note the proviso(*) under #15.)

An example of input data for the BERMUDA−1DN is shown in Fig. 5.1.

5.1.3 Output Data

The output data of BERMUDA-1DN are stored on the magnetic disk FT01 (Jxxxx. FLUX1DN. DATA; see Sec. 5. 1. 1 ($2)) and are also given on the printer.

The data on the output disk are as follows:

(1) In case of IPS=0, the following FORTRAN record is repeated for each group i (i=1, ···, IMAX) in the binary form,

((PHI (N, L), N=1, 260), L=1, 20), (TPHI (N), N=1, 260),
((FEMK (M, MK), M=1, 10), MK=1, 20), ((FTMK (M, MK), M=1, 10), MK=1, 20),

where PHI (N, L) : $\phi^i(r_N, \omega_L)$,

TPHI (N) : $\Phi^i(r_N) = 2\pi \sum_{L=1}^{20} W_L \phi^i (r_N, \omega_L)$,

FEMK (M, MK) : $\bar{f}_e^{Mi}$ for mixture MK (see Sec. 2. 2 and Sec. 3. 1) and
FTMK (M, MK) : $\bar{f}_t^{Mi}$ for mixture MK (see Sec. 2. 2).

(2) In case of IPS=1, the following FORTRAN record is repeated for each group i (i=1, ···, IMAX) in the binary form,

```
                DATA SET NAME : J1057.BERMUDA.DATA(DATA1DN)
----+----1----+----2----+----3----+----4----+----5----+----6----+----7----+----8
 300.                                                                        #01
  0                                                                          #02
  1                                                                          #03
      J.N.S.T. VOL.14,210  BY SEKI,MAEKAWA        LI-C ASSEMBLY             #04
 117   2   4    4 125   9   0   1   0 1.455    +7 1.0      -3                #05
  4  6  5  4                                                                #06
     1     2     3     4                                                    #07
    20    44    66    82                                                    #08
 0.5  1.0058.96136.91938                                                    #09
 0.          0.          0.          0.          0.          0.            #10
 0.          0.          0.          0.                                     "
   240   260   280   250                                                    #12
    36    37   240   260   280   250                                        "
    60   240   260   280   250                                              "
   240   260   280   250                                                    "
 1.751    -3 6.349    -3 7.303    -4 8.185    -5                           #13
 2.507    -3 3.128    -2 3.086    -3 1.075    -2 1.374    -3 2.023    -4   "
 6.930    -2 1.751    -3 6.349    -3 7.303    -4 8.185    -5               "
 1.161    -3 4.159    -3 4.821    -4 5.632    -5                           "
     1     1                                                              #14
 1.                                                                         #15
     1     1                                                              #16
 1.                                                                         #17
     1    20                                                              #18
 7.957747 -2 7.957747 -2 7.957747 -2 7.957747 -2 7.957747 -2 7.957747 -2  #19
 7.957747 -2 7.957747 -2 7.957747 -2 7.957747 -2 7.957747 -2 7.957747 -2   "
 7.957747 -2 7.957747 -2 7.957747 -2 7.957747 -2 7.957747 -2 7.957747 -2   "
 7.957747 -2 7.957747 -2                                                    "
```

Fig. 5.1 Example of input data for the BERMUDA-1DN

((PHI (N, L), N=1, 260), L=1, 20), (TPHI (N), N=1, 260),
((FEMK (M, MK), M=1, 10), MK=1, 20), ((FTMK (M, MK), M=1, 10), MK=1, 20),
(PHI0 (N), N=1, 260), (PHI00(L), L=1, 20),

where PHI (N, L) : ϕ^i (r_N, ω_L) (without component of uncollided flux),

TPHI (N) : $\Phi^i(r_N) = 2\pi \sum_{L=1}^{20} W_L \phi^i(r_N, \omega_L) + \Phi_0^i(r_N)$,

FEMK (M, MK) : see above (1),
FTMK (M, MK) : see above (1),
PHI0 (N) : $\Phi_0^i(r_N)$ (uncollided flux) and
PHI00 (L) : $S^i(0, \omega_L)$ (point source at the origin).

The data on the output print are as follows:

(a) list of input file Jxxxx. DATA1DN. DATA (see Sec. 5. 1. 1 ($4)) like Fig. 5. 1,
(b) list of the main input parameters with explanatory captions,

(The items (c) ~ (f) below are repeated for each energy group i (i=1, ···, IMAX).)

(c) CPU+VU time (sec) accumulated from the start of computation (EXEC LMGO) until the end of each main calculational item,
(d) when the convergence has been attained or ITMAX iterations have been finished for the 10–th grid,
- neutron balance parameters; F, GAIN, ABBS, SELF, XLEK (see Sec. 3. 7) integrated over the entire spatial region dealing with it as a single coarse mesh region,
- group no. i, iteration times IT, residual VERGF,

where $VERGF = \max_{N, L} |\{\phi^{i(IT-1)}(r_N, \omega_L)/\phi^{i(IT)}(r_N, \omega_L) - 1| < \varepsilon$

(N, L : except the cases where $\phi^{i(IT)}(r_N, \omega_L) = 0$),
IT : iteration times (IT=1, 2, ···),

(When the energy grid model is used for the group i, these printed neutron balance parameters and VERGF are meaningless, because the iteration is terminated by ITMAX ($\leq$3) times. In addition, these parameters are obtained only from the data of the last (10–th) grid in the group i.)

(e) • the upper energy boundary EUP (i) (eV),
• the lower energy boundary EUP (i+1) (eV),
• the energy width ΔE_i (eV) and
(f) neutron scalar flux $\Phi^i(r_N)$ for N=1, ···, NMAX.

The STOP code 2222 indicates that the input fixed source for the group 1 is 0.

5.2 BERMUDA-2DN

5.2.1 JCL

The JCL for the BERMUDA-2DN execution on the FACOM/VP2600 computer in JAERI is as follows;

```
//JCLG JOB
// EXEC JCLG
//SYSIN DD DATA, DLM='++'
// JUSER xxxxxxxx,xx.xxxxxxxx, xxxx. xx
      T.12 W.06 C.00 I.10 E.04 SRP
      OPTP MSGCLASS=X, MSGLEVEL=(1, 1, 2), CLASS=7, NOTIFY=Jxxxx($1)
      OPTP PASSWORD=xxxxxxxx
//    EXEC LMGO, LM=J9091. BERMD2DN,A='HIO=(01, 09)' ($2)
//FT01F001 DD DISP=SHR, DSN=Jxxxx. FLX601. DATA($3)
//FT02F001 DD DISP=SHR, DSN=Jxxxx. BOUNDFLX. DATA($4)
//FT03F001 DD UNIT=WK10, SPACE=(TRK, (100, 50)), DISP=(NEW, DELETE, DELETE),
//    DSN=&&WORK, DCB=(RECFM=VBS, LRECL=23472, BLKSIZE=23476, DSORG=PS)
//FT04F001 DD DISP=SHR, DSN=J3931. BERM125X. DATA. LABEL=(, , , IN)
//SYSIN    DD DISP=SHR, DSN=Jxxxx. DATA2DN. DATA($5)
//FT08F001 DD DISP=SHR, DSN=Jxxxx. FLUX2DN. DATA($6)
//FT09F001 DD DISP=SHR, DSN=Jxxxx. FLX609. DATA($7)
//FT12F001 DD DISP=SHR, DSN=Jxxxx. SDB2DN. DATA($8)
++
//
```

($1) "CLASS=7" is a night job for free submission. Beside this, there are the classes 6 and 8 which need an approval of the Computing and Information Systems Center of JAERI for submission, and of which the class 8 is a night job. For these classes, permitted CPU time (T. xx), print lines (W. xx) and I/O times (EXCP I. xx) have different values from those of the class 7.

($2) There has already been a load module J9091. BERMD2DN. LOAD prepared for a public use in JAERI.

If necessary, a new load module is able to be created on a disk from the source module J9091. BERMUDA. FORT77 (BERMD2DN). The JCL for creating a new load module is as follows:

```
//JCLG JOB
// EXEC JCLG
//SYSIN DD DATA, DLM='++'
// JUSER xxxxxxxx, xx. xxxxxxxx, xxxx. xx
      T.02 W.03 C.02 I.02 E.00 SRP
      OPTP MSGCLASS=X, MSGLEVEL=(1, 1, 2), NOTIFY=Jxxxx, PASSWORD=xxxxxxxx
//    EXEC FORT77VE, SO=J9091. BERMUDA,
//      A='ELM(BERMD2DN), SOURCE, NOVMSG, NOVSOURCE', LCT=62
//    EXEC LKEDCT77, LM=Jxxxx. BERMD2DN, UNIT=xxxxx, MODS='11, 11, 1', A=MAP
++
//
```

These steps of compilation and linkage are executed rather rapidly on the FACOM/M780 scalar computer. The new load module is applied by replacing the above "LM=J9091.BERMD2DN"($2) with "LM=Jxxxx.BERMD2DN".

($3) The HIO (high-speed input/output) work file for the angular and scalar fluxes Jxxxx. FLX601. DATA has to be allocated beforehand as:

```
//FT01F001 DD UNIT=TSSWK, SPACE=(CYL, 250,, CONTIG),
//     DISP=(NEW, CATLG, CATLG), DSN=Jxxxx. FLX601. DATA,
//     DCB=(RECFM=F, LRECL=23000, BLKSIZE=23000, DSORG=PS)
```

This file contains the spatial distributions of the angular and scalar neutron fluxes for all of the calculated energy groups as a HIO work file for calculating the slowing down source from the upper energy groups.

So, this file can be deleted after the job has been successfully terminated in TMAX sec (see Sec. 5. 2. 2) because the same data are stored in the FT08 (Jxxxx. FLUX2DN. DATA($6)) for restarting the job. The main purpose of the FT01($3) and FT09($7) is to utilize the HIO option for saving the I/O times (EXCP). In fact, the TSSWK is automatically deleted at 8:00 a. m. (the TSSWK2 at 5: 00 p. m.) in JAERI. The HIO option needs to allocate the file 'contiguously' on the disk (CONTIG), and the FT01 and FT09 need to be allocated every time (or every day) before submitting the restarting job.

At the present, the specifications of the disk in JAERI are as follows:

1 VOL=1,326 CYL×2 (=19, 890 TRK×2),
1 CYL=15 TRK and
1 TRK=47, 476 bytes.

However, BLKSIZE cannot exceed 32, 767 bytes.

($4) The boundary flux file Jxxxx. BOUNDFLX. DATA has to be allocated beforehand as:

```
//FT02F001 DD UNIT=xxxxx, SPACE=(TRK, (20, 05)),
//     DISP=(NEW, CATLG, CATLG), DSN=Jxxxx. BOUNDFLX. DATA,
//     DCB=(RECFM=VBS, LRECL=23472, BLKSIZE=23476, DSORG=PS)
```

This file contains the boundary flux in case of the bootstrap option (see Sec. 3. 6. 2). In the first step, the boundary flux is written in this file; and in the second step, the boundary flux is supplied from the file. When the bootstrap option is not used (ISTEP=0 in Sec. 5. 2. 2), the one line of the JCL($4) is not necessary as well as allocation of the file.

($5) The input data file Jxxxx. DATA2DN. DATA has to be allocated beforehand as:

```
//FT05F001 DD UNIT=xxxxx, SPACE=(TRK, (01, 01)),
//     DISP=(NEW, CATLG, CATLG), DSN=Jxxxx. DATA2DN. DATA,
//     DCB=(RECFM=FB, LRECL=80, BLKSIZE=3120, DSORG=PS)
```

The content of this file is described in Sec. 5. 2. 2.
Otherwise, the one line of the JCL($5) is substituted with

```
//SYSIN     DD  *
      [input data described in Sec. 5. 2. 2]
/*
```

without allocating the Jxxxx. DATA2DN. DATA.

($6) The flux file Jxxxx. FLUX2DN. DATA has to be allocated as:

```
//FT08F001 DD UNIT=xxxxx, SPACE=(TRK, (3650, 50)),
//     DISP=(NEW, CATLG, CATLG), DSN=Jxxxx. FLUX2DN. DATA,
//     DCB=(RECFM=VBS, LRECL=23472, BLKSIZE=23476, DSORG=PS)
```

This file contains the angular and spatial distributions of neutron flux etc. for all of the calculated energy groups. It is used for restarting the job for energy group continuation. After the computation has been completed for all of the energy groups and the bootstrap steps, it is processed for the output data edition with the post-processing codes.[6)]

Note that the contents of the Jxxxx. FLUX2DN. DATA for the bootstrap step 1 vanish when the same file is used in the step 2. Usually comparison of the output data with the measured data concerns the region of the step 2. However, if it is necessary to save the data obtained in the step 1, dual files have to be allocated as Jxxxx. FLUX2DN1. DATA and Jxxxx. FLUX2DN2. DATA for each step.

($7) The HIO work file for the uncollided flux and the resonancne self-shielding factors Jxxxx. FLX609. DATA has to be allocated beforehand as:

```
//FT09F001 DD UNIT=TSSWK, SPACE=(CYL, 13,, CONTIG),
//     DISP=(NEW, CATLG, CATLG), DSN=Jxxxx. FLX609. DATA,
//     DCB=(RECFM=F, LRECL=23000, BLKSIZE=23000, DSORG=PS)
```

This file contains the spatial distribution of the uncollided neutron flux etc. for all of the calculated energy groups as a HIO work file for calculating the first collision source from the self and the upper groups in Eq. (3. 23). If IPS=0, it contains only the resonance self-shielding factors of which the $\bar{f}_e^{mi}$ is used in the F_L^{mj} in Eq. (3. 3). So '13 CYL' is too much, and '1 CYL' may be sufficient when IPS=0.

This file can also be deleted after the job has been successfully terminated in TMAX sec same as the FT01, because the same data are stored in the FT08 for restarting the job.

($8) The grid source file Jxxxx. SBD2DN. DATA has to be allocated beforehand as:

```
//FT12F001 DD UNIT=xxxxx, SPACE=(TRK, (280, 20)),
//     DISP=(NEW, CATLG, CATLG), DSN=Jxxxx. SDB2DN. DATA,
//     DCB= (RECFM=VBS, LRECL=23472, BLKSIZE=23476, DSORG=PS)
```

This file is necessary for restarting the job as well as the FT08, and can be deleted after the calculation up to the IMAX-th group has been completed (in case of ISTEP≠0, up to the IMAX-th group in the step 2). The contents of the FT12 are:

(1) the group no. i_R (Up to the i_R group the calculation has been completed.) and

(2) the grid source into the ten grids within the group (i_R+1) from the groups $1\sim(i_R-1)$ and from the ten grids within the group i_R.

5.2.2 Input Data

#01 (F6.0) 1 line

- TMAX : CPU time (sec) to terminate the job and to prepare the disk files for restarting the next job
  (If CLASS=7, then TMAX=6900.)

#02 (4I3) 1 line

- IRSTRT : group no. to be restarted (initially≡1)
- ISTEP : step no. for bootstrap option

$$\text{ISTEP}=\begin{cases}0 \cdots \text{no bootstrap option}\\ 1 \cdots \text{the first step}\\ 2 \cdots \text{the second step}\end{cases}$$

- IFACE : interface z-mesh point no. for bootstrap option (0 when ISTEP=0)
  IFACE must be on the bottom boundary mesh point of a partition in the z-direction. (The numbering method for mesh points is described in #10.)
  When ISTEP=2, IFACE is different value from that in ISTEP=1.
- ITMAX : maximum number of iteration times for each energy grid
  (ITMAX=1, 2 or 3)
  (ITMAX is defined as 1, if 0 or blank is input.)

#03 (18A4) 1 line

- Problem title : any characters, numbers or blanks describing the problem on columns 1~72

#04 (9I4, 2E12. 5) 1 line

- IMAX : total number of energy groups for this problem (≦125)
- MMAX : number of mixtures (≦20)
- KMAX : number of spatial regions (MMAX≦KMAX)
  Definition of a 'region' is that it is a rectangular part on the (r, z) plane, where mixture is assigned to be homogeneous.
  The (r, z) plane must be completely covered with the KMAX regions. Actually a 'region' is a ring-shaped volume made by rotating the rectangle around the axis of the cylinder (r=0).
- IMAXL : total number of groups of the group constants library used
  (for example, IMAXL=125 for J3931. BERM125X. DATA)
- I1LIB : group no. "on the group constants library" where the group 1 of this problem is to be defined
  (for example, IMAX+I1LIB≦126 for J3931. BERM125X. DATA)

In BERMUDA, the I1LIB-th group on the library is called as "group 1".

- IFIS(≡0) : dummy
- IPS : type of the fixed source

$$\text{IPS}=\begin{cases}0 \cdots \text{spatially distributed source}\\ \text{IZPS} \cdots \text{point source on the z-axis of the cylinder (IZPS}\geqq 1)\end{cases}$$

The IZPS is the z-mesh point no. for the point source. When IZPS=1, z (IZPS)=0

(origin). The numbering method for the mesh points is described in #10. The point source cannot be placed on an interface between partitions in the z-direction.

- NRR : number of partitions in the r-direction (NRR≦20)
  In each partition, mesh sizes (Δr) are assigned to be equal to each other.
- NRZ : number of partitions in the z-direction (NRZ≦20)
  In each partition, mesh sizes (Δz) are assigned to be equal to each other.
- ER : upper energy (eV) for the group 1 of the problem
  EUP (I1LIB+1)<ER≦EUP (I1LIB)
- EPS : convergence criterion (for angular flux) to be used to terminate the thermal group iteration (usually 10^{-3})

#05 (20I3) 1 line

- (MM (MK), MK=1, MMAX) : number of nuclides to be included in each mixture
  (1≦MM (MK)≦10)
  (For a vacuum, assign one dummy nuclide which is contained in another mixture. Input its code number in #12 and atomic number density (0.) in #13.)
  In a problem, maximum 20 nuclides can be selected out of 30 or 24 nuclides in the libraries. The definition of the maximum 'number' is that a nuclide contained commonly in plural number of mixtures is counted as 1, notwithstanding that the nuclide has equal or not equal atomic number densities in those mixtures.

#06 (10I6) [(NRR+9)/10] lines

The brackets [···] means the integer discarding the fractions.

- (INTERR (KR), KR=1, NRR) : number of mesh intervals between the origin and the outer boundary of each partition in the r-direction
  (Either even or odd numbers are valid.)
  (1≦INTERR (1)<INTERR (2)<···<INTERR (NRR)≦60-NRR)

#07 (10F6.3) [(NRR+9)/10] lines

- (DRR (KR), KR=1, NRR) : mesh size Δr (cm) for each partition in the r-direction
  (not the partition thickness)

#08 (10I6) [(NRZ+9)/10] lines

- (INTERZ (KZ), KZ=1, NRZ) : number of mesh intervals between the origin and the top boundary of each partition in the z-direction
  (Either even or odd numbers are valid.)
  (1≦INTERZ (1)<INTERZ (2)<···<INTERZ (NRZ)≦110-NRZ)

#09 (10F6. 3) [(NRZ+9)/10] lines

- (DZZ (KZ), KZ=1, NRZ) : mesh size Δz (cm) for each partition in the z-direction
  (not the partition thickness)

#10 (5I6) KMAX lines

- (J1 (K), J2 (K), I1 (K), I2 (K), MR (K), K=1, KMAX) : assignment of composition
  J1 (K) : left mesh point no. of the region K

J2 (K) : right mesh point no. of the region K
I1 (K) : bottom mesh point no. of the region K
I2 (K) : top mesh point no. of the region K
MR (K) : mixture no. for the region K (≡MK defined in #05)
($1 \leqq J1 < J2 \leqq NRMAX \leqq 60$ and $1 \leqq I1 < I2 \leqq NZMAX \leqq 110$)

In BERMUDA, the numbering of the mesh points is as follows:
(1) "1" for the origin,
(2) doubly (twice) numbered as "INTERR(KR)+KR" and "INTERR(KR)+KR+1" for the interface between the KR-th and the (KR+1)-th partitions in the r-direction where KR= 1, ···, NRR-1 (for treating spatial discontinuity of the macroscopic cross sections and the source distribution at the interfaces) and
(3) "NRMAX=INTERR (NRR)+NRR"≦60 for the outermost mesh point in the r-direction.
And it is same for the z-direction except "NZMAX=INTERZ (NRZ)+NRZ"≦110.

#11 (2F6.3) 1 line
- BCTOP : top boundary condition for z=z (NZMAX)
- BCBOT : bottom boundary condition for z=0.

$$\text{boundary conditions} \equiv \begin{cases} -1. \cdots \text{symmetry condition} \\ 0. \cdots \text{vacuum boundary condition} \end{cases}$$

#12 (10I6) MMAX lines
- (MCODE (M, MK), M=1, MM (MK)) : code no. of each nuclide in the mixture MK defined in the group constants library to be used (for example, see Table 2. 2)
(The order of nuclides in a mixture is able to be arbitrary.)

Repeat this in the order of MK=1, ···, MMAX renewing the line for each mixture.

#13 (6E12. 5) [{MM(MK)+5} /6] lines for each mixture
- (AN (M, MK), M=1, MM(MK)) : effective number density ($10^{24}cm^{-3}$) of each nuclide in the mixture MK
(The order of nuclides in a mixture must be same as in #12.)

Repeat this in the order of MK=1, ···, MMAX renewing the line for each mixture.

#14 (4I6) 1 line
- IZ1 : the first mesh point no. to give axial distribution of non-zero independent source in #15
- IZ2 : the last mesh point no. to give axial distribution of non-zero independent source in #15
- JR1 : the first mesh point no. to give radial distribution of non-zero independent source in #15
- JR2 : the last mesh point no. to give radial distribution of non-zero independent source in #15

These mesh points must be given in the definition of (1)~(3) in #10 ($1 \leqq IZ1 \leqq IZ2 \leqq$ NZMAX and $1 \leqq JR1 \leqq JR2 \leqq$ NRMAX). When IPS=0 in #04 and IZ1<IZ2 and JR1< JR2, S1 in #15 is a volume source. When IPS≠0, S1 is a point source (IZ1=IZ2=IPS and JR1=JR2=1).

#15 (6E12.5) {[(JR2-JR1)/6] +1} lines
- (S1 (JR, IZ), JR=JR1, JR2) : spatial distribution of independent source

Independent source is given in the form of a function with separation of variables as

S1 (JR, IZ)×S2 (I)×S3 (L).

(Each of the S1, S2 and S3 should be normalized to its correct magnitude, respectively. However, it is also valid that the product of the S1, S2 and S3 has the correct normalized value for each energy group (*).)

Repeat this in the order of IZ=IZ1, ···, IZ2.

#16 (216) 1 line

- I1 : the first energy group no. to give energy spectre of non-zero independent source in #17
- I2 : the last energy group no. to give energy spectre of non-zero independent source in #17

If the source is of mono-energy (monochromatic), I1=I2=1.

Otherwise, $1 \leqq I1 < I2 \leqq IMAX$.

#17 (6E12. 5) {[(I2-I1)/6] +1} lines

- (S2 (I), I=I1, I2) : energy spectre of independent source

(As BERMUDA has been programmed not in a continuous energy model but in a usual multigroup model, only the S2 (except the S1 and S3) must be given as integrated value for group i over ΔE_i.)

The S2 (I) is generally normalized to be 1 integrated over energy, that is,

$$\sum_{I=I1}^{I2} S2(I) = 1.$$

(However, note the proviso (*) under #15.)

#18 (2I6) 1 line

- L1 : the first ordinate no. to give angular distribution of non-zero independent source in #19 (see Fig. 3. 3)
- L2 : the last ordinate no. to give angular distribution of non-zero independent source in #19

If the source is mono-directional, L1=L2.

Otherwise, $1 \leqq L1 < L2 \leqq 40$. (S3 (L) for L=41, ···, 48 are automatically assumed to have equal values to the adjacent (just right) ordinates, respectively.)

#19 (6E12.5) {[(L2-L1)/6] +1} lines

- (S3 (L), L=L1, L2) : angular distribution of independent source The S3 (L) is generally normalized to be 1 integrated over the unit sphere, that is,

$$\sum_{L=L1}^{L2} \Delta\vec{\Omega}_L S3\ (L) = 1.$$

(However, note the proviso (*) under #15.)

Some examples of input data for the BERMUDA-2DN are shown in Fig. 5. 2. and 5. 3.

5.2.3 Output Data

The output data of BERMUDA-2DN are stored on the magnetic disk FT08 (Jxxxx. FLUX2DN. DATA; see Sec. 5. 2. 1 ($6)) and are also given on the printer.

The data on the output disk are as follows:

(1) In case of IPS=0, the following FORTRAN record is repeated for each group i (i=1, ···, IMAX) in the binary form.

```
                DATA SET NAME : J1057.BERMUDA.DATA(DATA2DN1)
----+----1----+----2----+----3----+----4----+----5----+----6----+----7----+----8
 6900.                                                                        #01
  1  1 33  1                                                                 #02
  SECOND TARGET ROOM SYMM. 19/11/86 TUE. ENERGY 66G MESH TUNNING              #03
  66   4  11 125   5   0   1   8   5 1.5488   +7 5.0      -3                  #04
  2 10  7  9                                                                  #05
     6     7     8    10    11    36    37    42                             #06
3.75  0.8   2.5   4.6   0.8   8.488 2.0   12.0                               #07
    16    17    27    28    45                                              #08
15.5  2.0   7.8   1.6   4.0                                                  #09
     1    42     1    17     1    REG 1 AIR FRONT PART                       #10
    43    44     1    17     2    REG 2 MORTAR                                "
    45    50     1    19     3    REG 3 ROOM WALL                             "
     1    14    18    30     1    REG 1-2 AIR FRONT PART                      "
    15    16    18    30     4    REG 4 FE TEST PORT FLAME                    "
    17    44    18    19     2    REG 2-2 MORTAR                              "
    17    50    20    32     3    REG 3-2 ROOM WALL                           "
     1     7    31    32     1    REG 1-3 AIR FRONT PART                      "
     8    16    31    32     4    REG 4-3 FE TEST PORT SUS316                 "
     1     9    33    50     4    REG 4-4 FE TEST PORT SUS316                 "
    10    50    33    50     3    REG 3-3 ROOM WALL                           "
 0.   -1.                                                                     #11
    70    80                                                                 #12
    11    80    80   130   130   130   140   140   140   260                 "
    80    11   130   130   130   140   260                                   "
    60   140   140   140   240   250   260   280   420                       "
3.8810   -5 1.0400   -5                                                     #13
9.4246   -3 7.4297   -4 3.7680   -2 5.0802   -4 4.6874   -4 1.9408   -3      "
1.1347   -2 3.3427   -4 3.7143   -3 6.8100   -4                              "
4.31509  -2 7.9740   -3 5.4090   -4 7.8590   -4 3.0194   -3 1.7903   -2      "
5.8590   -4                                                                  "
3.1729   -4 1.6962   -3 6.9211   -5 4.4572   -5 1.5575   -2 1.7343   -3      "
5.5740   -2 9.7339   -3 1.2421   -3                                          "
     1     1     1     1                                                    #14
7.95775E-02                                                                 #15
     1    66                                                                #16
  2.0282-08   1.6009-05   2.2393-04   2.1827-03   1.0623-01   7.0219-01    #17
  4.0324-02   8.6730-03   2.8072-03   1.9716-03   2.1199-03   2.1551-03     "
  1.7718-03   1.3596-03   1.1058-03   9.8002-04   9.2473-04   8.2910-04     "
  7.5409-04   6.0028-04   5.4624-04   5.1257-04   4.8040-04   4.1078-04     "
  4.5049-04   4.1154-04   4.7600-04   4.9296-04   1.8409-03   1.8610-03     "
  1.7291-03   1.8799-03   1.9314-03   1.8899-03   1.7907-03   1.6436-03     "
  1.5582-03   1.6650-03   1.6286-03   1.7793-03   1.8020-03   1.9477-03     "
  1.9063-03   1.9100-03   1.9603-03   2.2028-03   2.1438-03   2.2946-03     "
  2.2418-03   2.1865-03   2.3360-03   2.3938-03   2.1764-03   2.1903-03     "
  2.3662-03   2.2569-03   4.1317-03   4.4672-03   4.3554-03   4.1279-03     "
  3.9131-03   3.7597-03   3.4531-03   3.1428-03   2.8487-03   2.6150-03     "
     1    40                                                                #18
 1.          1.          1.          1.          1.          1.             #19
 1.          1.          1.          1.          1.          1.              "
 1.          1.          1.          1.          1.          1.              "
 1.          1.          1.          1.          1.          1.              "
 1.          1.          1.          1.          1.          1.              "
 1.          1.          1.          1.          1.          1.              "
 1.          1.          1.          1.                                      "
```

Fig. 5.2 Example of input data for the BERMUDA-2DN (ISTEP=1)

(((PHI (JR, IZ, L), L=1, LMAX), IZ=1, NZMAX), JR=1, NRMAX),
((TPHI (JR, IZ), IZ=1, NZMAX), JR=1, NRMAX),
((FEMK (M, MK), M=1, 10), MK=1, 20), ((FTMK (M, MK), M=1, 10), MK=1, 20),

where PHI (JR, IZ, L) : $\phi^i(r_{JR}, z_{IZ}, \vec{\Omega}_L)$,

DATA SET NAME : J1057.BERMUDA.DATA(DATA2DN2)

```
----+----1----+----2----+----3----+----4----+----5----+----6----+----7----+----8
 6900.                                                                      #01
  1  2  9  1                                                                #02
 STEP-2 SUS316 ASSEMBLY DEEP PENETRATION 21/11/86 FRI. 66G MESH TUNNING     #03
  66   4  13 125   5   0   1   8   8 1.5488   +7 5.0      -3                 #04
  2 10  7  9                                                                #05
     6     7     8    10    11    36    37    42                           #06
3.75  0.8   2.5   4.6   0.8   8.488 2.0   12.0                             #07
     1     2     3     4    14    24    34    42                           #08
248.0 2.0   78.0  1.6   2.96  2.96  3.06  3.825                            #09
     1    42     1     2     1    REG 1 AIR FRONT PART                     #10
    43    44     1     2     2    REG 2 MORTAR                              "
    45    50     1     4     3    REG 3 ROOM WALL                           "
     1    14     3     6     1    REG 1-2 AIR FRONT PART                    "
    15    16     3     8     4    REG 4 FE TEST PORT FLAME                  "
    17    44     3     4     2    REG 2-2 MORTAR                            "
    17    50     5     8     3    REG 3-2 ROOM WALL                         "
     1     7     7     8     1    REG 1-3 AIR FRONT PART                    "
     8    14     7     8     4    REG 4-2 FE TEST PORT FLAME                "
     1     9     9    30     4    REG 4-3 FE TEST PORT SUS316               "
    10    50     9    30     3    REG 3-3 ROOM WALL                         "
     1    11    31    50     4    REG 4-4 FE TEST PORT SUS316               "
    12    50    31    50     3    REG 3-4 ROOM WALL                         "
 0.   -1.                                                                   #11
    70    80                                                               #12
    11    80    80   130   130   130   140   140   140   260               "
    80    11   130   130   130   140   260                                 "
    60   140   140   140   240   250   260   280   420                     "
 3.8810   -5 1.0400   -5                                                   #13
 9.4246   -3 7.4297   -4 3.7680   -2 5.0802   -4 4.6874   -4 1.9408   -3   "
 1.1347   -2 3.3427   -4 3.7143   -3 6.8100   -4                           "
 4.31509  -2 7.9740   -3 5.4090   -4 7.8590   -4 3.0194   -3 1.7903   -2   "
 5.8590   -4                                                               "
 3.1729   -4 1.6962   -3 6.9211   -5 4.4572   -5 1.5575   -2 1.7343   -3   "
 5.5740   -2 9.7339   -3 1.2421   -3                                       "
     1     1     1     1                                                  #14
 7.95775E-02                                                              #15
     1    66                                                              #16
   2.0282-08   1.6009-05   2.2393-04   2.1827-03   1.0623-01   7.0219-01  #17
   4.0324-02   8.6730-03   2.8072-03   1.9716-03   2.1199-03   2.1551-03   "
   1.7718-03   1.3596-03   1.1058-03   9.8002-04   9.2473-04   8.2910-04   "
   7.5409-04   6.0028-04   5.4624-04   5.1257-04   4.8040-04   4.1078-04   "
   4.5049-04   4.1154-04   4.7600-04   4.9296-04   1.8409-03   1.8610-03   "
   1.7291-03   1.8799-03   1.9314-03   1.8899-03   1.7907-03   1.6436-03   "
   1.5582-03   1.6650-03   1.6286-03   1.7793-03   1.8020-03   1.9477-03   "
   1.9063-03   1.9100-03   1.9603-03   2.2028-03   2.1438-03   2.2946-03   "
   2.2418-03   2.1865-03   2.3360-03   2.3938-03   2.1764-03   2.1903-03   "
   2.3662-03   2.2569-03   4.1317-03   4.4672-03   4.3554-03   4.1279-03   "
   3.9131-03   3.7597-03   3.4531-03   3.1428-03   2.8487-03   2.6150-03   "
     1    40                                                              #18
 1.          1.          1.          1.          1.          1.            #19
 1.          1.          1.          1.          1.          1.             "
 1.          1.          1.          1.          1.          1.             "
 1.          1.          1.          1.          1.          1.             "
 1.          1.          1.          1.          1.          1.             "
 1.          1.          1.          1.          1.          1.             "
 1.          1.          1.          1.                                     "
```

Fig. 5.3 Example of input data for the BERMUDA-2DN (ISTEP=2)

LMAX = { 40···when calculation has been completed until the group IMAX,
48···when calculation is to be restarted from the group (i_R+1),

NZMAX, NRMAX : see Sec.5.2.2 (#10).

TPHI (JR, IZ) : $\Phi^i(r_{JR}, z_{IZ}) = \sum_{L=1}^{40} \Delta\vec{\Omega}_L \phi^i(r_{JR}, z_{IZ}, \vec{\Omega}_L)$,

FEMK (M, MK) : $\bar{f}_e^{Mi}$ for mixture MK (see Sec.2.2 and Sec.3.1) and
FTMK (M, MK) : $\bar{f}_t^{Mi}$ for mixture MK (see Sec.2.2).

(2) In case of IPS≠0, the following FORTRAN record is repeated for each group i (i=1, ···, IMAX) in the binary form,

(((PHI (JR, IZ, L), L=1, LMAX), IZ=1, NZMAX), JR=1, NRMAX),
((PHI0 (JR, IZ), IZ=1, NZMAX), JR=1, NRMAX), (PHI00 (L), L=1, 40),
((TPHI (JR, IZ), IZ=1, NZMAX), IZ=1, NRMAX),
((FEMK (M, MK), M=1, 10), MK=1, 20), ((FTMK (M, MK), M=1, 10), MK=1, 20),

where PHI (JR, IZ, L) : $\phi^i(r_{JR}, z_{IZ}, \vec{\Omega}_L)$ (without component of uncollided flux),
LMAX, NZMAX, NRMAX : see above (1),
PHI0 (JR, IZ) : $\Phi_0^i(r_{JR}, z_{IZ})$ (uncollided flux),
PHI00 (L) : $S^i(0, z_{IZPS}, \vec{\Omega}_L)$ (point source),
TPHI (JR, IZ) : $\Phi^i(r_{JR}, z_{IZ}) = \sum_{L=1}^{40} \Delta\vec{\Omega}_L \phi^i(r_{JR}, z_{IZ}, \vec{\Omega}_L) + \Phi_0^i(r_{JR}, z_{IZ})$,
FEMK (M, MK) : see above (1) and
FTMK (M, MK) : see above (1).

The data on the output print are as follows:

(a) list of input file Jxxxx.DATA2DN.DATA (see Sec.5.2.1 ($5)) like Fig. 5. 2 or Fig. 5. 3,
(b) list of the main input parameters with explanatory captions,

(The items (c)~(f) below are repeated for each energy group i (i=1, ···, IMAX).)

(c) CPU+VU time (sec) accumulated from the start of computation (EXEC LMGO) until the end of each main calculational item,
(d) when the convergence has been attained or ITMAX iterations have been finished for the 10-th grid,
- neutron balance parameters; F, GAIN, ABBS, SELF, XLEK (see Sec. 3. 7) integrated over the entire spatial region dealing with it as a single coarse mesh region,
- group no. i, iteration times IT, residual VERGF,

where $VERGF = \max_{JR, IZ, L} |\{\phi^{i(IT-1)}(r_{JR}, z_{IZ}, \vec{\Omega}_L)/\phi^{i(IT)}(r_{JR}, z_{IZ}, \vec{\Omega}_L)\} - 1| < \varepsilon$
(JR, IZ, L : except the cases where $\phi^{i(IT)}(r_{JR}, z_{IZ}, \vec{\Omega}_L) = 0$),
IT : iteration times (IT=1, 2, ···),

(When the energy grid model is used for the group i, these printed neutron balance parameters and VERGF are meaningless, because the iteration is terminated by ITMAX ($\leqq 3$) times. In addition, these parameters are obtained only from the data of the last (10–th) grid in the group i.)

(e) • the upper energy boundary EUP (i) (eV),
• the lower energy boundary EUP (i+1) (eV),
• the energy width ΔE_i (eV) and
(f) neutron scalar flux Φ^i (r_{JR}, z_{IZ}) for JR=1, ···, 10 and for IZ=NZMIN, ···, NZMAX,

where

$$\text{NZMIN}=\begin{cases} 1 \text{ for ISTEP}\neq 2 \text{ and} \\ \text{IFACE for ISTEP}=2 \text{ (see Sec. 5. 2. 2 (\#2))}. \end{cases}$$

The STOP codes are as follows:

(1) 1001 : KMAX regions do not cover completely the whole (r, z) plane, or some regions overlap (error in J1 (K), J2 (K), I1 (K) and I2 (K) in input data #10).
(2) 2001 : IFACE in input data #02 is not on the bottom boundary of a partition in the z–direction,
(3) 2222 : The input fixed source for the group 1 is zero (error in input data #14~#19) and
(4) 9876 : Total number of nuclides exceeds 20 (error in input data #05 or #12).

5.3 BERMUDA–2DN–S16

5.3.1 JCL

The JCL for the BERMUDA–2DN–S16 execution on the FACOM/VP2600 computer in JAERI is as follows;

```
//JCLG JOB
// EXEC JCLG
//SYSIN DD DATA, DLM='++'
// JUSER xxxxxxxx, xx. xxxxxxxx, xxxx. xx
        T.14 W.08 C.00 I.10 E.13 SRP
        OPTP MSGCLASS=X, MSGLEVEL=(1, 1, 2), CLASS=8, NOTIFY=Jxxxx($1)
        OPTP PASSWORD=xxxxxxxx
//     EXEC LMGO, LM=J9091. BM2DNS16, A='HIO=(01, 09)'($2)
//FT01F001 DD DISP=SHR, DSN=Jxxxx. FX601S16. DATA($3)
//FT02F001 DD DISP=SHR, DSN=Jxxxx. BNDFXS16. DATA($4)
//FT03F001 DD UNIT=WK10, SPACE=(TRK, (100, 50)), DISP=(NEW, DELETE, DELETE),
//     DSN=&&WORK, DCB=(RECFM=VBS, LRECL=23472, BLKSIZE=23476, DSORG=PS)
//FT04F001 DD DISP=SHR, DSN=J3931. BERM125X. DATA. LABEL=(, , , IN)
//SYSIN    DD DISP=SHR, DSN=Jxxxx. DT2DNS16. DATA($5)
//FT08F001 DD DISP=SHR, DSN=Jxxxx. FX2DNS16. DATA($6)
//FT09F001 DD DISP=SHR, DSN=Jxxxx. FX609S16. DATA($7)
//FT12F001 DD DISP=SHR, DSN=Jxxxx. SB2DNS16. DATA($8)
++
//
```

($1) "CLASS=8" is a night job which needs an approval of the Computing and Information Systems Center of JAERI for submission. Besides this, there is the class 6 which also needs an approval but is not a night job. For this class 6, permitted CPU time (T. xx), print lines (W. xx) and I/O times (I. xx) have different values from those of the class 8.

($2) There has already been a load module J9091. BM2DNS16. LOAD prepared for a public use in JAERI.

If necessary, a new load module is able to be created on a disk from the source module J9091. BERMUDA. FORT77 (BM2DNS16). The JCL for creating a new load module is as follows:

```
//JCLG JOB
// EXEC JCLG
//SYSIN DD DATA, DLM='++'
// JUSER xxxxxxxx, xx. xxxxxxxx, xxxx. xx
        T.02 W.03 C.02 I.02 E.00 SRP
        OPTP MSGCLASS=X, MSGLEVEL=(1, 1, 2), NOTIFY=Jxxxx, PASSWORD=xxxxxxxx
//    EXEC FORT77VE, SO=J9091. BERMUDA,
//      A='ELM (BM2DNS16), SOURCE, NOVMSG, NOVSOURCE', LCT=62
//    EXEC LKEDCT77, LM=Jxxxx. BM2DNS16, UNIT=xxxxx, MODS='11, 11, 1', A=MAP
++
//
```

These steps of compilation and linkage are executed rather rapidly on the FACOM/M780 scalar computer. The new load module is applied by replacing the above "LM=J9091.BM2DNS16"($2) with "LM=Jxxxx.BM2DNS16".

($3) The HIO (high-speed input/output) work file for the angular and scalar fluxes Jxxxx.FX601S16. DATA has to be allocated beforehand as:

```
//FT01F001 DD UNIT=TSSWK, SPACE=(CYL, 780,, CONTIG),
//    DISP=(NEW, CATLG, CATLG), DSN=Jxxxx. FX601S16. DATA,
//    DCB=(RECFM=F, LRECL=23000, BLKSIZE=23000, DSORG=PS)
```

This file contains the spatial distributions of the angular and scalar neutron fluxes for all of the calculated energy groups as a HIO work file for calculating the slowing down source from the upper energy groups.

So, this file can be deleted after the job has been successfully terminated in TMAX sec (see Sec. 5. 3. 2) because the same data are stored in the FT08 (Jxxxx. FX2DNS16. DATA($6)) for restarting the job. The main purpose of the FT01 ($3) and FT09($7) is to utilize the HIO option for saving the I/O times (EXCP). In fact, the TSSWK is automatically deleted at 8: 00 a. m. (the TSSWK2 at 5: 00 p. m.) in JAERI. The HIO option needs to allocate the file 'contiguously' on the disk (CONTIG), and the FT01 and FT09 need to be allocated every time (or every day) before submitting the restarting job.

At the present, the specifications of the disk in JAERI are as follows:

1 VOL=1, 326 CYL×2 (=19, 890 TRK×2),
1 CYL=15 TRK and
1 TRK=47, 476 bytes.

However, BLKSIZE cannot exceed 32, 767 bytes.

(\$4) The boundary flux file Jxxxx. BNDFXS16. DATA has to be allocated beforehand as:

```
//FT02F001 DD UNIT=xxxxx,SPACE=(TRK, (60, 05)),
//     DISP=(NEW, CATLG, CATLG), DSN=Jxxxx. BNDFXS16. DATA,
//     DCB=(RECFM=VBS, LRECL=23472, BLKSIZE=23476, DSORG=PS)
```

This file contains the boundary flux in case of the bootstrap option (see Sec. 3. 6. 2). In the first step, the boundary flux is written in this file; and in the second step, the boundary flux is supplied from the file. When the bootstrap option is not used (ISTEP=0 in Sec. 5. 3. 2), the one line of the JCL (\$4) is not necessary as well as allocation of the file.

(\$5) The input data file Jxxxx. DT2DNS16. DATA has to be allocated beforehand as:

```
//FT05F001 DD UNIT=xxxxx, SPACE=(TRK, (01, 01)),
//     DISP=(NEW, CATLG, CATLG), DSN=Jxxxx. DT2DNS16. DATA,
//     DCB=(RECFM=FB, LRECL=80, BLKSIZE=3120, DSORG=PS)
```

The content of this file is described in Sec. 5. 3. 2.
Otherwise, the one line of the JCL(\$5) is substituted with

```
//SYSIN     DD  *
        [input data described in Sec. 5. 3. 2]
/*
```

without allocating the Jxxxx. DT2DNS16. DATA.

(\$6) The flux file Jxxxx. FX2DNS16. DATA has to be allocated as:

```
//FT08F001 DD UNIT=xxxxx, SPACE=(TRK, (11500, 100)),
//     DISP=(NEW, CATLG, CATLG), DSN=Jxxxx. FX2DNS16. DATA,
//     DCB=(RECFM=VBS, LRECL=23472, BLKSIZE=23476, DSORG=PS)
```

This file contains the angular and spatial distributions of neutron flux etc. for all of the calculated energy groups. It is used for restarting the job for energy group continuation. After the computation has been completed for all of the energy groups and the bootstrap steps, it is processed for the output data edition with the post-processing codes.[6]

Note that the contents of the Jxxxx. FX2DNS16. DATA for the bootstrap step 1 vanish when the same file is used in the step 2. Usually comparison of the output data with the measured data concerns the region of the step 2. However, if it is necessary to save the data obtained in the step 1, dual files have to be allocated as Jxxxx. F2DNS161. DATA and Jxxxx. F2DNS162. DATA for each step.

(\$7) The HIO work file for the uncollided flux and the resonancne self-shielding factors Jxxxx. FX609S16. DATA has to be allocated beforehand as:

```
//FT09F001 DD UNIT=TSSWK,SPACE=(CYL, 13,, CONTIG),
//     DISP=(NEW, CATLG, CATLG), DSN=Jxxxx. FX609S16. DATA,
//     DCB=(RECFM=F, LRECL=23000, BLKSIZE=23000, DSORG=PS)
```

This file contains the spatial distribution of the uncollided neutron flux etc. for all of the calculated energy groups as a HIO work file for calculating the first collision source from the self and the upper groups in Eq. (3. 23). If IPS=0, it contains only the resonance self-shielding factors of which the $\tilde{f}_e^{mi}$ is used in the F_L^{mj} in Eq. (3. 3). So '13 CYL' is too much, and '1 CYL' may be sufficient when IPS=0.

This file can also be deleted after the job has been successfully terminated in TMAX sec same as the FT01, because the same data are stored in the FT08 for restarting the job.

($8) The grid source file Jxxxx. SB2DNS16. DATA has to be allocated beforehand as:

```
//FT12F001 DD UNIT=xxxxx, SPACE=(TRK, (950, 50)),
//     DISP=(NEW, CATLG, CATLG), DSN=Jxxxx. SB2DNS16. DATA,
//     DCB=(RECFM=VBS, LRECL=23472, BLKSIZE=23476, DSORG=PS)
```

This file is necessary for restarting the job as well as the FT08, and can be deleted after the calculation up to the IMAX-th group has been completed (in case of ISTEP≠0, up to the IMAX-th group in the step 2). The contents of the FT12 are:

(1) the group no. i_R (Up to the i_R group the calculation has been completed.) and

(2) the grid source into the ten grids within the group (i_R+1) from the groups $1\sim(i_R-1)$ and from the ten grids within the group i_R.

5.3.2 Input Data

#01 (F6.0) 1 line

- TMAX : CPU time (sec) to terminate the job and to prepare the disk files for restarting the next job
  (If CLASS=8, then TMAX=10000.)

#02 (4I3) 1 line

- IRSTRT : group no. to be restarted (initially≡1)
- ISTEP : step no. for bootstrap option

$$\text{ISTEP}=\begin{cases}0 \cdots \text{no bootstrap option}\\ 1 \cdots \text{the first step}\\ 2 \cdots \text{the second step}\end{cases}$$

- IFACE : interface z-mesh point no. for bootstrap option (0 when ISTEP=0)
  IFACE must be on the bottom boundary mesh point of a partition in the z-direction. (The numbering method for mesh points is described in #10.)
  When ISTEP=2, IFACE is different value from that in ISTEP=1.
- ITMAX : maximum number of iteration times for each energy grid
  (ITMAX=1, 2 or 3)
  (ITMAX is defined as 1, if 0 or blank is input.)

#03 (18A4) 1 line

- Problem title : any characters, numbers or blanks describing the problem on columns 1~72

#04 (9I4, 2E12. 5) 1 line

- IMAX : total number of energy groups for this problem (≦125)
- MMAX : number of mixtures (≦20)
- KMAX : number of spatial regions (MMAX≦KMAX)
  Definition of a 'region' is that it is a rectangular part on the (r, z) plane, where mixture is

assigned to be homogeneous.

The (r, z) plane must be completely covered with the KMAX regions. Actually a 'region' is a ring-shaped volume made by rotating the rectangle around the axis of the cylinder (r=0).

- IMAXL : total number of groups of the group constants library used
  (for example, IMAXL=125 for J3931. BERM125X. DATA)
- I1LIB : group no. "on the group constants library" where the group 1 of this problem is to be defined
  (for example, IMAX+I1LIB≦126 for J3931. BERM125X. DATA)

In BERMUDA, the I1LIB-th group on the library is called as "group 1".

- IFIS(≡0) : dummy
- IPS : type of the fixed source

$$IPS=\begin{cases} 0 \cdots \text{spatially distributed source} \\ IZPS \cdots \text{point source on the z-axis of the cylinder } (IZPS \geqq 1) \end{cases}$$

The IZPS is the z-mesh point no. for the point source. When IZPS=1, z (IZPS)=0 (origin). The numbering method for the mesh points is described in #10. The point source cannot be placed on an interface between partitions in the z-direction.

- NRR : number of partitions in the r-direction (NRR≦20)
  In each partition, mesh sizes (Δr) are assigned to be equal to each other.
- NRZ : number of partitions in the z-direction (NRZ≦20)
  In each partition, mesh sizes (Δz) are assigned to be equal to each other.
- ER : upper energy (eV) for the group 1 of the problem
  EUP (I1LIB+1)<ER≦EUP (I1LIB)
- EPS : convergence criterion (for angular flux) to be used to terminate the thermal group iteration
  (usually 10^{-3})

#05 (20I3) 1 line

- (MM (MK), MK=1, MMAX) : number of nuclides to be included in each mixture
  (1≦MM (MK)≦10)
  (For a vacuum, assign one dummy nuclide which is contained in another mixture. Input its code number in #12 and atomic number density (0.) in #13.)
  In a problem, maximum 20 nuclides can be selected out of 30 or 24 nuclides in the libraries. The definition of the maximum 'number' is that a nuclide contained commonly in plural number of mixtures is counted as 1, notwithstanding that the nuclide has equal or not equal atomic number densities in those mixtures.

#06 (10I6) [(NRR+9)/10] lines

The brackets [···] means the integer discarding the fractions.

- (INTERR (KR), KR=1, NRR) : number of mesh intervals between the origin and the outer boundary of each partition in the r-direction
  (Either even or odd numbers are valid.)
  (1≦INTERR (1)<INTERR (2)<···<INTERR (NRR)≦60−NRR)

#07 (10F6.3) [(NRR+9)/10] lines

• (DRR (KR), KR=1, NRR) : mesh size Δr (cm) for each partition in the r-direction (not the partition thickness)

#08 (10I6) [(NRZ+9)/10] lines

• (INTERZ (KZ), KZ=1, NRZ) : number of mesh intervals between the origin and the top boundary of each partition in the z-direction
(Either even or odd numbers are valid.)
(1≦INTERZ (1)<INTERZ (2)<⋯<INTERZ (NRZ)≦110−NRZ)

#09 (10F6. 3) [(NRZ+9)/10] lines

• (DZZ (KZ), KZ=1, NRZ) : mesh size Δz (cm) for each partition in the z-direction (not the partition thickness)

#10 (5I6) KMAX lines

• (J1 (K), J2(K), I1 (K), I2(K), MR(K), K=1, KMAX) : assignment of composition
J1 (K) : left mesh point no. of the region K
J2 (K) : right mesh point no. of the region K
I1 (K) : bottom mesh point no. of the region K
I2 (K) : top mesh point no. of the region K
MR (K) : mixture no. for the region K (≡MK defined in #05)
(1≦J1<J2≦NRMAX≦60 and 1≦I1<I2≦NZMAX≦110)

In BERMUDA, the numbering of the mesh points is as follows:
(1) "1" for the origin,
(2) doubly (twice) numbered as "INTERR (KR)+KR" and "INTERR (KR)+KR+1" for the interface between the KR-th and the (KR+1)-th partitions in the r-direction where KR=1, ⋯, NRR-1 (for treating spatial discontinuity of the macroscopic cross sections and the source distribution at the interfaces) and
(3) "NRMAX=INTERR (NRR)+NRR"≦60 for the outermost mesh point in the r-direction.
And it is same for the z-direction except "NZMAX=INTERZ (NRZ)+NRZ"≦110.

#11 (2F6.3) 1 line

• BCTOP : top boundary condition for z=z (NZMAX)
• BCBOT : bottom boundary condition for z=0.

$$\text{boundary conditions} \equiv \begin{cases} -1. \cdots \text{symmetry condition} \\ 0. \cdots \text{vacuum boundary condition} \end{cases}$$

#12 (10I6) MMAX lines

• (MCODE (M, MK), M=1, MM (MK)) : code no. of each nuclide in the mixture MK defined in the group constants library to be used (for example, see Table 2. 2)
(The order of nuclides in a mixture is able to be arbitrary.)

Repeat this in the order of MK=1, ⋯, MMAX renewing the line for each mixture.

#13 (6E12.5) [{MM (MK)+5} /6] lines for each mixture

• (AN (M, MK), M=1, MM (MK)) : effective number density (10^{24}cm^{-3}) of each nuclide in the mixture MK

(The order of nuclides in a mixture must be same as in #12.)

Repeat this in the order of MK=1, ···, MMAX renewing the line for each mixture.

#14 (4I6) 1 line

- IZ1 : the first mesh point no. to give axial distribution of non-zero independent source in #15
- IZ2 : the last mesh point no. to give axial distribution of non-zero independent source in #15
- JR1 : the first mesh point no. to give radial distribution of non-zero independent source in #15
- JR2 : the last mesh point no. to give radial distribution of non-zero independent source in #15

These mesh points must be given in the definition of (1)~(3) in #10 ($1 \leqq IZ1 \leqq IZ2 \leqq NZMAX$ and $1 \leqq JR1 \leqq JR2 \leqq NRMAX$). When IPS=0 in #04 and IZ1<IZ2 and JR1<JR2, S1 in #15 is a volume source. When IPS≠0, S1 is a point source (IZ1=IZ2=IPS and JR1=JR2=1).

#15 (6E12.5) {[(JR2-JR1)/6] +1} lines

- (S1 (JR, IZ), JR=JR1, JR2) : spatial distribution of independent source

Independent source is given in the form of a function with separation of variables as S1 (JR, IZ)×S2 (I)×S3 (L).

(Each of the S1, S2 and S3 should be normalized to its correct magnitude, respectively. However, it is also valid that the product of the S1, S2 and S3 has the correct normalized value for each energy group(*).)

Repeat this in the order of IZ=IZ1, ···, IZ2.

#16 (2I6) 1 line

- I1 : the first energy group no. to give energy spectre of non-zero independent source in #17
- I2 : the last energy group no. to give energy spectre of non-zero independent source in #17

If the source is of mono-energy (monochromatic), I1=I2=1.

Otherwise, $1 \leqq I1 < I2 \leqq IMAX$.

#17 (6E12.5) {[(I2-I1)/6] +1} lines

- (S2 (I), I=I1, I2) : energy spectre of independent source

(As BERMUDA has been programmed not in a continuous energy model but in a usual multigroup model, only the S2 (except the S1 and S3) must be given as integrated value for group i over ΔE_i.)

The S2 (I) is generally normalized to be 1 integrated over energy, that is,

$$\sum_{I=I1}^{I2} S2\ (I) = 1.$$

(However, note the proviso (*) under #15.)

#18 (2I6) 1 line

- L1 : the first ordinate no. to give angular distribution of non-zero independent source in #19 (see Fig. 3. 4)
- L2 : the last ordinate no. to give angular distribution of non-zero independent source in #19

If the source is mono-directional, L1=L2.

Otherwise, $1 \leqq L1 < L2 \leqq 144$. (S3 (L) for L=145, ···, 160 are automatically assumed to have equal values to the adjacent (just right) ordinates, respectively.)

#19 (6E12. 5) {[(L2–L1)/6] +1} lines

• (S3 (L), L=L1, L2) : angular distribution of independent source

The S3 (L) is generally normalized to be 1 integrated over the unit sphere, that is,

$$\sum_{L=L1}^{L2} \Delta\vec{\Omega}_L S3(L) = 1.$$

(However, note the proviso (*) under #15.)

An example of input data for the BERMUDA–2DN–S16 is shown in Fig.5.4 where a case of ISTEP =0 is shown. However, ISTEP≠0 is also possible.

```
                DATA SET NAME : J1057.BERMUDA.DATA(DT2DNS16)

----+----1----+----2----+----3----+----4----+----5----+----6----+----7----+----8

10000.                                                                      #01
  1  0  0  1                                                                #02
    SUS316 ASSEMBLY DEEP PENETRATION 21/11/86 FRI. 66G MESH TUNNING         #03
  66   4  13 125   5   0   1   8   8 1.5488   +7 5.0      -3                 #04
  2 10  7  9                                                                #05
     6     7     8    10    11    36    37    42                           #06
3.75  0.8   2.5   4.6   0.8   8.488 2.0   12.0                              #07
    16    17    27    28    38    48    58    66                           #08
15.5  2.0   7.8   1.6   2.96  2.96  3.06  3.825                            #09
     1    42     1    17     1    REG 1 AIR FRONT PART                     #10
    43    44     1    17     2    REG 2 MORTAR                              "
    45    50     1    19     3    REG 3 ROOM WALL (CONCRETE)                "
     1    14    18    30     1    REG 1-2 AIR FRONT PART                    "
    15    16    18    32     4    REG 4 FE TEST PORT FLAME                  "
    17    44    18    19     2    REG 2-2 MORTAR                            "
    17    50    20    32     3    REG 3-2 ROOM WALL                         "
     1     7    31    32     1    REG 1-3 AIR FRONT PART                    "
     8    14    31    32     4    REG 4-2 FE TEST PORT FLAME                "
     1     9    33    54     4    REG 4-3 FE TEST PORT SUS316               "
    10    50    33    54     3    REG 3-3 ROOM WALL                         "
     1    11    55    74     4    REG 4-4 FE TEST PORT SUS316               "
    12    50    55    74     3    REG 3-4 ROOM WALL                         "
 0.   -1.                                                                   #11
    70    80                                                                #12
    11    80    80   130   130   130   140   140   140   260               "
    80    11   130   130   130   140   260                                 "
    60   140   140   140   240   250   260   280   420                     "
 3.8810   -5 1.0400   -5                                                   #13
 9.4246   -3 7.4297   -4 3.7680   -2 5.0802   -4 4.6874   -4 1.9408   -3   "
 1.1347   -2 3.3427   -4 3.7143   -3 6.8100   -4                           "
 4.31509  -2 7.9740   -3 5.4090   -4 7.8590   -4 3.0194   -3 1.7903   -2   "
 5.8590   -4                                                               "
 3.1729   -4 1.6962   -3 6.9211   -5 4.4572   -5 1.5575   -2 1.7343   -3   "
 5.5740   -2 9.7339   -3 1.2421   -3                                       "
     1     1     1     1                                                   #14
 7.95775E-02                                                              #15
     1    66                                                              #16
   2.0282-08   1.6009-05   2.2393-04   2.1827-03   1.0623-01   7.0219-01  #17
   4.0324-02   8.6730-03   2.8072-03   1.9716-03   2.1199-03   2.1551-03   "
   1.7718-03   1.3596-03   1.1058-03   9.8002-04   9.2473-04   8.2910-04   "
   7.5409-04   6.0028-04   5.4624-04   5.1257-04   4.8040-04   4.1078-04   "
   4.5049-04   4.1154-04   4.7600-04   4.9296-04   1.8409-03   1.8610-03   "
   1.7291-03   1.8799-03   1.9314-03   1.8899-03   1.7907-03   1.6436-03   "
   1.5582-03   1.6650-03   1.6286-03   1.7793-03   1.8020-03   1.9477-03   "
   1.9063-03   1.9100-03   1.9603-03   2.2028-03   2.1438-03   2.2946-03   "
   2.2418-03   2.1865-03   2.3360-03   2.3938-03   2.1764-03   2.1903-03   "
   2.3662-03   2.2569-03   4.1317-03   4.4672-03   4.3554-03   4.1279-03   "
   3.9131-03   3.7597-03   3.4531-03   3.1428-03   2.8487-03   2.6150-03   "
```

Fig. 5.4 Example of input data for the BERMUDA–2DN–S16 (ISTEP=0)

```
                  DATA SET NAME : J1057.BERMUDA.DATA(DT2DNS16)

----+----1----+----2----+----3----+----4----+----5----+----6----+----7----+----8

    1    144                                                              #18
1.          1.          1.          1.          1.          1.            #19
1.          1.          1.          1.          1.          1.             "
1.          1.          1.          1.          1.          1.             "
1.          1.          1.          1.          1.          1.             "
1.          1.          1.          1.          1.          1.             "
1.          1.          1.          1.          1.          1.             "
1.          1.          1.          1.          1.          1.             "
1.          1.          1.          1.          1.          1.             "
1.          1.          1.          1.          1.          1.             "
1.          1.          1.          1.          1.          1.             "
1.          1.          1.          1.          1.          1.             "
1.          1.          1.          1.          1.          1.             "
1.          1.          1.          1.          1.          1.             "
1.          1.          1.          1.          1.          1.             "
1.          1.          1.          1.          1.          1.             "
1.          1.          1.          1.          1.          1.             "
1.          1.          1.          1.          1.          1.             "
1.          1.          1.          1.          1.          1.             "
1.          1.          1.          1.          1.          1.             "
1.          1.          1.          1.          1.          1.             "
1.          1.          1.          1.          1.          1.             "
1.          1.          1.          1.          1.          1.             "
1.          1.          1.          1.          1.          1.             "
1.          1.          1.          1.          1.          1.             "
```

Fig. 5.4 Example of input data for the BERMUDA-2DN-S16 (ISTEP=0) (continued)

5.3.3 Output Data

The output data of BERMUDA-2DN-S16 are stored on the magnetic disk FT08 (Jxxxx. FX2DNS16.DATA; see Sec.5.3.1 ($6)) and are also given on the printer.

The data on the output disk are as follows:

(1) In case of IPS=0, the following FORTRAN record is repeated for each group i (i=1, ⋯, IMAX) in the binary form,

(((PHI (JR, IZ, L), L=1, LMAX), IZ=1, NZMAX), JR=1, NRMAX),
((TPHI (JR, IZ), IZ=1, NZMAX), JR=1, NRMAX),
((FEMK (M, MK), M=1, 10), MK=1, 20), ((FTMK (M, MK), M=1, 10), MK=1, 20),

where PHI (JR, IZ, L) : $\phi^i (r_{JR}, z_{IZ}, \vec{\Omega}_L)$,

$$\mathrm{LMAX}=\begin{cases}144\cdots\text{when calculation has been completed until the group IMAX,}\\ 160\cdots\text{when calculation is to be restarted from the group } (i_R+1),\end{cases}$$

NZMAX, NRMAX : see Sec. 5. 3. 2 (#10).

TPHI (JR, IZ) : $\Phi^i (r_{JR}, z_{IZ}) = \sum_{L=1}^{144} \Delta\vec{\Omega}_L \phi^i (r_{JR}, z_{IZ}, \vec{\Omega}_L)$,

FEMK (M, MK) : $\bar{f}_e^{Mi}$ for mixture MK (see Sec. 2. 2 and Sec. 3. 1) and

FTMK (M, MK) : $\bar{f}_t^{Mi}$ for mixture MK (see Sec. 2. 2).

(2) In case of IPS≠0, the following FORTRAN record is repeated for each group i (i=1, ⋯, IMAX) in the binary form,

(((PHI (JR, IZ, L), L=1, LMAX), IZ=1, NZMAX), JR=1, NRMAX),
((PHI0 (JR, IZ), IZ=1, NZMAX), JR=1, NRMAX), (PHI00 (L), L=1, 40),
((TPHI (JR, IZ), IZ=1, NZMAX), IZ=1, NRMAX),
((FEMK (M, MK), M=1, 10), MK=1, 20), ((FTMK (M, MK), M=1, 10), MK=1, 20),

where PHI (JR, IZ, L) : ϕ^i (r_{JR}, z_{IZ}, $\vec{\Omega}_L$) (without component of uncollided flux),
LMAX,NZMAX,NRMAX : see above (1),
PHI0(JR, IZ) : Φ_0^i (r_{JR}, z_{IZ}) (uncollided flux),
PHI00 (L) : S^i (0, z_{IZPS}, $\vec{\Omega}_L$) (point source),
TPHI (JR, IZ) : $\Phi^i(r_{JR}, z_{IZ})=\sum_{L=1}^{144} \Delta\vec{\Omega}_L \phi^i (r_{JR}, z_{IZ}, \vec{\Omega}_L)+\Phi_0^i (r_{JR}, z_{IZ})$,
FEMK (M, MK) : see above (1) and
FTMK (M, MK) : see above (1).

The data on the output print are as follows:

(a) list of input file Jxxxx. DT2DNS16. DATA (see Sec. 5. 3. 1 ($5)) like Fig. 5. 4,
(b) list of the main input parameters with explanatory captions,

(The items (c)~(f) below are repeated for each energy group i (i=1, ···, IMAX).)

(c) CPU+VU time (sec) accumulated from the start of computation (EXEC LMGO) until the end of each main calculational item,
(d) when the convergence has been attained or ITMAX iterations have been finished for the 10-th grid,
- neutron balance parameters; F, GAIN, ABBS, SELF, XLEK (see Sec. 3. 7) integrated over the entire spatial region dealing with it as a single coarse mesh region,
- group no. i, iteration times IT, residual VERGF,

where $VERGF=\max_{JR, IZ, L} |\{\phi^{i\,(IT-1)} (r_{JR}, z_{IZ}, \vec{\Omega}_L)/\phi^{i\,(IT)} (r_{JR}, z_{IZ}, \vec{\Omega}_L)\}-1|<\varepsilon$
(JR, IZ, L : except the cases where $\phi^{i\,(IT)} (r_{JR}, z_{IZ}, \vec{\Omega}_L)=0$),
IT : iteration times (IT=1, 2, ···),

(When the energy grid model is used for the group i, these printed neutron balance parameters and VERGF are meaningless, because the iteration is terminated by ITMAX ($\leqq$3) times. In addition, these parameters are obtained only from the data of the last (10-th) grid in the group i.)

(e) • the upper energy boundary EUP (i) (eV),
• the lower energy boundary EUP (i+1) (eV),
• the energy width ΔE_i (eV) and
(f) neutron scalar flux Φ^i (r_{JR}, z_{IZ}) for JR=1, ···, 10 and for IZ=NZMIN, ···, NZMAX.

where

$$NZMIN=\begin{cases} 1 \text{ for ISTEP}\neq 2 \text{ and} \\ \text{IFACE for ISTEP}=2 \text{ (see Sec.5.3.2 (\#2))}. \end{cases}$$

The STOP codes are as follows:

(1) 1001 : KMAX regions do not cover completely the whole (r, z) plane, or some regions overlap (error in J1 (K), J2 (K), I1 (K) and I2 (K) in input data #10).
(2) 2001 : IFACE in input data #02 is not on the bottom boundary of a partition in the z-direction,
(3) 2222 : The input fixed source for the group 1 is zero (error in input data #14~#19) and
(4) 9876 : Total number of nuclides exceeds 20 (error in input data #05 or #12).

5.4 BERMUDA-3DN

5.4.1 JCL

The JCL for the BERMUDA-3DN execution on the FACOM/VP2600 computer in JAERI is as follows;

```
//JCLG JOB
// EXEC JCLG
//SYSIN DD DATA,DLM='++'
// JUSER xxxxxxxx, xx. xxxxxxxx, xxxx. xx
        T.15 W.09 C.00 I.15 E.44 SRP
        T=(1440, 00)
        OPTP MSGCLASS=X, MSGLEVEL=(1, 1, 2), CLASS=9, NOTIFY=Jxxxx($1)
        OPTP PASSWORD=xxxxxxxx
//     EXEC LMGO, LM=J9091. BERMD3DN, A='HIO=(01, 11, 21)'($2)
//FT01F001 DD DISP=SHR, DSN=Jxxxx. FLX601. DATA($3)
//FT02F001 DD DISP=SHR, DSN=Jxxxx. BOUNDFLX. DATA($4)
//FT03F001 DD UNIT=WK10, SPACE=(TRK, (100, 50)), DISP=(NEW, DELETE, DELETE),
//     DSN=&&WORK, DCB=(RECFM=VBS, LRECL=23472, BLKSIZE=23476, DSORG=PS)
//FT04F001 DD DISP=SHR, DSN=J3931. BERM125X. DATA, LABEL=(, , , IN)
//SYSIN    DD DISP=SHR, DSN=Jxxxx. DATA3DN. DATA($5)
//FT08F001 DD DISP=SHR, DSN=Jxxxx. FLUX3DN. DATA($6)
//FT11F001 DD DISP=SHR, DSN=Jxxxx. FLX611. DATA($7)
//FT21F001 DD DISP=SHR, DSN=Jxxxx. FLX621. DATA($8)
++
//
```

($1) "CLASS=9" is a specially reserved job for occupying the almost all of the '500MB extended memory' (that is, 440MB (E.44)) and the FACOM/VP2600 computer through one day or more.

So, this is a closed job for 'a weekend' once a month or once per two months, and the Jxxxx may be a personnel no. of some staff in the Computing and Information Systems Center of JAERI.

'T.15' is dummy and 'T=(1440, 00)' means that CPU+VU time may be unlimited until the next Monday morning.

($2) There has already been a load module J9091. BERMD3DN. LOAD prepared for a public use in JAERI.

If necessary, a new load module is able to be created on a disk from the source module J9091. BERMUDA. FORT77 (BERMD3DN). The JCL for creating a new load module is as follows:

```
//JCLG JOB
// EXEC JCLG
//SYSIN DD DATA, DLM='++'
// JUSER xxxxxxxx, xx. xxxxxxxx, xxxx. xx
        T.02 W.03 C.02 I.02 E.00 SRP
        OPTP MSGCLASS=X, MSGLEVEL=(1, 1, 2), NOTIFY=Jxxxx, PASSWORD=xxxxxxxx
//    EXEC FORT77VE, SO=J9091. BERMUDA,
//    A='ELM (BERMD3DN), SOURCE, NOVMSG, NOVSOURCE', LCT=62
//    EXEC LKEDCT77, LM=Jxxxx. BERMD3DN, UNIT=xxxxx, MODS='12, 12, 1', A=MAP
++
//
```

These steps of compilation and linkage are executed rather rapidly on the FACOM/M780 scalar computer. The new load module is applied by replacing the above "LM=J9091.BERMD3DN"($2) with "LM=Jxxxx. BERMD3DN".

"A='HIO=(01, 11, 21)' " is necessary when $97 \leqq IMAX \leqq 125$. If $49 \leqq IMAX \leqq 96$, then A='HIO=(01, 11)', and if $1 \leqq IMAX \leqq 48$, then A='HIO=(01)' must be substituted in place of A='HIO=(01, 11, 21)'. The IMAX is the total number of energy groups (see Sec. 5. 4. 2 (#4)).

($3) The HIO (high-speed input/output) work file for the angular and scalar fluxes Jxxxx. FLX601. DATA has to be allocated beforehand as:

```
//FT01F001 DD UNIT=TSSWK,SPACE=(CYL, 1320,, CONTIG),
//    DISP=(NEW, CATLG, CATLG), DSN=Jxxxx. FLX601. DATA,
//    DCB=(RECFM=F, LRECL=23000, BLKSIZE=23000, DSORG=PS)
```

This file contains the spatial distributions of the angular and scalar neutron fluxes for the energy groups 1~48 as a HIO work file for calculating the slowing down source from these energy groups.

So, this file can be deleted after the job has been terminated if the angular flux is not necessary to be saved, because the scalar flux is stored in the FT08 (Jxxxx.FLUX3DN. DATA($6)) for output data edition. The main purpose of the FT01($3), FT11($7)and FT21($8) is to utilize the HIO option for saving the I/O times (EXCP) and to use the TSSWK for saving the user's disk file from occupying the gigantic space for the angular flux memory. In fact, the TSSWK is automatically deleted at 8:00 a.m. on the next Monday. The HIO option needs to allocate the file 'contiguously' on the disk (CONTIG), and the FT01, FT11 and FT21 need to be allocated every time before executing the special large job.

At the present, the specifications of the disk in JAERI are as follows:

1 VOL=1, 326 CYL×2 (=19, 890 TRK×2),
1 CYL=15 TRK and
1 TRK=47, 476 bytes.

However, BLKSIZE cannot exceed 32,767 bytes.

($4) The boundary flux file Jxxxx. BOUNDFLX. DATA has to be allocated beforehand as:

```
//FT02F001 DD UNIT=xxxxx, SPACE=(TRK, (400, 10)),
//    DISP=(NEW, CATLG, CATLG), DSN=Jxxxx. BOUNDFLX. DATA,
//    DCB=(RECFM=VBS, LRECL=23472, BLKSIZE=23476, DSORG=PS)
```

This file contains the boundary flux in case of the bootstrap option (see Sec. 3. 6. 2). In the first step, the boundary flux is written in this file; and in the second step, the boundary flux is supplied from the file. When the bootstrap option is not used (ISTEP=0 in Sec. 5. 4. 2), the one line of the JCL(\$4) is not necessary as well as allocation of the file.

(\$5) The input data file Jxxxx. DATA3DN. DATA has to be allocated beforehand as:

```
//FT05F001 DD UNIT=xxxxx, SPACE=(TRK, (01, 01)),
//     DISP=(NEW, CATLG, CATLG), DSN=Jxxxx. DATA3DN. DATA,
//     DCB=(RECFM=FB, LRECL=80, BLKSIZE=3120, DSORG=PS)
```

The content of this file is described in Sec. 5. 4. 2.
Otherwise, the one line of the JCL(\$5) is substituted with

```
//SYSIN     DD  *
        [input data described in Sec. 5. 4. 2]
/*
```

without allocating the Jxxxx.DATA3DN.DATA.

(\$6) The flux file Jxxxx.FLUX3DN. DATA has to be allocated as:

```
//FT08F001 DD UNIT=xxxxx, SPACE=(TRK, (600, 50)),
//     DISP=(NEW, CATLG, CATLG), DSN=Jxxxx. FLUX3DN. DATA,
//     DCB=(RECFM=VBS, LRECL=23472, BLKSIZE=23476, DSORG=PS)
```

This file contains the spatial distribution of neutron scalar flux etc. for all of the calculated energy groups. It is processed for the output data edition with the post-processing codes.[6]

Note that the contents of the Jxxxx. FLUX3DN. DATA for the bootstrap step 1 vanish when the same file is used in the step 2. Usually comparison of the output data with the measured data concerns the region of the step 2. However, if it is necessary to save the data obtained in the step 1, dual files have to be allocated as Jxxxx. FLUX3DN1. DATA and Jxxxx. FLUX3DN2. DATA for each step.

(\$7) The HIO work file for the angular and scalar fluxes Jxxxx. FLX611. DATA has to be allocated beforehand as:

```
//FT11F001 DD UNIT=TSSWK, SPACE=(CYL, 1320,, CONTIG),
//     DISP=(NEW, CATLG, CATLG), DSN=Jxxxx. FLX611. DATA,
//     DCB=(RECFM=F, LRECL=23000, BLKSIZE=23000, DSORG=PS)
```

This file contains the spatial distributions of the angular and scalar neutron fluxes for the energy groups 49~96 as a HIO work file for calculating the slowing down source from these energy groups.

So, this file can be deleted after the job has been terminated if the angular flux is not necessary to be saved, because the scalar flux is stored in the FT08 for output data edition. If IMAX$\leqq$48, then the one line of the JCL(\$7) is not necessary as well as allocation of the file.

($8) The HIO work file for the angular and scalar fluxes Jxxxx. FLX621. DATA has to be allocated beforehand as:

```
//FT21F001 DD UNIT=TSSWK, SPACE=(CYL, 800,, CONTIG),
//     DISP=(NEW, CATLG, CATLG), DSN=Jxxxx. FLX621. DATA,
//     DCB=(RECFM=F, LRECL=23000, BLKSIZE=23000, DSORG=PS)
```

This file contains the spatial distributions of the angular and scalar neutron fluxes for the energy groups 97～125 as a HIO work file for calculating the slowding down source from these energy groups.

So, this file can be deleted after the job has been terminated if the angular flux is not necessary to be saved, because the scalar flux is stored in the FT08 for output data edition. If IMAX≦96, then the one line of the JCL($8) is not necessary as well as allocation of the file.

5.4.2 Input Data

#01 (F6.0) 1 line

- TMAX : CPU time (sec) to terminate the job (≡1.0E+6 for CLASS=9)

#02 (4I3) 1 line

- IRSTRT : group no. to be restarted (≡1 for CLASS=9)
- ISTEP : step no. for bootstrap option

$$\text{ISTEP}=\begin{cases}0 \cdots \text{no bootstrap option}\\ 1 \cdots \text{the first step}\\ 2 \cdots \text{the second step}\end{cases}$$

- IFACE : interface z-mesh point no. for bootstrap option (0 when ISTEP=0)
  IFACE must be on the bottom boundary mesh point of a partition in the z-direction. (The numbering method for mesh points is described in #12.)
  When ISTEP=2, IFACE is different from that in ISTEP=1.
- ITMAX : maximum number of iteration times for each energy grid
  (ITMAX=1, 2 or 3)
  (ITMAX is defined as 1, if 0 or blank is input.)

#03 (18A4) 1 line

- Problem title : any characters, numbers or blanks describing the problem on columns 1～72

#04 (9I4, 2E12. 5) 1 line

- IMAX : total number of energy groups for this problem (≦125)
- MMAX : number of mixtures (≦20)
- KMAX : number of spatial regions (MMAX≦KMAX)
  Definition of a 'region' is that it is a rectangular parallelpiped part in the (x, y, z) whole volume, where mixture is assigned to be homogeneous.
  The (x, y, z) whole volume must be completely filled up with the KMAX regions.
- IMAXL : total number of groups of the group constants library used
  (for example, IMAXL=125 for J3931. BERM125X. DATA)
- I1LIB : group no. "on the group constants library" where the group 1 of this problem is to be defined
  (for example, IMAX+I1LIB≦126 for J3931. BERM125X. DATA)

In BERMUDA, the I1LIB-th group on the library is called as "group 1".

- IPS : type of the fixed source

$$IPS = \begin{cases} 0 \cdots \text{spatially distributed source} \\ IYPS \cdots \text{point source on the y-axis of the rectangular parallelpiped } (IYPS \geqq 1) \end{cases}$$

The IYPS is the y-mesh point no. for the point source. When IYPS=1, y (IYPS)=0 (origin). The numbering method for the mesh points is described in #12. The point source cannot be placed on an interface between partitions in the y-direction.

- NRX : number of partitions in the x-direction (NRX≦20)
  In each partition, mesh sizes (Δx) are assigned to be equal to each other.
- NRY : number of partitions in the y-direction (NRY≦20)
  In each partition, mesh sizes (Δy) are assigned to be equal to each other.
- NRZ : number of partitions in the z-direction (NRZ≦20)
  In each partition, mesh sizes (Δz) are assigned to be equal to each other.
- ER : upper energy (eV) for the group 1 of the problem
  EUP (I1LIB+1)<ER≦EUP (I1LIB)
- EPS : convergence criterion (for angular flux) to be used to terminate the thermal group iteration (usually 10^{-3})

#05 (20I3) 1 line

- (MM (MK), MK=1, MMAX) : number of nuclides to be included in each mixture
  (1≦MM (MK)≦10)
  (For a vacuum, assign one dummy nuclide which is contained in another mixture. Input its code number in #14 and atomic number density (0.) in #15.)
  In a problem, maximum 20 nuclides can be selected out of 30 or 24 nuclides in the libraries. The definition of the maximum 'number' is that a nuclide contained commonly in plural number of mixtures is counted as 1, notwithstanding that the nuclide has equal or not equal atomic number densities in those mixtures.

#06 (10I6) [(NRX+9)/10] lines

The brackets [···] means the integer discarding the fractions.

- (INTERX (KX), KX=1, NRX) : number of mesh intervals between the origin and the front boundary of each partition in the x-direction
  (Either even or odd numbers are valid.)
  (1≦INTERX (1)<INTERX (2)<···<INTERX (NRX)≦30−NRX)

The origin is placed at the back, left and bottom corner of the calculated volume.

#07 (10F6.3) [(NRX+9)/10] lines

- (DXX (KX), KX=1, NRX) : mesh size Δx (cm) for each partition in the x-direction
  (not the partition thickness)

#08 (10I6) [(NRY+9)/10] lines

- (INTERY (KY), KY=1, NRY) : number of mesh intervals between the origin and the right

boundary of each partition in the y-direction
(Either even or odd numbers are valid.)
$(1 \leqq \text{INTERY}(1) < \text{INTERY}(2) < \cdots < \text{INTERY}(\text{NRY}) \leqq 30 - \text{NRY})$

#09 (10F6.3) [(NRY+9)/10] lines

- (DYY (KY), KY=1, NRY) : mesh size Δy (cm) for each partition in the y-direction (not the partition thickness)

#10 (10I6) [(NRZ+9)/10] lines

- (INTERZ (KZ), KZ=1, NRZ) : number of mesh intervals between the origin and the top boundary of each partition in the z-direction
(Either even or odd numbers are valid.)
$(1 \leqq \text{INTERZ}(1) < \text{INTERZ}(2) < \cdots < \text{INTERZ}(\text{NRZ}) \leqq 60 - \text{NRZ})$

#11 (10F6.3) [(NRZ+9)/10] lines

- (DZZ (KZ), KZ=1, NRZ) : mesh size Δz (cm) for each partition in the z-direction (not the partition thickness)

#12 (7I6) KMAX lines

- (KX1 (K), KX2 (K), JY1 (K), JY2 (K), IZ1 (K), IZ2 (K), MR (K), K=1, KMAX) : assignment of composition
KX1 (K) : back mesh point no. of the region K
KX2 (K) : front mesh point no. of the region K
JY1 (K) : left mesh point no. of the region K
JY2 (K) : right mesh point no. of the region K
IZ1 (K) : bottom mesh point no. of the region K
IZ2 (K) : top mesh point no. of the region K
MR (K) : mixture no. for the region K (≡MK defined in #05)
$(1 \leqq \text{KX1} < \text{KX2} \leqq \text{NXMAX} \leqq 30,\ 1 \leqq \text{JY1} < \text{JY2} \leqq \text{NYMAX} \leqq 30$ and $1 \leqq \text{IZ1} < \text{IZ2} \leqq \text{NZMAX} \leqq 60)$

In BERMUDA, the numbering of the mesh points is as follows:

(1) "1" for the origin,

(2) doubly (twice) numbered as "INTERX (KX)+KX" and "INTERX (KX)+KX+1" for the interface between the KX-th and the (KX+1)-th partitions in the x-direction where KX =1, ···, NRX-1 (for treating spatial discontinuity of the macroscopic cross sections and the source distribution at the interfaces) and

(3) "NXMAX=INTERX (NRX)+NRX" ≦30 for the outermost mesh point in the x-direction.

And it is same for the y-direction, "NYMAX=INTERY(NRY)+NRY" ≦30 and also same for the z-direction except "NZMAX=INTERZ (NRZ)+NRZ" ≦60.

#13 (6F6. 3) 1 line

- BCX1 : back boundary condition for x=0.
- BCX2 : front boundary condition for x=x (NXMAX)
- BCY1 : left boundary condition for y=0.
- BCY2 : right boundary condition for y=y (NYMAX)
- BCZ1 : bottom boundary condition for z=0.

• BCZ2 : top boundary condition for z=z (NZMAX)

$$\text{boundary conditions} \equiv \begin{cases} -1. \cdots \text{symmetry condition} \\ 0. \cdots \text{vacuum boundary condition} \end{cases}$$

#14 (10I6) MMAX lines

• (MCODE (M, MK), M=1, MM (MK)) : code no. of each nuclide in the mixture MK defined in the group constants library to be used (for example, see Table 2. 2)
(The order of nuclides in a mixture is able to be arbitrary.)

Repeat this in the order of MK=1, ···, MMAX renewing the line for each mixture.

#15 (6E12. 5) [{MM(MK)+5} /6] lines for each mixture

• (AN (M, MK), M=1, MM (MK)) : effective number density (10^{24}cm^{-3}) of each nuclide in the mixture MK
(The order of nuclides in a mixture must be same as in #14.)

Repeat this in the order of MK=1, ···, MMAX renewing the line for each mixture.

#16 (6I6) 1 line

• KXS1 : the first mesh point no. to give x-distribution of non-zero independent source in #17
• KXS2 : the last mesh point no. to give x-distribution of non-zero independent source in #17
• JYS1 : the first mesh point no. to give y-distribution of non-zero independent source in #17
• JYS2 : the last mesh point no. to give y-distribution of non-zero independent source in #17
• IZS1 : the first mesh point no. to give z-distribution of non-zero independent source in #17
• IZS2 : the last mesh point no. to give z-distribution of non-zero independent source in #17

These mesh points must be given in the definition of (1)~(3) in #12 ($1 \leqq KXS1 \leqq KXS2 \leqq NXMAX$, $1 \leqq JYS1 \leqq JYS2 \leqq NYMAX$ and $1 \leqq IZS1 \leqq IZS2 \leqq NZMAX$). When IPS=0 in #04 and KXS1<KXS2, JYS1<JYS2 and IZS1<IZS2, S1 in #17 is a volume source. When IPS≠0, S1 is a point source (KXS1=KXS2=1, JYS1=JYS2=IPS and IZS1=IZS2=1).

#17 (6E12. 5) {[(JYS2-JYS1)/6] +1} lines for each (KX,IZ) point

• (S1(KX, JY, IZ), JY=JYS1, JYS2) : spatial distribution of independent source

Independent source is given in the form of a function with separation of variables as S1(KX, JY, IZ)×S2 (I)×S3 (L).
(Each of the S1, S2 and S3 should be normalized to its correct magnitude, respectively. However, it is also valid that the product of the S1, S2 and S3 has the correct normalized value for each energy group (*).)

Repeat it in the order of KX=KXS1, ···, KXS2 renewing the line for each KX.

And repeat "the above set over JY and KX" in the order of IZ=IZS1, ···, IZS2.

#18 (2I6) 1 line

• I1 : the first energy group no. to give energy spectre of non-zero independent source in #19
• I2 : the last energy group no. to give energy spectre of non-zero independent source in #19

If the source is of mono-energy (monochromatic), I1=I2=1.
Otherwise, $1 \leqq I1 < I2 \leqq IMAX$.

#19 (6E12.5) {[(I2–I1)/6] +1} lines

• (S2 (I), I=I1, I2) : energy spectre of independent source

(As BERMUDA has been programmed not in a continuous energy model but in a usual multigroup model, only the S2 (except the S1 and S3) must be given as integrated value for group i over ΔE_i.)

The S2 (I) is generally normalized to be 1 integrated over energy, that is,

$$\sum_{I=I1}^{I2} S2(I)=1.$$

(However, note the proviso (*) under #17.)

#20 (2I6) 1 line

• L1 : the first ordinate no. to give angular distribution of non–zero independent source in #21 (see Fig. 3.6)

• L2 : the last ordinate no. to give angular distribution of non–zero independent source in #21

If the source is mono–directional, L1=L2.

Otherwise, $1 \leqq L1 < L2 \leqq 80$.

#21 (6E12.5) {[(L2–L1)/6] +1} lines

• (S3 (L), L=L1, L2) : angular distribution of independent source

The S3 (L) is generally normalized to be 1 integrated over the unit sphere, that is,

$$\sum_{L=L1}^{L2} \Delta\vec{\Omega}_L S3\ (L)=1.$$

(However, note the proviso (*) under #17.)

Some examples of input data for the BERMUDA–3DN are shown in Figs. 5. 5 and 5. 6.

5.4.3 Output Data

The output data of BERMUDA–3DN are stored on the magnetic disk FT08 (Jxxxx. FLUX3DN. DATA; see Sec. 5. 4. 1 ($6)) and are also given on the printer.

The data on the output disk are as follows:

(1) In case of IPS=0, the following FORTRAN record is repeated for each group i (i=1, ···, IMAX) in the binary form,

(PHI (1, 1, NZMAX, L), L=1, 80), (DUMMY (L), L=1, 80),
(((TPHI (KX, JY, IZ), IZ=1, NZMAX), JY=1, NYMAX), KX=1, NXMAX),

where PHI (1, 1, NZMAX, L) : $\phi^i(0, 0, z_{NZMAX}, \vec{\Omega}_L)$,

TPHI (KX, JY, IZ) : $\Phi^i(x_{KX}, y_{JY}, z_{IZ}) = \sum_{L=1}^{80} \Delta\vec{\Omega}_L \phi^i\ (x_{KX}, y_{JY}, z_{IZ}, \vec{\Omega}_L)$ and

NXMAX, NYMAX, NZMAX: see Sec. 5. 4. 2. (#12).

(2) In case of IPS≠0, the following FORTRAN record is repeated for each group i (i=1, ···, IMAX) in the binary form,

(PHI (1, 1, NZMAX, L), L=1, 80), (PHI0 (1, 1, NZMAX, L), L=1, 80),
(((TPHI (KX, JY, IZ), IZ=1, NZMAX), JY=1, NYMAX), KX=1, NXMAX),

where PHI (1, 1, NZMAX, L) : $\phi^i(0, 0, z_{NZMAX}, \vec{\Omega}_L)+\phi_0^i(0, 0, z_{NZMAX}, \vec{\Omega}_L)$,
PHI0 (1, 1, NZMAX, L) : $\phi_0^i(0, 0, z_{NZMAX}, \vec{\Omega}_L)$,

DATA SET NAME : J1057.BERMUDA.DATA(DATA3DN1)

```
----+----1----+----2----+----3----+----4----+----5----+----6----+----7----+----8
1.0E+6                                                                      #01
  1  0  0  1                                                               #02
 NEUTRON BEHAIVIOR IN CAVITY BERM-3DN '91.2.12                              #03
  58   4  32 125   5   1   9   9  10 1.5488   +7 5.0      -3                #04
  2 10  8 10                                                                #05
     5     7     8    11    12    16    17    20    21                     #06
 3.20  2.0   2.0   4.333 5.0   2.0   2.0   6.666 2.0                        #07
     3     5     6     9    10    16    17    20    21                     #08
 4.0   4.0   2.0   4.333 5.0   6.333 2.0   6.666 2.0                        #09
     8    12    18    26    27    29    30    47    48    50               #10
31.0  19.5  20.33318.125 2.0  10.0   2.0   5.647 2.0  16.0                  #11
     1    30     1    30     1     9     1    REG 1  AIR TARGET ROOM       #12
     1    15     1    13    10    14     1    REG 2  1ST AIR PORT           "
     1    15    14    30    10    14     2    REG 3  UPPER ROOM WALL        "
    16    30     1    30    10    14     2    REG 4  SIDE ROOM WALL         "
     1     9     1     7    15    21     1    REG 5  2ND AIR PORT           "
     1     9     8    30    15    21     2    REG 6  UPPER REAR PORT        "
    10    30     1    30    15    21     2    REG 7  SIDE ROOM WALL         "
     1     6     1     4    22    30     1    REG 8  3RD AIR PORT           "
     1     6     5     7    22    30     3    REG 9  SS304                  "
     7     9     1     7    22    30     3    REG 10 SS304                  "
     1     9     8    15    22    30     4    REG 11 MORTAR                 "
    10    17     1    15    22    30     4    REG 12 MORTAR                 "
     1    17    16    30    22    30     1    REG 13 AMBIENT AIR            "
    18    30     1    30    22    30     1    REG 14 AMBIENT AIR            "
     1     9     1     7    31    37     1    REG 15 CAVITY ENTRANSE        "
     1     9     8     9    31    37     3    REG 16 SS304                  "
    10    11     1     9    31    37     3    REG 17 SS304                  "
     1    11    10    28    31    32     3    REG 18 SS304                  "
    12    28     1    28    31    32     3    REG 19 SS304                  "
     1    11    10    24    33    35     4    REG 20 MORTAR                 "
    12    24     1    24    33    35     4    REG 21 MORTAR                 "
     1    11    10    24    36    37     3    REG 22 SS304                  "
    12    24     1    24    36    37     3    REG 23 SS304                  "
     1    22     1    22    38    55     1    REG 24 CAVITY                 "
     1    22    23    24    38    55     3    REG 25 SS304                  "
    23    24     1    24    38    55     3    REG 26 SS304                  "
     1    24     1    24    56    57     3    REG 27 SS304                  "
     1    24    25    28    33    57     4    REG 28 MORTAR                 "
    25    28     1    28    33    57     4    REG 29 MORTAR                 "
     1    28     1    28    58    60     4    REG 30 MORTAR                 "
     1    28    29    30    31    60     3    REG 32 SS304                  "
    29    30     1    30    31    60     3    REG 31 SS304                  "
-1.   0.    -1.   0.    -1.   0.                                            #13
    70    80                                                              #14
    11    60    80   110   130   130   140   140   200   260               "
    60   140   140   140   240   250   260   280                           "
    11    60    80   110   130   130   140   140   200   260               "
 4.2000   -5 1.1300   -5                                                  #15
 7.9740   -3 5.4090   -4 4.3150   -2 7.8590   -4 3.8200   -4 2.6400   -3    "
 1.4800   -2 5.2900   -4 2.5600   -3 5.8600   -4                          "
 3.1729   -4 1.6962   -3 6.9211   -5 4.4572   -5 1.7400   -2 1.7343   -3    "
 5.7900   -2 8.1100   -3                                                  "
 4.8000   -3 3.8000   -2 4.3900   -2 1.0200   -3 3.1400   -4 3.4400   -3    "
 1.5900   -2 7.3500   -4 1.7400   -3 5.0500   -4                          "
```

Fig. 5.5 Example of input data for the BERMUDA-3DN (1)

```
                DATA SET NAME : J1057.BERMUDA.DATA(DATA3DN1)

----+----1----+----2----+----3----+----4----+----5----+----6----+----7----+----8

    1     1     1     1     1     1                                          #16
7.95775E-02                                                                #17
    1    66                                                                #18
0.20838E-07 0.16448E-04 0.23007E-03 0.22425E-02 0.10914E+00 0.72143E+00    #19
0.41429E-01 0.89107E-02 0.28841E-02 0.20256E-02 0.21780E-02 0.22142E-02     "
0.18204E-02 0.13969E-02 0.11361E-02 0.10069E-02 0.95007E-03 0.85182E-03     "
0.77476E-03 0.61673E-03 0.56121E-03 0.52662E-03 0.49357E-03 0.42204E-03     "
0.46284E-03 0.42282E-03 0.48904E-03 0.50647E-03 0.18914E-02 0.19120E-02     "
0.17765E-02 0.19314E-02 0.19843E-02 0.19417E-02 0.18398E-02 0.16886E-02     "
0.16009E-02 0.17106E-02 0.16732E-02 0.18281E-02 0.18514E-02 0.20011E-02     "
0.19585E-02 0.19623E-02 0.20140E-02 0.22632E-02 0.22026E-02 0.23575E-02     "
0.23032E-02 0.22464E-02 0.24000E-02 0.24594E-02 0.22360E-02 0.22503E-02     "
0.24310E-02 0.23188E-02 0.42449E-02 0.45896E-02 0.44748E-02 0.42410E-02     "
0.40203E-02 0.38627E-02 0.35477E-02 0.32289E-02 0.29268E-02 0.26867E-02     "
    1    80                                                                #20
1.          1.          1.          1.          1.          1.            #21
1.          1.          1.          1.          1.          1.             "
1.          1.          1.          1.          1.          1.             "
1.          1.          1.          1.          1.          1.             "
1.          1.          1.          1.          1.          1.             "
1.          1.          1.          1.          1.          1.             "
1.          1.          1.          1.          1.          1.             "
1.          1.          1.          1.          1.          1.             "
1.          1.          1.          1.          1.          1.             "
1.          1.          1.          1.          1.          1.             "
1.          1.          1.          1.          1.          1.             "
1.          1.          1.          1.          1.          1.             "
1.          1.          1.          1.          1.          1.             "
1.          1.                                                            "
```

Fig. 5.5 Example of input data for the BERMUDA-3DN (1) (continued)

TPHI (KX, JY, IZ) : $\Phi^i(x_{KX}, y_{JY}, z_{IZ}) = \sum_{L=1}^{80} \Delta\vec{\Omega}_L \{\phi^i(x_{KX}, y_{JY}, z_{IZ}, \vec{\Omega}_L) + \phi_0^i(x_{KX}, y_{JY}, z_{IZ}, \vec{\Omega}_L)\}$ and

NXMAX, NYMAX, NZMAX: see above (1).

The data on the output print are as follows:

(a) list of input file Jxxxx. DATA3DN. DATA (see Sec. 5. 4. 1 ($5)) like Fig. 5. 5 or Fig. 5. 6,
(b) list of the main input parameters with explanatory captions,

(The items (c)~(g) below are repeated for each energy group i (i=1, ···, IMAX).)

(c) CPU+VU time (sec) accumulated from the start of computation (EXEC LMGO) until the end of each main calculational item,
(d) when the convergence has been attained or ITMAX iterations have been finished for the 10-th grid,
- neutron balance parameters; F, GAIN, ABBS, SELF, XLEK (see Sec. 3. 7) integrated over the entire spatial region dealing with it as a single coarse mesh region,
- group no. i, iteration times IT, residual VERGF,

where $VERGF = \max_{KX, JY, IZ, L} |\{\phi^{i\,(IT-1)}(x_{KX}, y_{JY}, z_{IZ}, \vec{\Omega}_L)/\phi^{i\,(IT)}(x_{KX}, y_{JY}, z_{IZ}, \vec{\Omega}_L)\} - 1| < \varepsilon$

(KX, JY, IZ, L : except the cases where $\phi^{i\,(IT)}(x_{KX}, y_{JY}, z_{IZ}, \vec{\Omega}_L) = 0$),

IT : iteration times (IT=1, 2, ···),

(When the energy grid model is used for the group i, these printed neutron balance parameters and VERGF are meaningless, because the iteration is terminated by ITMAX (≦3) times. In addition, these parameters are obtained only from the data of the last (10-th) grid in the group i.)

(e) • the upper energy boundary EUP(i) (eV),

```
                DATA SET NAME : J1057.BERMUDA.DATA(DATA3DN2)

----+----1----+----2----+----3----+----4----+----5----+----6----+----7----+----8

1.0E+6                                                                        #01
  1  0  0  2                                                                 #02
 OFFSET GAP STREAMING CASE-1 BERM-3DN '91.5.29                                #03
  58   3  19 125   5  13   5  11   5 1.5488   +7 5.0      -3                  #04
  2 10  8                                                                     #05
    15    17    18    20    25                                               #06
1.3333 3.75  3.0   2.25  29.0                                                 #07
     3     4     5     7     9    10    12    14    15    16                  #08
    19                                                                        "
 30.0  3.0   12.0  9.25  1.5   1.0   1.5   7.25 12.0   3.0                   #09
 30.0                                                                         "
    10    15    25    35    55                                               #10
 24.8 15.6  12.2   4.00  2.50                                                 #11
     1    30     1    30     1    11     1    REG 1  AIR TARGET ROOM         #12
     1    24     5    25    12    17     1    REG 2  AIR FRONT PORT           "
     1    24     1     4    12    17     2    REG 3  SIDE ROOM WALL           "
     1    24    26    30    12    17     2    REG 4  SIDE ROOM WALL           "
    25    30     1    30    12    17     2    REG 5  UPPER ROOM WALL          "
     1    16     9    22    18    28     1    REG 6  AIR REAR PORT            "
     1    16     1     8    18    28     2    REG 7  SIDE ROOM WALL           "
     1    16    23    30    18    28     2    REG 8  SIDE ROOM WALL           "
    17    30     1    30    18    28     2    REG 9  UPPER ROOM WALL          "
     1    19    12    14    29    39     1    REG 10 FIRST GAP               "
     1    19     7    11    29    39     3    REG 11 SS304                   "
     1    19    15    24    29    39     3    REG 12 SS304                   "
     1    19    17    19    40    60     1    REG 13 SECOND GAP              "
     1    19     7    16    40    60     3    REG 14 SS304                   "
     1    19    20    24    40    60     3    REG 15 SS304                   "
    20    21     7    24    29    60     3    REG 16 SS304                   "
     1    21     1     6    29    60     1    REG 17 AMBIENT AIR             "
     1    21    25    30    29    60     1    REG 18 AMBIENT AIR             "
    22    30     1    30    29    60     1    REG 19 AMBIENT AIR             "
-1.   0.    0.    0.    -1.   0.                                             #13
    70    80                                                                #14
    80    11    60   110   130   130   140   140   200   260                "
    60   140   140   140   240   250   260   280                            "
 3.8810   -5 1.0400   -5                                                    #15
 4.3150   -2 7.9740   -3 5.4090   -4 7.8590   -4 3.8200   -4 2.6400   -3    "
 1.4800   -2 5.2900   -4 2.5600   -3 5.8600   -4                            "
 3.1729   -4 1.6962   -3 6.9211   -5 4.4572   -5 1.7400   -2 1.7343   -3    "
 5.7900   -2 8.1100   -3                                                    "
     1     1    13    13     1     1                                        #16
 7.95775E-02                                                               #17
     1    66                                                               #18
 0.20838E-07 0.16448E-04 0.23007E-03 0.22425E-02 0.10914E+00 0.72143E+00    #19
 0.41429E-01 0.89107E-02 0.28841E-02 0.20256E-02 0.21780E-02 0.22142E-02    "
 0.18204E-02 0.13969E-02 0.11361E-02 0.10069E-02 0.95007E-03 0.85182E-03    "
 0.77476E-03 0.61673E-03 0.56121E-03 0.52662E-03 0.49357E-03 0.42204E-03    "
 0.46284E-03 0.42282E-03 0.48904E-03 0.50647E-03 0.18914E-02 0.19120E-02    "
 0.17765E-02 0.19314E-02 0.19843E-02 0.19417E-02 0.18398E-02 0.16886E-02    "
 0.16009E-02 0.17106E-02 0.16732E-02 0.18281E-02 0.18514E-02 0.20011E-02    "
 0.19585E-02 0.19623E-02 0.20140E-02 0.22632E-02 0.22026E-02 0.23575E-02    "
 0.23032E-02 0.22464E-02 0.24000E-02 0.24594E-02 0.22360E-02 0.22503E-02    "
 0.24310E-02 0.23188E-02 0.42449E-02 0.45896E-02 0.44748E-02 0.42410E-02    "
 0.40203E-02 0.38627E-02 0.35477E-02 0.32289E-02 0.29268E-02 0.26867E-02    "
```

Fig. 5.6 Example of input data for the BERMUDA-3DN (2)

```
                DATA SET NAME : J1057.BERMUDA.DATA(DATA3DN2)
----+----1----+----2----+----3----+----4----+----5----+----6----+----7----+----8
    1    80                                                              #20
1.          1.          1.          1.          1.          1.          #21
1.          1.          1.          1.          1.          1.           "
1.          1.          1.          1.          1.          1.           "
1.          1.          1.          1.          1.          1.           "
1.          1.          1.          1.          1.          1.           "
1.          1.          1.          1.          1.          1.           "
1.          1.          1.          1.          1.          1.           "
1.          1.          1.          1.          1.          1.           "
1.          1.          1.          1.          1.          1.           "
1.          1.          1.          1.          1.          1.           "
1.          1.          1.          1.          1.          1.           "
1.          1.          1.          1.          1.          1.           "
1.          1.          1.          1.          1.          1.           "
1.          1.                                                           "
```

Fig. 5.6 Example of input data for the BERMUDA-3DN (2) (continued)

- the lower energy boundary EUP(i+1) (eV),
- the energy width ΔE_i (eV) and

(f) neutron scalar flux over the x=0 plane,

Φ^i (0, y_{JY}, z_{IZ}) for JY=1, ···, NYMAX and for IZ=NZMIN, ···, NZMAX,

where

$$NZMIN = \begin{cases} 1 \text{ for ISTEP} \neq 2 \text{ and} \\ \\ \text{IFACE for ISTEP} = 2 \text{ (see Sec. 5. 4. 2 (\#2)) and} \end{cases}$$

(g) neutron scalar flux over the $z = z_{NZMAX}$ plane,

Φ^i (x_{KX}, y_{JY}, z_{NZMAX}) for KX=1, ···, NXMAX and for JY=1, ···, NYMAX.

The STOP codes are as follows:

(1) 1001 : KMAX regions do not cover completely the whole (x, y, z) volume, or some regions overlap (error in KX1 (K), KX2 (K), JY1 (K) JY2 (K), IZ1 (K) and IZ2 (K) in input data #12).

(2) 2001 : IFACE in input data #02 is not on the bottom boundary of a partition in the z-direction,

(3) 2222 : The input fixed source for the group 1 is zero (error in input data #16~#21) and

(4) 9876 : Total number of nuclides exceeds 20 (error in input data #05 or #14).

6. Concluding Remarks

Four neutron transport codes in the radiation transport code system BERMUDA have been developed for one–, two– and three–dimensional geometries. To solve the transport equation numerically, the deterministic direct integration method was adopted in a multigroup model, because it simulates the neutron transport phenomenon in the natural, direct and simple equation. The energy group model is convenient to take into account the neutron balance especially in the thermal energy group, and also to derive adjoint equation. The Legendre polynomial expansion method was not used considering the strong anisotropy of both angular flux and scattering cross section in the high energy region above 10MeV.

In course of development, it was found that a very fine treatment was necessary for variables of energy E and direction $\vec{\Omega}$ so as to simulate precisely the neutron transport process. Validity of the codes was tested by analyzing the shielding benchmark experiments using DT neutron source of the FNS facility in JAERI. The results have shown a good agreement especially for the deep penetration problems. The energy grid model dividing a group into ten fine groups has shown to be very effective to enhance accuracy of the penetration calculation. The remained problem is to achieve efficiency in computation or to save computer resources.

As to the three–dimensional calculation, it is not so practical in terms of computing time. However, the computer itself is progressing very rapidly in speed, memory and data storage media. If the progress in these aspects will be attained, the deterministic code will be possible to produce accurate solutions over a whole calculated region attenuating to 10^{-10} or less in magnitude.

The present code system has been developed in the following seven steps:

(1) coding the source program from the beginning,
(2) mathematical or numerical consideration on the method to solve the basic transport equation,
(3) developing programs for the group constants library,
(4) planning and performing the benchmark experiments,
(5) execution of the validity tests,
(6) consideration on the cause of discrepancy between the calculated and the measured results and
(7) improvements of the codes to achieve accuracy repeated many times.

These steps were carried out by each of the authors in a good cooperating relation.

In a strict sense, a code system is necessary to be always improved incorporating the newest knowledge acquired through usage experiences and comparison with experiments. However, it has already taken more than twelve years for the development work including preparation of the present report. The source programs of the four neutron transport codes:

(1) BERMUDA–1DN,
(2) BERMUDA–2DN,
(3) BERMUDA–2DN–S16 and
(4) BERMUDA–3DN

will be available to the public through the Code Center of JAERI within 1992.

A neutron transport code for three–dimensional (r,θ,z) geometry BERMUDA–RTZN, gamma rays transport codes BERMUDA–1DG, –2DG, –3DG and adjoint neutron transport codes BERMUDA–1DNA, –2DNA and –3DNA have also been developed as preliminary versions. They need further

improvements and validity tests as well as enhancement in the group constants library. On these unfinished codes and data, manuals will be published as Part II and III after improvements.

An expert system is being developed as a code package on an engineering work station to facilitate usage of transport codes such as input data preparation and graphic display of results obtained from data of flux distribution on the output disk and data in the group constants library. With this convenient package and the BERMUDA code system, a standard shielding calculation code system INTEL-BERMUDA is now under development as well as a standard shielding database which mainly consists of group constants.

Acknowledgments

The authors would like to express their sincere thanks to Drs. Y. Ishiguro, H. Maekawa, Y. Seki and Y. Oyama of JAERI and also to Dr. K. Takeuchi of the Ship Research Institute for their cooperation, discussion and encouragement from the early period of this development work. The authors are also indebted to Dr. M. Akimoto, Messrs. K. Yamazaki, M. Tomiyama and K. Okada of the Computing and Information Systems Center of JAERI for their cooperation in executing the special large jobs of the BERMUDA-3DN on holidays. Thanks are also due to Drs. Y. Nakajima and N. Sasamoto of JAERI for their critical reading of the manuscript.

References

1) Engle W.W.Jr.: "A User's Manual for ANISN, A One Dimensional Discrete Ordinates Transport Code with Anisotropic Scattering," K-1693 (1967).
2) Rhodes W.A., Mynatt F.R.: "The DOT III Two-Dimensional Discrete Ordinates Transport Code," ORNL-TM-4280 (1973).
3) Takeuchi K.: "Study on a Numerical Approach to the Boltzmann Transport Equation for the Purpose of Analyzing Neutron Shields," Report of Ship Research Institute, vol.9, no.6 (1972) (in Japanese).
4) Hasegawa A.: "Development of EDFSRS : Evaluated Data Files Storage and Retrieval System," JAERI 1295 (1985).
5) Hasegawa A.: "PROF-GROUCH-G/B : A Code System for Processing Evaluated Nuclear Data to Produce Group Constants for BERMUDA or Other Transport Codes," to be published.
6) Kosako K.: "INTERF : The Reaction Rates and Spectra Editing Code for Analysis of Fusion Neutronics Experiments," JAERI-M 90-199 (1990) (in Japanese) and
Hasegawa A. et al.: "TSGPLT, GPLOTB1N and GPLOTB2N Codes," private communication.
7) Weinberg A.M., Wigner E.P.: "The Physical Theory of Neutron Chain Reactors," Chapters IX and X, The University of Chicago Press (1958).
8) Radiation Shielding Information Center, ORNL : CCC-276, page 177, "Common Symmetric Quadratures and the DOQDP Computer Code," by J.P. Jenal (1975).
9) Suzuki T. et al.: "14MeV Neutron Penetration into Fe Assembly - Accuracy Improvement of the BERMUDA Code -," Proc. First Int. Conf. on Supercomputing in Nucl. Appl. (SNA'90), 145, published by Nuclear Energy Data Center (1990).
10) Nakashima H. et al.: "Experiment and Analysis of 14MeV Neutron Deep Penetration in a Type 316L Stainless Steel Assembly," Fusion Eng. Design, vol.10, 121 (1989).
11) Radiation Shielding Information Center, ORNL : "FORIST Spectra Unfolding Code," PSR-92 (1975).
12) Nakashima H., Tanaka S., Suzuki T.: "Experiment and Analysis of the Behavior of 14-MeV Neutrons in a Large Cavity," Fusion Technology, vol.16, 365 (1989).
13) LANL : "MCNP : A General Purpose Monte Carlo Code for Neutron and Photon Transport, Version 3A," LA-7396-M (1986).
14) "ENDF-201 : ENDF/B Summary Documentation," BNL-17541, 2nd ed. Compiled by D. Garber (1975).
15) "Summary of JENDL-2 General Purpose File," JAERI-M 84-103, Edited by T. Nakagawa (1984).
16) "JENDL-3 PR1 and PR2 : Japanese Evaluated Nuclear Data Library, Version 3 Preliminary Version-1 & 2," Nuclear Data Center, JAERI (1984).
17) Takahashi A. et al.: "Method for Calculating Anisotropic Neutron Transport Using Scattering Kernel without Polynomial Expansion," J. Nucl. Sci. Technol., vol.16, 1 (1979).
18) Oyama Y. et al.: "Development of a Spherical NE213 Spectrometer with 14mm Diameter," JAERI-M 84-124 (1984) (in Japanese).
19) Nakashima H.: "Study on Shielding Design Methods for Fusion Reactors Using Benchmark Experiments," JAERI-M 92-025 (1992) (in Japanese).
20) Mori T., Nakagawa M., Sasaki M.: "One-, Two- and Three-Dimensional Transport Codes Using Multi-Group Doulbe-Differential Form Cross Sections," JAERI 1314 (1988).

21) Nakamura T. et al.: "A D–T Neutron Source for Fusion Neutronics Experiments at the JAERI," Proc. Seventh Symp. Ion and Plasma–Assisted Techniques, Kyoto, Japan (1983).
22) Oyama Y. et al.: "Neutron Field Characteristics in a Concrete Cavity Having a DT Neutron Source," Fusion Technol., vol.10, 585 (1986).
23) Nishimura T. et al.: "Development of Discrete Ordinates S_N Code in Three–Dimensional (X,Y,Z) Geometry for Shielding Design," J. Nucl. Sci. Technol., vol.17, 539 (1980).
24) Sasamoto N.: "A Study on Direct Integration Method for Solving Neutron Transport Equation in Three–Dimensional Geometry," JAERI–M 82–167 (1983).
25) Radiation Shielding Information Center, ORNL: "TORT : Three–Dimensional Discrete Ordinates Transport," CCC–543/TORT, ORNL–6268 (1987).
26) Kosako K. et al.: "Neutron Cross Section Libraries for Analysis of Fusion Neutronics Experiments," JAERI–M 88–076 (1988) (in Japanese).
27) Kosako K. et al.: "FSXLIB–J3 : MCNP Continuous Energy Cross Section Library Based on JENDL–3," JAERI–M 91–187 (1991) (in Japanese).

Appendix. Examples of Source Program Lists

A source program list of MAIN routine is convenient to see the summary of the structure and calculational flow of the entire code. In addition, the comments in it give the history of development and improvements on each item of calculation.

In the following, the list of the MAIN routine is shown for each of the four neutron transport codes described in the text:

(1) MAIN routine of the BERMUDA-1DN,
(2) MAIN routine of the BERMUDA-2DN,
(3) MAIN routine of the BERMUDA-2DN-S16 and
(4) MAIN routine of the BERMUDA-3DN.

And the subroutines AZIM2 and WGC in the BERMUDA-2DN for calculating the azimuthal weights $\Delta\phi$ described in Sec.3.4.2 are given as:

(5) SUBROUTINE AZIM2 and SUBROUTINE WGC in the BERMUDA-2DN

which needed a work involving much elaboration preceding the start of development of the two-dimensional code in August 1981. These subroutines had been written since May 1981. There only the surface of unit sphere is dealt with.

(1) MAIN routine of the BERMUDA-1DN

```
C      PROGRAM BERMUDA-1DN
C       ONE-DIMENSIONAL NEUTRON TRANSPORT PROGRAM
C       IN PLANE AND SPHERICAL GEOMETRIES
C                              OCT.,1979 BY TOMOO SUZUKI , JAERI
C                   MODIFIED MARCH,1984
C                       (1) SELF-SHIELDING FACTOR
C                       (2) NUCLIDES UP TO 30
C                       (3) GZI-M' TO THETA-M'
C                       (4) RELATIVITY , DIRECT BEAM , ETC.
C                   MODIFIED MAY,1989
C                       (1) POINT KERNEL MODEL
C                            RO=DR(K)
C                            PHID=PHI(N1,L)*RSQ(N1,L)/RSQ(N,L)
C                            SND=S(N1,L)
C                             FOR (L.EQ. 1).AND.(N.GT.2) (SLAB & SPHERE)
C                                 (L.EQ.20).AND.(N.LT.NMAX-1) (SLAB)
C                   MODIFIED JUNE,1989
C                       (1) INFINETE DILUTION SIGT TO OBTAIN UNCOLLIDED
C                           FLUX
C                       (2) 10 GRIDS IN A GROUP EXCEPT THERMAL, AND
C                       (3) ITMAX ITERATIONS FOR EACH GRID
C                       (4) 10 GRIDS IN THE PREVIOUS GROUP
C                   MODIFIED OCTOBER,1989
C                       (1) MAXIMUM NUMBER OF MESH INTERVALS 100 ==> 240
C                   MODIFIED DECEMBER,1989
C                       (1) WG(N,L,M) HAS BEEN OBTAINED AS AN AVERAGE OF
C                           5 POINTS OF L, AND NORMALIZED TO 2.*PI NOT
C                           WITH RESPECT TO 'N' BUT 'L'.
C
C         MAIN ROUTINE
C
      COMMON /LBLPG/HEAD(18),IPAGE,IT,TMAX,IRSTRT,INTPS,IIB,IBMAX,ITMAX
      COMMON /LBLIN/I,IMAX,IP,EQIN(1007)
    1 FORMAT(18A4)
    2 FORMAT(2I3)
    3 FORMAT(F6.3)
      CALL DTLIST
      CALL STIMER
      REWIND 1
      REWIND 2
      REWIND 3
      REWIND 4
      READ (5,3) TMAX
      READ (5,2) KIND
      READ (5,2) IRSTRT,ITMAX
      READ (5,1) HEAD
      IF(ITMAX.EQ.0) ITMAX=1
      IPAGE=0
      CALL PAGE
      CALL INPUT
      CALL CROSS
      CALL AZIM
      IMAX1=IMAX
      DO 500 II=1,IMAX1
      IF(II.LT.IRSTRT) GO TO 500
      I=II
      CALL SELF
      DO 400 IB=1,IBMAX
```

```
      IIB=IB
      CALL SELFB
      IT=0
  200 IT=IT+1
      CALL SOURCE
      IF(IP.NE.0) GO TO 250
      CALL PLANE
      GO TO 300
  250 CALL SPHERE
  300 CALL CONV
      IF(IT.GT.0) GO TO 200
      CALL SLDOWN
      CALL SLDWNB
  400 CALL OUTPUT
  500 CONTINUE
      REWIND 1
      REWIND 2
      STOP
      END
```

(2) MAIN routine of the BERMUDA-2DN

```
C      PROGRAM BERMUDA-2DN
C       TWO-DIMENSIONAL NEUTRON TRANSPORT PROGRAM
C       IN R-Z CYLINDRICAL GEOMETRY
C                          AUG.,1981 BY TOMOO SUZUKI , JAERI
C                  MODIFIED MAY,1984
C                       (1) NUCLIDES UP TO 20 ( 0 < MML < 21 )
C                       (2) GZI-M' TO THETA-M'
C                       (3) INTEGRATION WITH RESPECT TO MU INSTEAD OF E
C                       (4) RELATIVITY , DIRECT BEAM ON EASTSIDE ARC
C                       (5) POINT SOURCE ON Z-AXIS EVEN Z>0
C                  MODIFIED JUNE,1985
C                       (1) AZIM2 : AVERAGE OF 25 POINTS
C                  MODIFIED AUGUST,1985
C                       (1) STEP CALCULATION IN Z DIRECTION
C                           ( CONCRETE OR MORTAR ROOM TREATMENT )
C                  MODIFIED MARCH,1986
C                       (1) COMPLETELY SYMMETRIC S8 METHOD (LQ8)
C                  MODIFIED AUGUST,1986
C                       (1) JSSL INTERPOLATION ROUTINES FOR REBALANCING
C                       (2) EXPONENTIAL INTERPOLATION ON X<P-1> POINT
C                       (3) F(MU):HISTOGRAM TO PIECEWISE LINEAR FUNCTION
C                       (4) ANGULAR FLUX ON WESTSIDE ARC
C                  MODIFIED SEPTEMBER,1986
C                       (1) F(MU):MU ---- 81 POINTS
C                       (2) TRIGGER FOR (48,110,60) POINTS (LOGICAL*1)
C                       (3) COARSE MESH REBALANCING (CMR)
C                  MODIFIED NOVEMBER,1986
C                       (1) A(LL,MK) REMOVED
C                  MODIFIED DECEMBER,1986
C                       (1) ORDER OF REBALANCED COARSE MESHES IS FIXED
C                           AFTER SOME ITERATIONS.
C                  MODIFIED JANUARY,1987
C                       (1) CMR WITHOUT ANGULAR FLUXES COMING INTO A CM
C                  MODIFIED FEBRUARY,1987
C                       (1) ENERGY GROUP STRUCTURE 125G
C                           LIBRARY : J3931.BERM125X
C                       (2) HIO ( FT01 & FT09 )
C                  MODIFIED JUNE,1988
C                       (1) 10 GRIDS IN A GROUP EXCEPT THERMAL, AND
C                       (2) ITMAX ITERATIONS FOR EACH GRID (FT10)
C                       (3) EXTENDED COMMON SECTIONS
C                  MODIFIED NOVEMBER,1988-FEBRUARY,1989
C                       (1) 10 GRIDS IN THE PREVIOUS GROUP (FT11 & FT12)
C                  MODIFIED FEBRUARY,1989
C                       (1) SYMMETRIC ANGULAR SOURCE ON Z-AXIS
C                  MODIFIED JUNE,1989
C                       (1) POINT KERNEL MODEL FOR
C                             (L.EQ. 2).AND.(JR.EQ.  1)
C                             (L.EQ.40).AND.(JR.EQ.  1)
C                             (L.EQ.13).AND.(IZ.EQ.IPS)
C                             (L.EQ.21).AND.(IZ.EQ.IPS)
C                       (2) INFINITE DILUTION SIGT TO OBTAIN UNCOLLIDED
C                           FLUX
C                  MODIFIED JULY-AUGUST,1989
C                       (1) 'BACKSPACE 3' REMOVED. PREVIOUS CALCULATION
C                           OF SLOWING DOWN SOURCES FOR TEN GRIDS IN THE
C                           NEXT GROUP ( FT10 & FT11 HAVE BEEN REMOVED.)
C                  MODIFIED DECEMBER,1989
```

```
C                       (1) FILES FOR RESTART ( FT08 & FT12 ) ARE
C                           PREPARED AFTER EACH GROUP CALCULATION.
C
C          MAIN ROUTINE
C
      COMMON /LBLPG/HEAD(18),IPAGE,II,IMAX1,IT,TMAX,IRSTRT,ISTEP,IFACE,
     1NZMIN,KKZMIN,IIB,IBMAX,ITMAX,EQPG
    1 FORMAT(F6.3)
    2 FORMAT(4I3)
    3 FORMAT(18A4)
      CALL DTLIST
      CALL STIMER
      READ (5,1) TMAX
      READ (5,2) IRSTRT,ISTEP,IFACE,ITMAX
      READ (5,3) HEAD
      IF(ITMAX.EQ.0) ITMAX=1
      REWIND 1
      IF(ISTEP.NE.0) REWIND 2
      REWIND 3
      REWIND 4
      REWIND 8
      REWIND 9
      REWIND 12
      IPAGE=0
      CALL PAGE
      CALL EARTH
      CALL INPUT2
      CALL CROSS2
      CALL AZIM2
      IMAX=IMAX1
      DO 500 I=1,IMAX
      IF(I.LT.IRSTRT) GO TO 500
      II=I
      CALL DWNSC2
      CALL SLFK2N
      CALL SELSC2
      DO 300 IB=1,IBMAX
      IIB=IB
      CALL SELSCB
      IT=0
  200 IT=IT+1
      CALL SOURC2
      CALL RZ2N1
      CALL RZ2N2
      CALL CONV2
      IF(IT.GT.0) GO TO 200
      CALL DWNSCB
  300 CALL OUTPT2
  500 CONTINUE
      REWIND 1
      IF(ISTEP.NE.0) REWIND 2
      REWIND 8
      REWIND 9
      STOP
      END
```

(3) MAIN routine of the BERMUDA-2DN-S16

```
C      PROGRAM BERMUDA-2DN-S16
C       TWO-DIMENSIONAL NEUTRON TRANSPORT PROGRAM
C       IN R-Z CYLINDRICAL GEOMETRY
C                              AUG.,1981 BY TOMOO SUZUKI , JAERI
C                    MODIFIED MAY,1984
C                         (1) NUCLIDES UP TO 20 ( 0 < MML < 21 )
C                         (2) GZI-M' TO THETA-M'
C                         (3) INTEGRATION WITH RESPECT TO MU INSTEAD OF E
C                         (4) RELATIVITY , DIRECT BEAM ON EASTSIDE ARC
C                         (5) POINT SOURCE ON Z-AXIS EVEN Z>0
C                    MODIFIED JUNE,1985
C                         (1) AZIM2 : AVERAGE OF 25 POINTS
C                    MODIFIED AUGUST,1985
C                         (1) STEP CALCULATION IN Z DIRECTION
C                             ( CONCRETE OR MORTAR ROOM TREATMENT )
C                    MODIFIED MARCH,1986
C                         (1) COMPLETELY SYMMETRIC S8 METHOD (LQ8)
C                    MODIFIED AUGUST,1986
C                         (1) JSSL INTERPOLATION ROUTINES FOR REBALANCING
C                         (2) EXPONENTIAL INTERPOLATION ON X<P-1> POINT
C                         (3) F(MU):HISTOGRAM TO PIECEWISE LINEAR FUNCTION
C                         (4) ANGULAR FLUX ON WESTSIDE ARC
C                    MODIFIED SEPTEMBER,1986
C                         (1) F(MU):MU ---- 81 POINTS
C                         (2) TRIGGER FOR (48,110,60) POINTS (LOGICAL*1)
C                         (3) COARSE MESH REBALANCING (CMR)
C                    MODIFIED NOVEMBER,1986
C                         (1) A(LL,MK) REMOVED
C                    MODIFIED DECEMBER,1986
C                         (1) ORDER OF REBALANCED COARSE MESHES IS FIXED
C                             AFTER SOME ITERATIONS.
C                    MODIFIED JANUARY,1987
C                         (1) CMR WITHOUT ANGULAR FLUXES COMING INTO A CM
C                    MODIFIED FEBRUARY,1987
C                         (1) ENERGY GROUP STRUCTURE 125G
C                             LIBRARY : J3931.BERM125X
C                         (2) HIO ( FT01 & FT09 )
C                    MODIFIED AUGUST,1988 -- FEBRUARY,1989
C                         (1) ANGULAR QUADRATURE S8 ====> S16 (NAKASHIMA)
C                         (2) 10 GRIDS IN A GROUP EXCEPT THERMAL, AND
C                         (3) ITMAX ITERATIONS FOR EACH GRID (FT10)
C                         (4) EXTENDED COMMON SECTIONS
C                    MODIFIED FEBRUARY,1989
C                         (1) 10 GRIDS IN THE PREVIOUS GROUP (FT11 & FT12)
C                         (2) SYMMETRIC ANGULAR SOURCE ON Z-AXIS
C                    MODIFIED JUNE,1989
C                         (1) POINT KERNEL MODEL FOR
C                               (L.EQ.  2).AND.(JR.EQ.  1)
C                               (L.EQ.144).AND.(JR.EQ.  1)
C                               (L.EQ. 57).AND.(IZ.EQ.IPS)
C                               (L.EQ. 73).AND.(IZ.EQ.IPS)
C                         (2) INFINETE DILUTION SIGT TO OBTAIN UNCOLLIDED
C                             FLUX
C                    MODIFIED JULY-AUGUST,1989
C                         (1) 'BACKSPACE 3' REMOVED. PREVIOUS CALCULATION
C                             OF SLOWING DOWN SOURCES ( SDB ) FOR TEN
C                             GRIDS IN THE NEXT GROUP ( FT10 & FT11 )
C                    MODIFIED DECEMBER,1989
```

```
C                       (1) FILES FOR RESTART ( FT08 & FT12 ) ARE
C                           PREPARED AFTER EACH GROUP CALCULATION.
C                   MODIFIED JULY,1991
C                       (1) SDB ==> AE  ( FT10 & 11 HAVE BEEN REMOVED. )
C
C          MAIN ROUTINE
C
      COMMON /LBLPG/HEAD(18),IPAGE,II,IMAX1,IT,TMAX,IRSTRT,ISTEP,IFACE,
     1NZMIN,KKZMIN,IIB,IBMAX,ITMAX,EQPG
    1 FORMAT(F6.3)
    2 FORMAT(4I3)
    3 FORMAT(18A4)
      CALL DTLIST
      CALL STIMER
      READ (5,1) TMAX
      READ (5,2) IRSTRT,ISTEP,IFACE,ITMAX
      READ (5,3) HEAD
      IF(ITMAX.EQ.0) ITMAX=2
      REWIND 1
      IF(ISTEP.NE.0) REWIND 2
      REWIND 3
      REWIND 4
      REWIND 8
      REWIND 9
      REWIND 12
      IPAGE=0
      CALL PAGE
      CALL EARTH
      CALL INPUT2
      CALL CROSS2
      CALL AZIM2
      IMAX=IMAX1
      DO 500 I=1,IMAX
      IF(I.LT.IRSTRT) GO TO 500
      II=I
      CALL DWNSC2
      CALL SLFK2N
      CALL SELSC2
      DO 300 IB=1,IBMAX
      IIB=IB
      CALL SELSCB
      IT=0
  200 IT=IT+1
      CALL SOURC2
      CALL RZ2N1
      CALL RZ2N2
      CALL CONV2
      IF(IT.GT.0) GO TO 200
      CALL DWNSCB
  300 CALL OUTPT2
  500 CONTINUE
      REWIND 1
      IF(ISTEP.NE.0) REWIND 2
      REWIND 8
      REWIND 9
      STOP
      END
```

(4) MAIN routine of the BERMUDA-3DN

```
C      PROGRAM BERMUDA-3DN
C       THREE-DIMENSIONAL NEUTRON TRANSPORT PROGRAM IN X-Y-Z GEOMETRY
C                  FEB.,1983 BY TOMOO SUZUKI , JAERI
C                   WITH CONTRIBUTIONS BY AKIRA HASEGAWA AND TOSHIMI MORI
C
C                    MODIFIED JULY-SEPTEMBER,1990
C                         (1) 10 GRIDS DIVISION, ETC. AS IN BERMUDA-2DN
C                    MODIFIED OCTOBER,1990
C                         (1) SUBROUTINE HREAD & HWRITE
C                    MODIFIED MAY,1991
C                         (1) 19800 TRACKS CAN BE ALLOCATED CONTIGUOUSLY
C                             FOR HIO SCRATCHES ( HREAD & HWRITE )
C                         (2) REMOVED THE SYMMETRY CONDITION WITH RESPECT
C                             TO Y=0 PLANE ( SLSC31 & SLSC32 )
C          MAIN ROUTINE
C
      COMMON /LBLPG/IT,TMAX,IMAX1,II,IRSTRT,IPAGE,HEAD(18),ISTEP,IFACE,
     1NZMIN,KKZMIN,IIB,IBMAX,ITMAX,LYPS
    1 FORMAT(E6.3)
    2 FORMAT(4I3)
    3 FORMAT(18A4)
      CALL DTLIST
      CALL STIMER
      READ (5,1) TMAX
      READ (5,2) IRSTRT,ISTEP,IFACE,ITMAX
      READ (5,3) HEAD
      IF(ITMAX.EQ.0) ITMAX=1
      REWIND 1
      IF(ISTEP.NE.0) REWIND 2
      REWIND 3
      REWIND 4
      REWIND 8
      IPAGE=0
      CALL PAGE
      CALL EARTH3
      CALL INPUT3
      CALL CROSS3
      CALL AZIM3
      IMAX=IMAX1
      IF(IMAX.GT.48) REWIND 11
      IF(IMAX.GT.96) REWIND 21
      DO 500 I=1,IMAX
      IF((ITMAX.EQ.2).AND.(I.EQ.8)) ITMAX=1
      IF(I.LT.IRSTRT) GO TO 500
      II=I
      CALL DWNSC3
      CALL SELSCK
      CALL SLSC31
      CALL SLSC32
      DO 300 IB=1,IBMAX
      IIB=IB
      CALL SELSCB
      IT=0
  200 IT=IT+1
      CALL SOURC3
      CALL XYZ1
      CALL XYZ2
      CALL CONV3
```

```
      IF(IT.GT.0) GO TO 200
      CALL DWNSCB
  300 CALL OUTPT3
  500 CONTINUE
      REWIND 1
      IF(ISTEP.NE.0) REWIND 2
      REWIND 8
      IF(IMAX.GT.48) REWIND 11
      IF(IMAX.GT.96) REWIND 21
      STOP
      END
```

(5) SUBROUTINE AZIM2 and SUBROUTINE WGC in the BERMUDA-2DN

```
      SUBROUTINE AZIM2
      COMMON /AAA/WP(40),WQ(40),WW(40),WBN(40),WBS(40),WBE(40),WBW(40)
      DOUBLE PRECISION WP,WQ,WW,WBN,WBS,WBE,WBW
      COMMON /WORK/GZI(80),GZISQ(80),SINM(80),COSLQ(40),WPSQ(40),
     1SINL(40),SINN(40),SINS(40),PI,X2,X1,GZL,WWL,WBNL,WBSL,WBWL,WBEL,
     2DWP,WPL,DWQ,SINLL,COSL,WQL,WPLB,COSLB,WQLB,WWN,WBNN,WBSN,WBWN,
     3WBEN,SINNN,SINSN,COSW,COSE,GZNW,GZNE,GZSW,GZSE,GZNL,GZSL,GZW,GZE,
     4COSWB,COSEB,GZNWB,GZNEB,GZSWB,GZSEB,GZNLB,GZSLB,GZWB,GZEB,WPG,SQR,
     5WMAX,WMIN,FACT,EQW(322420)
      DOUBLE PRECISION GZI,GZISQ,SINM,COSLQ,WPSQ,SINL,SINN,SINS,PI,X2,
     1X1,GZL,WWL,WBNL,WBSL,WBWL,WBEL,DWP,WPL,DWQ,SINLL,COSL,WQL,WPLB,
     2COSLB,WQLB,WWN,WBNN,WBSN,WBWN,WBEN,SINNN,SINSN,COSW,COSE,GZNW,
     3GZNE,GZSW,GZSE,GZNL,GZSL,GZW,GZE,COSWB,COSEB,GZNWB,GZNEB,GZSWB,
     4GZSEB,GZNLB,GZSLB,GZWB,GZEB,WPG,SQR,WMAX,WMIN,FACT
      COMMON /AZM/WG(40,40,80),GZ,WPSQL,GWP,GZSQ,ARG1,ARG2,TEMP2,TEMP1,
     1LN,LL,M,EQAZM,WGO(40,40,80)
      DOUBLE PRECISION GZ,WPSQL,GWP,GZSQ,ARG1,ARG2,TEMP2,TEMP1
    1 FORMAT(12HO END AZIM2 ,10X,6HTIME =,F8.2,6H (SEC))
      DO 105 LN=1,256020
  105 WG(LN,1,1)=0.
      PI=3.14159265358979300
      X2=PI/80.
      X1=-0.5*X2
      DO 110 M=1,40
      M1=81-M
      X1=X1+X2
      TEMP1=DCOS(X1)
      GZI(M )= TEMP1
      GZI(M1)=-TEMP1
      TEMP2=TEMP1*TEMP1
      GZISQ(M )=TEMP2
      GZISQ(M1)=TEMP2
      TEMP1=DSQRT(1.-TEMP2)
      SINM(M )=TEMP1
  110 SINM(M1)=TEMP1
      X2=X2*2.
      X1=-0.5*X2
      DO 115 LL=1,40
      X1=X1+X2
      TEMP1=DCOS(X1)
      COSLQ(LL)=TEMP1
      TEMP2=TEMP1*TEMP1
      WPSQ(LL)=TEMP2
      SINL(LL)=DSQRT(1.-TEMP2)
      TEMP1=WBN(LL)
      TEMP2=WBS(LL)
      SINN(LL)=DSQRT(1.-TEMP1*TEMP1)
  115 SINS(LL)=DSQRT(1.-TEMP2*TEMP2)
      GZL=1.
      DO 325 L=1,80
      LL=L
      IF(L.GT.40) GO TO 120
      FACT=0.04
      WBNL=WBN(L)
      WBSL=WBS(L)
      WBWL=WBW(L)
      WBEL=WBE(L)
      DWP=0.2*(WBNL-WBSL)
```

```
      WPL=WBNL+0.5*DWP
      DWQ=0.2*(WBWL-WBEL)
      LPMAX=5
      LQMAX=5
      GO TO 125
  120 WWL=2.
      L1=L-40
      WPL=COSLQ(L1)
      WPSQL=WPSQ(L1)
      SINLL=SINL(L1)
      COSL=SINLL
      WQL=0.
      LPMAX=1
      LQMAX=1
  125 DO 325 LP=1,LPMAX
      IF(L.GT.40) GO TO 130
      WPL=WPL-DWP
      WPLB=-WPL
      WPSQL=WPL*WPL
      SINLL=DSQRT(1.-WPSQL)
      COSL=SINLL
      COSLB=-SINLL
      WQL=WBEL-0.5*DWQ
  130 DO 325 LQ=1,LQMAX
      IF(L.GT.40) GO TO 135
      WQL=WQL+DWQ
      WQLB=PI-WQL
  135 DO 325 N=1,40
      LN=N
      WWN=WW(N)
      WBNN=WBN(N)
      WBSN=WBS(N)
      WBWN=WBW(N)
      WBEN=WBE(N)
      SINNN=SINN(N)
      SINSN=SINS(N)
      TEMP1=WPL*WBNN
      TEMP2=WPL*WBSN
      COSW =SINLL*DCOS(WQL-WBWN)
      COSE =SINLL*DCOS(WQL-WBEN)
      IF(DABS(COSW ).LT.1.0E-5) COSW =0.
      IF(DABS(COSE ).LT.1.0E-5) COSE =0.
      GZNW=TEMP1+SINNN*COSW
      GZNE=TEMP1+SINNN*COSE
      GZSW=TEMP2+SINSN*COSW
      GZSE=TEMP2+SINSN*COSE
      GZNL=TEMP1+SINNN*COSL
      GZSL=TEMP2+SINSN*COSL
      GZW =DSQRT(WPSQL+COSW *COSW )
      GZE =DSQRT(WPSQL+COSE *COSE )
      IF(COSW.LT.0.) GZW=-GZW
      IF(COSE.LT.0.) GZE=-GZE
      IF(L.GT.40) GO TO 140
      COSWB=SINLL*DCOS(WQL+WBWN)
      COSEB=SINLL*DCOS(WQL+WBEN)
      IF(DABS(COSWB).LT.1.0E-5) COSWB=0.
      IF(DABS(COSEB).LT.1.0E-5) COSEB=0.
      GZNWB=TEMP1+SINNN*COSWB
```

```
      GZNEB=TEMP1+SINNN*COSEB
      GZSWB=TEMP2+SINSN*COSWB
      GZSEB=TEMP2+SINSN*COSEB
      GZNLB=TEMP1+SINNN*COSLB
      GZSLB=TEMP2+SINSN*COSLB
      GZWB=DSQRT(WPSQL+COSWB*COSWB)
      GZEB=DSQRT(WPSQL+COSEB*COSEB)
      IF(COSWB.LT.0.) GZWB=-GZWB
      IF(COSEB.LT.0.) GZEB=-GZEB
      GO TO 145
  140 FACT=WWL/WWN
  145 DO 325 M1=1,40
      M=M1
      GZ=GZI(M1)
      GZSQ=GZISQ(M1)
      TEMP2=SINLL*SINM(M1)
      GWP=GZ*WPL
      WPG=WPL/GZ
      SQR=0.
      TEMP1=GZSQ-WPSQL
      IF(TEMP1.GE.0.) SQR=DSQRT(TEMP1)
      WMAX=GWP+TEMP2
      WMIN=GWP-TEMP2
      IF(WMAX.GT. 1.) WMAX= 1.
      IF(WMIN.LT.-1.) WMIN=-1.
      IF((WMAX.LE.WBSN).OR.(WMIN.GE.WBNN)) GO TO 325
      IF(WPG.LT.1.) GO TO 150
      IF(WQL.LE.WBEN) GO TO 180
      IF(WQL.GE.WBWN) GO TO 185
      IF(WPL.LE.WBSN) GO TO 200
      IF(WPL-WBNN) 230,200,200
  150 IF(WPG.GT.-1.) GO TO 155
      IF(WQL.LE.WBEN) GO TO 170
      IF(WQL.GE.WBWN) GO TO 175
      IF(WPL.LE.WBSN) GO TO 190
      IF(WPL-WBNN) 230,190,190
  155 IF(WQL.GT.WBEN) GO TO 160
      IF(GZ.GE.GZE) GO TO 325
      IF(WPG.LE.WBSN) GO TO 170
      IF(WPG-WBNN) 210,180,180
  160 IF(WQL.LT.WBWN) GO TO 165
      IF(GZ.GE.GZW) GO TO 325
      IF(WPG.LE.WBSN) GO TO 175
      IF(WPG-WBNN) 220,185,185
  165 IF(WPL.LE.WBSN) GO TO 190
      IF(WPL-WBNN) 230,200,200
  170 CALL WGC(GZNW,GZSE,WBNN,GZNE,COSE,WBSN,GZSW,COSW, 1.)
      GO TO 250
  175 CALL WGC(GZNE,GZSW,WBNN,GZNW,COSW,WBSN,GZSE,COSE, 1.)
      GO TO 250
  180 CALL WGC(GZSW,GZNE,WBNN,GZNW,COSW,WBSN,GZSE,COSE,-1.)
      GO TO 250
  185 CALL WGC(GZSE,GZNW,WBNN,GZNE,COSE,WBSN,GZSW,COSW,-1.)
      GO TO 250
  190 IF((WPG.LT.WBNN).AND.(WPG.GT.WBSN)) GO TO 195
      CALL WGC(GZNW,GZSL,WBNN,GZNL,COSL,WBSN,GZSW,COSW, 1.)
      CALL WGC(GZNE,GZSL,WBNN,GZNL,COSL,WBSN,GZSE,COSE, 1.)
      GO TO 250
```

```
195 CALL WGC(GZNW,GZSL,WBNN,GZNL,COSL,WPG ,GZW ,COSW, 1.)
    CALL WGC(GZSW,GZSL,WPG ,GZW ,COSW,WBSN,GZSL,COSL,-1.)
    CALL WGC(GZNE,GZSL,WBNN,GZNL,COSL,WPG ,GZE ,COSE, 1.)
    CALL WGC(GZSE,GZSL,WPG ,GZE ,COSE,WBSN,GZSL,COSL,-1.)
    GO TO 250
200 IF((WPG.LT.WBNN).AND.(WPG.GT.WBSN)) GO TO 205
    CALL WGC(GZSW,GZNL,WBNN,GZNW,COSW,WBSN,GZSL,COSL,-1.)
    CALL WGC(GZSE,GZNL,WBNN,GZNE,COSE,WBSN,GZSL,COSL,-1.)
    GO TO 250
205 CALL WGC(GZNW,GZNL,WBNN,GZNL,COSL,WPG ,GZW ,COSW, 1.)
    CALL WGC(GZSW,GZNL,WPG ,GZW ,COSW,WBSN,GZSL,COSL,-1.)
    CALL WGC(GZNE,GZNL,WBNN,GZNL,COSL,WPG ,GZE ,COSE, 1.)
    CALL WGC(GZSE,GZNL,WPG ,GZE ,COSE,WBSN,GZSL,COSL,-1.)
    GO TO 250
210 IF(GZ.GE.GZW) GO TO 215
    CALL WGC(GZNW,GZE ,WBNN,GZNE,COSE,WPG ,GZW ,COSW, 1.)
    CALL WGC(GZSW,GZE ,WPG ,GZW ,COSW,WBSN,GZSE,COSE,-1.)
    GO TO 250
215 CALL WGC(GZNW,GZE ,WBNN,GZNE,COSE,WPG ,GZ  ,SQR , 1.)
    CALL WGC(GZSW,GZE ,WPG ,GZ  ,SQR ,WBSN,GZSE,COSE,-1.)
    GO TO 250
220 IF(GZ.GE.GZE) GO TO 225
    CALL WGC(GZNE,GZW ,WBNN,GZNW,COSW,WPG ,GZE ,COSE, 1.)
    CALL WGC(GZSE,GZW ,WPG ,GZE ,COSE,WBSN,GZSW,COSW,-1.)
    GO TO 250
225 CALL WGC(GZNE,GZW ,WBNN,GZNW,COSW,WPG ,GZ  ,SQR , 1.)
    CALL WGC(GZSE,GZW ,WPG ,GZ  ,SQR ,WBSN,GZSW,COSW,-1.)
    GO TO 250
230 IF(GZ.GE.GZW) GO TO 235
    CALL WGC(GZNW,GZL ,WBNN,GZNL,COSL,WPG ,GZW ,COSW, 1.)
    CALL WGC(GZSW,GZL ,WPG ,GZW ,COSW,WBSN,GZSL,COSL,-1.)
    GO TO 240
235 CALL WGC(GZNW,GZL ,WBNN,GZNL,COSL,WPG ,GZ  ,SQR , 1.)
    CALL WGC(GZSW,GZL ,WPG ,GZ  ,SQR ,WBSN,GZSL,COSL,-1.)
240 IF(GZ.GE.GZE) GO TO 245
    CALL WGC(GZNE,GZL ,WBNN,GZNL,COSL,WPG ,GZE ,COSE, 1.)
    CALL WGC(GZSE,GZL ,WPG ,GZE ,COSE,WBSN,GZSL,COSL,-1.)
    GO TO 250
245 CALL WGC(GZNE,GZL ,WBNN,GZNL,COSL,WPG ,GZ  ,SQR , 1.)
    CALL WGC(GZSE,GZL ,WPG ,GZ  ,SQR ,WBSN,GZSL,COSL,-1.)
250 IF(L.GT.40) GO TO 325
    IF(WPG.LT.1.) GO TO 255
    IF(WQLB.LE.WBEN) GO TO 275
    IF(WQLB.GE.WBWN) GO TO 280
    IF(WPLB.LE.WBSN) GO TO 295
    IF(WPLB-WBNN) 325,295,295
255 IF(WPG.GT.-1.) GO TO 260
    IF(WQLB.LE.WBEN) GO TO 285
    IF(WQLB.GE.WBWN) GO TO 290
    IF(WPLB.LE.WBSN) GO TO 300
    IF(WPLB-WBNN) 325,300,300
260 IF(WQLB.GT.WBEN) GO TO 265
    IF(GZ.GE.GZWB) GO TO 325
    IF(WPG.LE.WBSN) GO TO 285
    IF(WPG-WBNN) 305,275,275
265 IF(WQLB.LT.WBWN) GO TO 270
    IF(GZ.GE.GZEB) GO TO 325
    IF(WPG.LE.WBSN) GO TO 290
```

```
      IF(WPG-WBNN) 315,280,280
  270 IF(WPLB.LE.WBSN) GO TO 295
      IF(WPLB-WBNN) 325,300,300
  275 CALL WGC(GZSEB,GZNWB,WBNN,GZNEB,COSEB,WBSN,GZSWB,COSWB,-1.)
      GO TO 325
  280 CALL WGC(GZSWB,GZNEB,WBNN,GZNWB,COSWB,WBSN,GZSEB,COSEB,-1.)
      GO TO 325
  285 CALL WGC(GZNEB,GZSWB,WBNN,GZNWB,COSWB,WBSN,GZSEB,COSEB, 1.)
      GO TO 325
  290 CALL WGC(GZNWB,GZSEB,WBNN,GZNEB,COSEB,WBSN,GZSWB,COSWB, 1.)
      GO TO 325
  295 CALL WGC(GZSLB,GZNWB,WBNN,GZNLB,COSLB,WBSN,GZSWB,COSWB,-1.)
      CALL WGC(GZSLB,GZNEB,WBNN,GZNLB,COSLB,WBSN,GZSEB,COSEB,-1.)
      GO TO 325
  300 CALL WGC(GZNLB,GZSWB,WBNN,GZNWB,COSWB,WBSN,GZSLB,COSLB, 1.)
      CALL WGC(GZNLB,GZSEB,WBNN,GZNEB,COSEB,WBSN,GZSLB,COSLB, 1.)
      GO TO 325
  305 IF(GZ.GE.GZEB) GO TO 310
      CALL WGC(GZNEB,GZWB ,WBNN,GZNWB,COSWB,WPG ,GZEB ,COSEB, 1.)
      CALL WGC(GZSEB,GZWB ,WPG ,GZEB ,COSEB,WBSN,GZSWB,COSWB,-1.)
      GO TO 325
  310 CALL WGC(GZNEB,GZWB ,WBNN,GZNWB,COSWB,WPG ,GZ   ,SQR  , 1.)
      CALL WGC(GZSEB,GZWB ,WPG ,GZ   ,SQR  ,WBSN,GZSWB,COSWB,-1.)
      GO TO 325
  315 IF(GZ.GE.GZWB) GO TO 320
      CALL WGC(GZNWB,GZEB ,WBNN,GZNEB,COSEB,WPG ,GZWB ,COSWB, 1.)
      CALL WGC(GZSWB,GZEB ,WPG ,GZWB ,COSWB,WBSN,GZSEB,COSEB,-1.)
      GO TO 325
  320 CALL WGC(GZNWB,GZEB ,WBNN,GZNEB,COSEB,WPG ,GZ   ,SQR  , 1.)
      CALL WGC(GZSWB,GZEB ,WPG ,GZ   ,SQR  ,WBSN,GZSEB,COSEB,-1.)
  325 CONTINUE
      DO 335 M=1,80
      DO 335 N=1,40
      X1=0.
      DO 330 L=1,40
  330 X1=X1+WG(N,L,M)*WW(L)
      X2=2.*PI*WW(N)/X1
      DO 335 L=1,40
  335 WG(N,L,M)=X2*WG(N,L,M)
      CALL TTIMER(TIME)
      WRITE (6,1) TIME
      RETURN
      END
```

```
      SUBROUTINE WGC(D1,D2,D3,D4,D5,D6,D7,D8,SIG1)
      DOUBLE PRECISION D1,D2,D3,D4,D5,D6,D7,D8
      COMMON /WORK/EQW1(978),FACT,A1,A2,A3,A4,A5,A6,A7,A8,B1,B2,C1,C2,
     1EQW2(322396)
      DOUBLE PRECISION FACT,A1,A2,A3,A4,A5,A6,A7,A8,B1,B2,C1,C2
      COMMON /AZM/WG(40,40,80),GZ,WPSQL,GWP,GZSQ,ARG1,ARG2,TEMP2,TEMP1,
     1LN,LL,M,EQAZM,WGO(40,40,80)
      DOUBLE PRECISION GZ,WPSQL,GWP,GZSQ,ARG1,ARG2,TEMP2,TEMP1
      A1=D1
      A2=D2
      IF((GZ.LE.A1).OR.(GZ.GE.A2)) GO TO 200
      A3=D3
      A4=D4
      A5=D5
      A6=D6
      A7=D7
      A8=D8
      SIG=SIG1
      B1=A3
      IF(SIG.EQ.1.) IF(GZ-A4) 120,120,115
      IF(GZ.GE.A4) GO TO 120
  115 C1=SIG*A5
      C2=WPSQL+C1*C1
      B1=(GWP+C1*DSQRT(C2-GZSQ))/C2
  120 B2=A6
      IF(SIG.EQ.1.) IF(GZ-A7) 130,135,135
      IF(GZ.LE.A7) GO TO 135
  130 C1=SIG*A8
      C2=WPSQL+C1*C1
      B2=(GWP+C1*DSQRT(C2-GZSQ))/C2
  135 ARG1=(B1-GWP)/TEMP2
      ARG2=(B2-GWP)/TEMP2
      IF(ARG1.GT. 1.) ARG1= 1.
      IF(ARG2.LT.-1.) ARG2=-1.
      TEMP1=FACT*(DACOS(ARG2)-DACOS(ARG1))
      M1=81-M
      IF(LL.GT.40) GO TO 150
      WG(LN,LL,M)=WG(LN,LL,M)+TEMP1
      LL1=41-LL
      WG(LN,LL1,M1)=WG(LN,LL1,M1)+TEMP1
      GO TO 200
  150 LL1=LL-40
      WGO(LL1,LN,M)=WGO(LL1,LN,M)+TEMP1
      LN1=41-LN
      WGO(LL1,LN1,M1)=WGO(LL1,LN1,M1)+TEMP1
  200 RETURN
      END
```